Universität Ulm
Medizinische Fakultät
Universitätsklinikum Ulm
Zentrum für Innere Medizin
Klinik für Innere Medizin I
Leiter: Prof. Dr. med. Guido Adler

Stress protein complexed multidomain vaccines identify subdominant CD8 T cells with enhanced anti-viral activity

Dissertation zur Erlangung des Doktorgrades der Humanbiologie (Dr. biol. hum.) der medizinischen Fakultät der Universität Ulm

vorgelegt von **Andreas Wieland**

geboren in Laupheim

Jahr der Vorlage im Promotionssekretariat: 2009

Amtierender Dekan: Prof. Dr. Klaus-Michael Debatin

1. Berichterstatter: Prof. Dr. Reinhold Schirmbeck

2. Berichterstatter: Prof. Dr. Uwe Knippschild

Tag der Promotion: 29. Mai 2009

For my parents

Contents

List of Figures

List of Tables

Abbreviations

General abbreviations

Ab	antibody
acc.no.	accession number
Ad	adenovirus
ALT	alanine aminotransferase
APC	antigen-presenting cell
Ara	DnaJ domain of Arabidopsis thaliana
Aralong	elongated DnaJ domain of Arabidopsis thaliana
ATP	adenosine triphosphate
B6	C57BL/6J
ß-ME	ß-mercaptoethanol
BFA	brefeldin A
BM	bone marrow
BM-DC	bone marrow derived dendritic cell
bp	basepair(s)
BSA	bovine serum albumin
C or HBcAg	hepatitis B virus core antigen
cat.no.	catalog number
ccc	covalently closed circular
CD	cluster of differentiation
Chl	DnaJ domain of Chlamydia trachomatis
CHO	chinese hamster ovary
Ci	curie
CIP	calf intestinal alkaline phosphatase
COI	cut-off-index
DC	dendritic cell

DEC205	dendritic cell receptor for endocytosis 205
DMEM	Dubelcco's Modified Eagle Medium
DMSO	dimethyl sulfoxide
DNA	deoxyribonuclein acid
dNTP	deoxyribonucleotide triphosphate
DS	double-stranded linear
E. coli	Escherichia coli
EDTA	ethylenediaminetetraacetic acid
ELISA	enzyme-linked immunosorbent assay
ER	endoplasmatic reticulum
F or Flu-Ma	influenza A matrix protein
FACS	fluorescence activated cell sorting
FCM	flow cytometry
FCS	fetal calf serum
FITC	fluorescein isothiocyanate
g	acceleration due to gravity
G or (e)GFP	(enhanced) green fluorescent protein
G418	geneticin
GM-CSF	granulocyte macrophage colony-stimulating factor
H&E	hematoxylin-eosin
HBV	hepatitis B virus
HEK 293	human embryonic kidney 293
HIV	human immunodeficiency virus
HLA	human leukocyte antigen
HRP	horseradish peroxidase
Hsp	heat shock protein
IFN	interferon
IgG	immunoglobulin G
IgG/HC	heavy chain of immunoglobulin G
IgG/LC	light chain of immunoglobulin G
IL	interleukin
IPTG	isopropyl ß-D-1-thiogalactopyranoside
kb	kilobase(s)
kDa	kiloDalton

L or LLO	listeriolysin-O
LB	luria bertani
LDM	liver digest medium
LOX-1	lectin-like oxidized low-density lipoportein receptor-1
LPM	liver perfusion medium
LPS	lipopolysaccharide
LS	large surface antigen of hepatitis B virus
M	molar
mAb	monoclonal antibody
MACS	magnetic activated cell sorting
MHC	major histocompatibility complex
MOI	multiplicity of infection
MS	middle surface antigen of hepatitis B virus
NPC	non-parenchymal cells
ODN	oligodeoxynucleotide
OVA	ovalbumin
P or Pol	hepatitis B virus polymerase
PAGE	polyacrylamid gel electrophoresis
PBS	phosphate-buffered saline
PCR	polymerase chain reaction
PE	phycoerthrin
PFA	paraformaldehyde
PPO	2,5-diphenyloxazole
RAG	recombination activating genes
RC	relaxed circular
RFP	red fluorescent protein
rpm	rounds per minute
RPMI	Roswell Park Memorial Institute
S or HBsAg	hepatitis B virus small surface antigen
SAP	streptavidin-conjugated alkaline phosphatase
SDS	sodium dodecylsulfate
SEM	standard error of the mean
SS	single-stranded linear
St	streptavidin-binding tag

SV40	simian virus 40
T or T-Ag	large tumor antigen of SV40
TAP	transporter associated with antigen processing
TB	terrific broth
TBS	tris-buffered saline
TCR	T cell receptor
tg	transgenic
Th	T helper
TLR	toll-like receptor
TNF	tumor necrose factor
UV	ultraviolet
V	volt
X	X antigen of hepatitis B virus

Nucleotide abbreviations

A	adenine
C	cytosine
G	guanine
T	thymine

Amino acid abbreviations

A	Ala	alanin	M	Met	methionine
C	Cys	cysteine	N	Asn	asparagine
D	Asp	aspartic acid	P	Pro	proline
E	Glu	glutamic acid	Q	Gln	glutamine
F	Phe	phenylalanin	R	Arg	arginine
G	Gly	glycine	S	Ser	serine
H	His	histidine	T	Thr	threonine
I	Ile	isoleucine	V	Val	valine
K	Lys	lysine	W	Trp	tryptophan
L	Leu	leucine	Y	Tyr	tyrosine

1. Introduction

Vaccines are one of the most effective developments in medicine. The smallpox vaccine is the figure-head of a large range of vaccines, as through a massive, worldwide vaccination program the smallpox –one of the most deadly and persistent human pathogenic diseases– was eradicated. Vaccines are thus the major weapon in fighting pathogens. The key to their success is the ability of the adaptive immune system to react specifically against pathogens and simultaneously to build up a immunological memory enabling the effective clearance of a later infection. Despite the success using the smallpox vaccine, after about 200 years of vaccine research there is only a limited number of effective vaccines available. Vaccines for 'new' pathogens including human immunodeficiency virus (HIV) as well as ancient scourges such as malaria and tuberculosis are still missing or ineffectively inducing a protective immunity. The lack of effective vaccines for the above mentioned diseases is likely caused by the requirement of a cellular immune response for effective protection from those. Although all currently available vaccines efficiently induce antibody responses, in regard of priming cellular immune responses most vaccines are inefficient. Despite the availability of a preventive HBV vaccine efficiently inducing HBsAg-specific antibodies, a therapeutic vaccine reconstituting the suboptimal cellular immune responses in chronically infected patients is still missing. Only live-attenuated organisms are able to mount an efficient cellular immune response, however their widespread use might be precluded by manufacturing and safety concerns. The major focus of current vaccine research is thus the efficient induction of cellular immune responses by novel vaccination strategies. In general, there are two distinct vaccination protocols under extensive research: a DNA-based (genetic) and a protein-based approach.

1.1. Genetic vaccination

Vector design

DNA vaccines are eukaryotic expression vectors engineered for optimal antigen expression in mammalian recipients. Because of their easy handling and propagation, plasmid DNA vectors are generally used for vaccination purposes (figure 1). They consist of two regions: i) the vector backbone necessary for the propagation in bacteria that contains the origin of replication (providing large copy numbers in bacteria and thus high yields) and an antibiotic resistance gene as selection marker, and ii) a vaccine unit providing a viral promotor, an intron and a polyadenylation signal ensuring high-level expression of the inserted gene of interest.

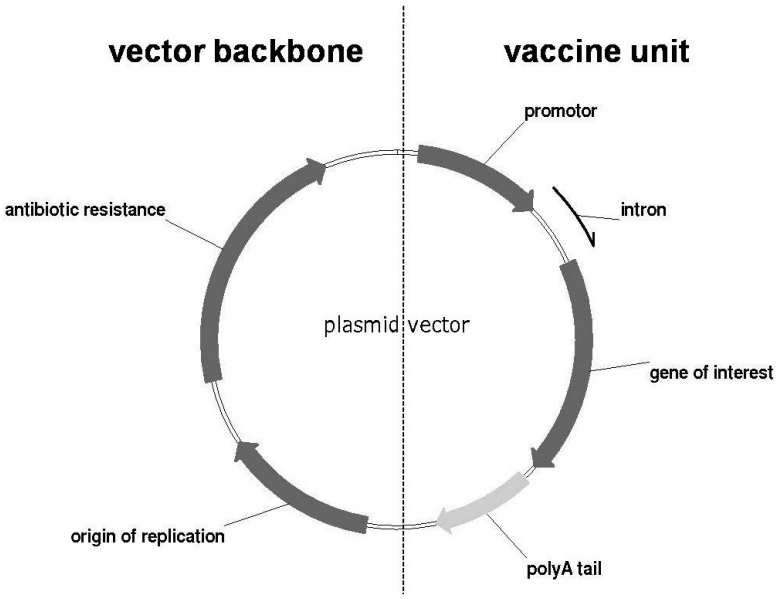

Figure 1.: Schematic presentation of an expression plasmid used for DNA vaccination. Plasmid vector contains the vector backbone consisting of the origin of replication and an antibiotic resistance gene, and the vaccine unit consisting of a viral promotor, an intron for enhanced expression, the gene coding for the antigen of interest and a polyadenylation signal.

DNA vaccination techniques

There are several techniques available, that efficiently deliver DNA vaccines in vivo and thus induce an immune response [45, 59, 72, 95]. However, there a two major techniques currently available that are broadly used and show high efficacy:

Intramuscular injection of high doses (50-100 µg per mouse) of non-packaged antigen encoding plasmid DNA ('naked') efficiently induces antigen-specific CD8 T cells and high titers of IgG2a antibodies, that are characteristic features of a Th1-biased response [34,58,134]. Although doses of 25-100 µg DNA per injection are sufficient to efficiently immunize mice, this amount of DNA seems not to be sufficient to efficiently prime the human CD8 T cell responses. A human study revealed, that 500-2500 µg plasmid DNA are required to induce enhanced CD8 T cell responses specific for a malaria antigen [131].

The amount of DNA necessary for the induction of a CD8 T cell response in mice can be markedly reduced by immunization with the gene gun. This approach uses low doses (0.1-1 µg per mouse) of plasmid DNA coated onto gold particles that are propelled directly into the cytosol of skin cells by a gas-driven biolistic device (gene gun) [132, 137, 140]. This immunization method results in higher transgene expression levels than those obtained by comparable amounts of 'naked' DNA. The enhanced expression can be partially explained by the protection of plasmid DNA from extracellular degradation by deoxyribonucleases [68]. In addition to enhanced antigen expression, delivery of low doses of DNA by gene gun immunization favors priming of Th2-directed immune responses inducing preferentially IgG1 antibodies and no or only low CD8 T cell responses [40].

Priming cellular immune responses by DNA vaccines

Adaptive immunity requires the activation of T lymphocytes by professional antigen presenting cells (APCs). Dendritic cells are supposed to be the main APC population that activate T cells by presentation of antigens bound to major histocompatibility complex (MHC) molecules. This antigen presentation proceeds through two pathways: the endogenous and exogenous antigen processing pathway. These two pathways of antigen processing strikingly differ in the source of antigen as well as the class of MHC molecule finally presenting the antigen –so-called epitope. Extracellular antigens enter the exogenous pathway resulting in endosomal and lysosomal degra-

dation with subsequent presentation of generated peptides by MHC-II molecules. MHC-II:peptide complexes located on the cell surface of APCs activate CD4 T cells specific for the generated MHC-II:peptide complexes [125]. The exogenous processing pathway and thus priming of CD4 T cells facilitates humoral immune responses. In contrast, intracellularly synthesized proteins enter the endogenous pathway utilizing the 'cytosolic' proteasome for degradation of proteins. The generated peptides are transported into the endoplasmatic reticulum (ER) by transporters associated with antigen processing (TAP) [82], followed by further trimming by ER-localized peptidases [106]. The processed peptides are loaded onto MHC-I molecules and the complexes are transported to the cell surface via the Golgi apparatus. Presentation of MHC-I:peptide complexes on the surface induces CD8 T cell responses.

A further pathway termed 'cross-presentation/cross-priming' enables APCs to activate CD8 T cells by processing of extracellular antigen and presentation via MHC-I molecules [86,96,139]. This pathway is required for immunity against pathogens that don't infect APCs directly, as otherwise –due to the inability of non-professional antigen presenting cells to activate T cells– pathogen-specific CD8 T cells couldn't be activated.

Upon intramuscular DNA vaccination, plasmid-encoded antigens are thought to activate CD8 T cells by two distinct mechanism. DNA vaccines can directly transfect APCs, antigens are thus processed and subsequently presented by MHC-I molecules via the conventional endogenous pathway (figure 2b). Naive CD8 T cells are then activated by the cell-surface expression of MHC-I:peptide complexes and co-stimulatory molecules necessary for activation. The second mechanism involves the above mentioned 'cross-priming' pathway. Myocytes or other somatic cells are transfected with the DNA vaccine and produce large amounts of antigen, as they lack co-stimulatory molecules no activation of naive CD8 T cells occurs. However, APCs can process secreted antigens of somatic cells by endocytosis or even take up apoptotic and necrotic bodies by phagocytosis [1–3]. The antigens are then processed and presented by MHC-I molecules on the cell surface together with co-stimulatory molecules resulting in activation of antigen-specific CD8 T cells (figure 2c).

In addition to activation of the adaptive immune system by vector encoded antigens, the presence of unmethylated cytidine-phosphate-guanosine (CpG) dinucleotide motifs in the bacterial plasmid DNA elicits innate immune responses characterized by the production of Th1-directing cytokines (e.g. IL-6, IL-12, TNFα, IFNγ and

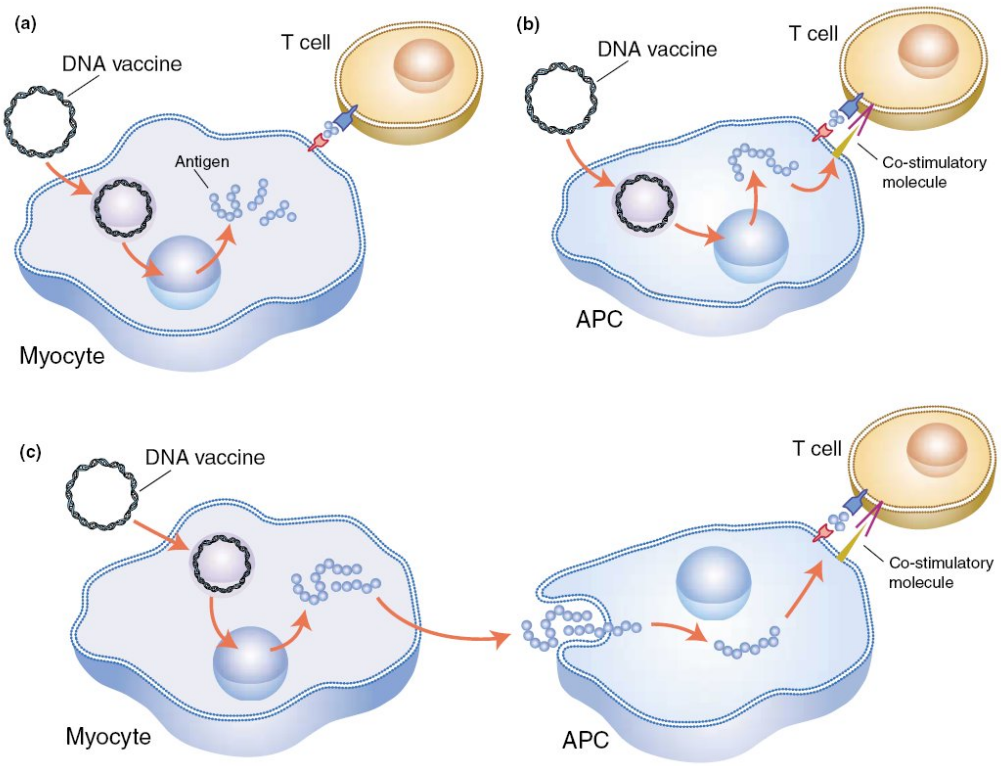

Figure 2.: Mechanisms stimulating T cells upon intramuscular DNA vaccination. **a** Myocytes take up DNA vaccine and express the antigen, resulting in presentation of MHC-I:peptide complexes. However, myocytes co-stimulatory molecules and thus fail to activate naive CD8 T cells. **b** Antigen presenting cells (APCs) can also take up DNA vaccine and directly express the antigen. Due to co-stimulatory molecules MHC-I:peptide complexes can efficiently activate naive CD8 T cells. **c** Alternative mechanism that involves the transfection of myocytes, followed by transfer of the myocyte-expressed antigen to an APC leading to activation of naive CD8 T cells. Adapted from Liu [71].

IFNα) and maturation of dendritic cells (DCs) [51, 62, 65]. These immunostimulatory motifs have thus a fundamental role in enhancing the immunogenicity of DNA vaccines.

Multivalent DNA vaccines

In contrast to immunization with live-attenuated organisms, plasmid vaccines encoding single antigens are supposed to deliver only a restricted amount of antigenic information for the induction of CD8 T cell responses resulting at worst in failed protection. Therefore, the delivery of multiple antigens is desirable to provide a large amount of antigenic information and thus elicit multispecific CD8 T cell responses. The design of fusion antigens consisting of defined T cell epitopes and/or antigenic domains is an attractive, commonly used approach to elicit an enhanced panel of CD8 T cell responses [41, 57, 93, 121]. This approach also allows the induction of CD8 T cell responses directed against multiple pathogens, as antigenic epitopes/domains of different sources can be easily combined. However, a potential roadblock in elicitation of multispecific CD8 T cell responses may be an overall decreased immunogenicity due to inefficient expression based on the chimeric, artificial character of the designed antigens. In addition, the combination of multiple epitopes on a single antigen may result in unexpected immunodominance hierarchies limiting the efficient induction of multispecific (subdominant) CD8 T cell responses.

Hsp-facilitated expression system for DNA vaccines

A Hsp-mediated expression system has been developed to facilitate the expression of chimeric, unstable antigens encoded by plasmid vaccines [37, 99, 109]. This system is based on the observation that the N-terminal domain of cytosolic T-Ag of SV40 is able to stably associate with Hsp70/73 in an ATP-dependent manner [22] mediated by a DnaJ-like structure of the T-Ag. For stable Hsp70/73 association the N-terminal 77 residues of the T-Ag are sufficient to form the required finger-like structure consisting of four α-helices. Multiple studies showed that the facilitated expression of Hsp-capturing chimeric antigens is accompanied by enhanced immunogenicity and independent of the origin and size of the fused antigen(s) [42, 97, 107, 111]. Expres-

sion of multivalent DNA vaccines in a Hsp-complexed form is thus an attractive approach to elicit enhanced multispecific CD8 T cell responses.

Risks and advantages of DNA vaccines

Although DNA vaccines have demonstrated high immunogenicity and the ability to induce protective immunity in multiple preclinical disease models, their application in humans is limited because of inefficient DNA delivery techniques [49]. In addition, a number of safety concerns about DNA vaccination have been raised including integration into the host genome [76], development of autoimmune diseases [46], and the induction of rather tolerizing T cell responses [56, 83]. Nevertheless, DNA vaccines are useful research tools helping to analyze the cellular response to endogenously processed antigens. The alteration and recombination of DNA vaccines is fast as well as cost-effective due to a large range of techniques of molecular biology.

1.2. Protein-based vaccination

Induction of CD8 T cells by protein-based vaccination approaches remains one of the primary goals in vaccinology. In general, protein-based vaccines enter the extracellular pathway resulting in presentation by MHC-II molecules and induction of CD4 T cells and antibodies. There are multiple approaches aiming at the increased priming of CD8 T cells by enhanced 'cross-priming' of antigens. These approaches include antigenic peptides fused to cationic tails [78, 100, 112], antigens fused to DC-specific antibodies (i.e. anti-DEC205) [74], Hsp/antigen fusion proteins [89] and Hsp loaded in vitro with antigenic peptides [14, 21, 67].

Hsp molecules mediate cross-priming

In addition to the 'traditional' housekeeping functions of Hsps such as protein folding, prevention of protein aggregration and facilitating transmembrane traffic [79], multiple studies have demonstrated that tumor-derived Hsp of different families (Hsp70 and Hsp90) initiate tumor-specific CD8 T cell responses and protective immunity [118]. The specific immunogenicity of Hsps derives from chaperoned antigenic peptides [20, 85]. Hsp molecules are thought to be internalized by receptor-

mediated endocytosis, resulting in presentation of chaperoned peptides by MHC-I molecules [15, 23]. Binding of Hsps to a number of cell surface receptors has been described, including CD91 [10, 17], CD40 [12], TLR2/4 [127], LOX-1 [35] and scavenger receptor-A [16]). However, it's unclear which receptors are responsible for the uptake of Hsps resulting in the 'cross-priming' of CD8 T cells.

In addition to their chaperoning activity, Hsp molecules have been described to possess strong immunostimulatory capacities that lead to maturation and activation of APCs [7, 77, 127, 128] as well as significant secretion of TNFα, IL-1β, IL-6, IL-12, IL-15 and IFNγ [6, 92, 115, 122]. Due to their dual function in the elicitation of immune responses, Hsps were thus termed 'chaperokines' [5]. However, recent studies showed that the immunostimulatory effects of Hsps are rather based on endotoxin contaminations [11, 13, 14, 75, 130] than on intrinsic, structure-related adjuvant activity of Hsp molecules. These findings are in accordance with the identification of the cellular Hsp-receptor TLR4 [127] that was initially described to bind LPS.

Currently available Hsp-mediated vaccination techniques

Different vaccination approaches have been established due to the enhanced cross-priming by Hsp molecules. Hsp molecules derived of tumor tissues have been shown to elicit protective tumor-specific CD8 T cell responses [31, 77, 101]. The specific immunogenicity is mediated by chaperoned tumor-derived peptides representing kind of a tumor fingerprint [20, 85]. Therefore, methods for the preparative isolation of in vivo formed Hsp/peptide complexes from tumor cells were developed in order to obtain tumor-specific vaccines [4, 38, 116, 117]. However, this approach covers only tumor-specific antigens and can't satisfy the needs of pathogen-specific vaccines.

Recombinant, purified Hsp molecules were also loaded in vitro with antigenic peptides in order to induce pathogen- as well as tumor-specific CD8 T cell responses. In vitro loaded Hsp/peptide complexes were shown to efficiently prime CD8 T cell responses [14, 21, 30, 67, 103] and enable the induction of mono-specific CD8 T cell responses. Although peptides loaded onto Hsp have demonstrated enhanced immunogenicity, a potential roadblock in elicitation of multispecific CD8 T cell responses is that only a small subset of peptides is able to bind Hsp with sufficient affinity [44]. To overcome hindrances based insufficient binding affinity to Hsp, hybrid peptides consisting of defined T cell epitopes as well as short hydrophobic Hsp binding sequences

were designed [43, 84]. However, the in vitro loading of peptides onto purified Hsp molecules is a demanding technique and the amount of antigenic information is limited to a maximum of about 20-30 residues thus limiting the usability.

Fusion proteins consisting of Hsp and a fused antigen are thought to overcome the limitations of above mentioned approaches, as they can deliver pathogen- as well as tumor-specific antigens of nearly infinite size. Enhanced immunogenicity of Hsp fusion proteins has been demonstrated by fusing CD8 T cell epitopes [28, 80] as well as entire antigens or fragments up to 25 kDa [53, 55, 75, 89, 119, 120]. Hsp fusion proteins are thus an attractive approach for vaccines aiming at enhanced cellular immune response.

1.3. Aim of the study

Induction of CD8 T cell responses by protein-based vaccines is one of the major challenges in vaccine research. We will use an expression system in which chimeric proteins with a Hsp-capturing, viral J domain fused to antigen-encoding sequences form stable complexes with eukaryotic (Hsp70, Hsp73) stress proteins to produce recombinant vaccines.

In the first part of the thesis the formation, isolation and immunogenicity of recombinant Hsp/antigen complexes should be characterized in detail. We will (i) design model antigens containing different (human and murine) MHC-I-restricted CD8 T cell epitopes; (ii) characterize the interactions of different J domains with Hsp70/73; (iii) develop a purification method that allows us to isolate native Hsp/antigen complexes from eukaryotic and bacterial lysates; and (iv) test the immunogenicity of these recombinant vaccines (with or without further adjuvant) in mice.

The Hsp-mediated expression system is exceptionally potent to induce multispecific CD8 T cell responses when used in DNA- or protein- based vaccines. It has been shown that immunodominance hierarchies operating in multispecific immune responses to viral antigens limit the diversity of the elicited T cell responses. In the second part of the thesis Hsp-binding vaccines containing different domains of HBV antigens should be generated in order to characterize immunodominant and subdominant CD8 T cell responses in wild type B6 mice and HBV transgenic mice. We will use HBV transgenic mice to test if the induced CD8 T cell responses deliver

anti-viral (replication-inhibiting) effector functions to the liver. This will allow us to investigate which vaccine-induced CD8 T cells can locally suppress HBV replication in hepatocytes.

2. Material and methods

2.1. Chemicals and reagents

All chemicals and reagents not separately mentioned in the text are listed in table 9 in the appendix.

2.2. Oligonucleotides and peptides

Oligonucleotides and synthetic peptides were purchased from Thermo Fisher Scientific (Ulm, Germany). Table 1 contains the oligonucleotides used for cloning of vaccine constructs. Oligonucleotides were dissolved in water yielding a concentration of 100 pM. Table 2 comprise the synthetic peptides used for in vitro stimulation of CD8 T cells. Peptides were dissolved at 10 mg/ml in DMSO.

2.3. Mice

C57BL/6J (B6) mice (H-2^b), BALB/c mice (H-2^d L^{d+}), H-2 class II deficient A$\alpha^{-/-}$ mice [63], K^b/OVA TCR-tg OT-I $RAG^{-/-}$ mice [32, 54, 81], HLA-A*0201-tg (HHD) mice [91], C57BL/6J-TgN(Alb1HBV)44Bri tg (Alb/HBs) mice [27] and 1.4 HBV-S^{mut} tg B6 mice [52] were bred and kept under standard pathogen-free conditions in the animal colony of Ulm University (Ulm, Germany). Male and female mice were used at 8-12 weeks of age. As HBV replication in the liver of 1.4 HBV-S^{mut} tg B6 males was higher and showed less variability [52], only 1.4 HBV-S^{mut} tg B6 males were used for vaccination studies. All animal experiments were performed according to the guidelines of the local Animal Use and Care Committee and the National Animal Welfare Law.

Table 1.: Oligonucleotides used for PCR

designation	sequence
C10 fow	5´-AAA AAG CTA GCG GAG CTA CTG TGG AGT TAC TCT CG-3´
C50 rev	5´-AAA AAG CGG CCG CTC ACC CGG GAG GTG AAC AAT GCT CAG GAG ACT C-3´
GFP rev	5´-TTT TAA GCT TGC GGC CGC TTT ACT TGT ACA GC
GFPmut fow	5´-GAT GCT GCA CCG GTC GCC ACC ACG GTG AGC AAG GGC GAG G-3´
GFPmut rev	5´-CCT CGC CCT TGC TCA CCG TGG TGG CGA CCG GTG CAG CAT C-3´
OVA246 fow	5´-AAA AAG AAT TCT TTG CCT GAT GAA GTC TCA GGC-3´
pCI rev	5´-CACTCCCAGTTCAATTACAGCTC-3´
S140 fow	5´-AAA AAC CCG GGA CCA AAC CTT CGG ACG GAA ATT G-3´
S140v2 fow	5´-AAA AAG AAT TCG ACC AAA CCT TCG GAC GGA AAT TG-3´
S2 fow	5´-AAA AAG GTA CCG CTC GAG AAC ATC ACA TCA GGA TTC CTA G-3´
S226 rev	5´-AAA AAG CGG CCG CTT AAA TGT ATA CCC AAA GAC AAA AGA AA-3´
S226v2 rev	5´-AAA AAG CGG CCG CAC CGG TAT GTA TAC CCA AAG ACA AAA GAA AAT TG-3´
S50 rev	5´-AAA AAG GTA CCC CAA GAC ACA CGG TAG TTC CC-3´
Strep fow	5´-AAA AGA ATT CAT TAA AGA GGA GAA ATT AAC TAT GGC CAG CTG GTC CCA CC-3´

Table 2.: Peptides used for stimulation of CD8 T cells. Peptides are listed according their antigenic origin. Their designation includes the respective MHC-I restriction and the localization of the epitope in the antigenic origin. Additionally, the respective sequences are shown in one letter amino acid code.

antigen	designation	sequence
HBcAg	K^d/C_{87-95}	SYVNTNMGL
HBcAg	K^b/C_{93-100}	MGLKFRQL
HBcAg	$A*0201/C_{18-27}$	FLPSDFFPSV
HBsAg	$K^b/S_{190-197}$	VWLSVIWM
HBsAg	$K^b/S_{208-215}$	ILSPFLPL
HBsAg	$A*0201/S_{20-28}$	FLLTRILTI
HBsAg	$A*0201/S_{185-194}$	GLSPTVWLSV
HBsAg	$A*0201/S_{208-216}$	ILSPFLPLL
HBV polymerase	$K^d/Pol_{140-148}$	HYFQTRHYL
HBV polymerase	$A*0201/Pol_{803-811}$	SLYADSPSV
Influenza A matrix protein	$A*0201/Flu\text{-}Ma_{58-66}$	GILGFVFTL
Listeriolysin-O	K^d/LLO_{91-98}	GYKDGNEYI
Ovalbumin	$K^b/OVA_{257-264}$	SIINFEKL

2.4. General techniques of molecular biology

Polymerase chain reaction (PCR)

PCR was performed using the ProofStart DNA polymerase (cat.no. 202205, Qiagen) in a total volume of 50 µl containing 1x PCR buffer, 2 µM dNTP, 10 pmol of forward and reverse primers, 50 ng template DNA and 2.5 U polymerase. The general PCR conditions are listed in table 3.

Table 3.: General PCR protocol. All PCR reactions for cloning purposes were performed according to the shown protocol.

cycle	temperature	duration
	95°C	5 min
1-35	94°C	30 s
	62°C	30 s
	72°C	60 s
	72°C	4 min
	4°C	∞

Restriction digests

Restriction digests were performed in a total volume of 50 µl containing 10 µg plasmid and at least 20 U restriction enzyme. The reactions were incubated at 37°C for 1 h. The target vector preparations were subsequently treated for 30 min at 37°C with 10 U of alkaline phosphatase (CIP) to remove 5´-phosphate groups avoiding self-ligation of the target vector. All enzymes were purchased from New England Biolabs and the appropriate reaction buffers were chosen according to the manufacturer's protocol.

Agarose gel electrophoresis

PCR and restriction digest products were subjected to agarose gel electrophoresis to separate the generated fragments. Depending on the size of the generated fragments 1-3% agarose gels were used. The appropriate amount of agarose was dissolved in 1x TAE buffer (40 mM Tris, 20 mM acetic acid, 1 mM EDTA) by heating-up. Ethidium bromide was added for later visualization of DNA fragments. Samples were loaded with 6x loading buffer (50% glycerol, 0.05% bromphenol blue, 0.05% xylencyanol). To estimate the size of the DNA fragments a 1 kb (cat.no. N3232) and 100 bp ladder (cat.no. N3231, both New England Biolabs) were loaded along with the samples. The electrophoresis was carried out at 120 V for 45 min. The DNA fragments were visualized using UV light and aquired using the GeneGenius system (Syngene).

Purification of DNA fragments from agarose gels

DNA fragments visualized using UV light were excised. DNA fragments smaller than 10 kb were purified using Qiaquick Gel Extraction Kit (cat.no. 28706, Qiagen) according to the manufacturer's instructions, whereas DNA fragments greater than 10 kb were purified using QIAEX II Gel Extraction Kit (cat.no. 20021, Qiagen).

DNA ligation

Purified DNA fragments were ligated in a total volume of 20 µl containing 2 µl 10x ligase buffer, 100 ng vector, 400 U T4 DNA ligase (cat.no. M0202, New England

Biolabs) and the appropriate amount of insert achieving a molar ratio of 1 (vector) to 5 (insert). The reaction mixture was incubated at room temperature for 2 h.

Transformation of *E. coli*

10 µl of the ligation reaction was added to 100 µl of competent *E. coli* DH5α and incubated on ice for 30 min. The bacteria were heat-shocked for 45 s at 42°C and immediately placed on ice for 3 min. 750 µl S.O.C. medium (cat.no. 15544-034, Invitrogen) were added and the bacteria were incubated for 45 min at 37°C. Varying amounts of the transformation reaction (50-300 µl) were plated onto LB agar plates (1% (w/v) bactotryptone, 0.5% (w/v) yeast extract, 0.5% (w/v) NaCl, 1.5% (w/v) agar) containing either 100 µg/ml ampicillin or 50 µg/ml kanamycin for selection of successfully transformed bacteria. The plates were incubated at 37°C overnight.

Plasmid purification

For plasmid purification (mini size) a single colony of transformed *E. coli* was picked and inoculated in 6 ml LB medium (1% (w/v) bactotryptone, 0.5% (w/v) yeast extract, 0.5% (w/v) NaCl) with the appropriate antibiotic. The culture was incubated at 37°C while shaking at 220 rpm overnight. The purification was performed using the Qiagen Plasmid Mini Kit (cat.no. 12123, Qiagen) according to the manufacturer's instructions, except adding directly the isopropanol to the cleared lysate and therefore skipping the purification via anion-exchange columns. For vaccination and cell-transfection purposes, the plasmids were purified using the Qiagen Plasmid Midi/Maxi/Mega Kit (cat.no. 12143/12163/12183, Qiagen) according to the manufacturer's instructions. Purified plasmids were dissolved in ddH_2O. Large scale plasmid DNA was produced and purified by PlasmidFactory GmbH (Bielefeld, Germany).

2.5. Plasmid vectors

All plasmid vectors used for transient expression and vaccination experiments are based on pCI vector (cat.no. E1731, Promega). The generation of the following plasmid vectors was previously described [36]:

- pCI/T-SFG encodes residues 1-77 of the T-Ag (T), residues 140-226 of HBsAg (S), residues 58-66 of influenza A matrix protein (F) and the entire enhanced green fluorescent protein (eGFP, G).
- pCI/T-SFG encodes the T-SFG sequence lacking residues 58-66 of influenza A matrix protein (F).
- pCI/T60-SFG encodes residues 1-60 of the T-Ag and the SFG sequence.
- pCI/StT-SFG encodes the T-SFG sequence plus a N-terminal streptavidin-binding tag (St).
- pCI/StT-C encodes the streptavidin-binding tag (St), residues 1-77 of the T-Ag (T) and residues 79-149 of the HBcAg (C).
- pCI/StT-PCL encodes the streptavidin-binding tag (St), residues 1-77 of the T-Ag (T), residues 131-160 and 791-832 of the hepatitis B polymerase (P), residues 79-149 of the HBcAg (C) and residues 81-106 of the *Listeria monocytogenes* listeriolysin-O (L).
- pCI/StChl-PCL encodes the same sequence as StT-PCL, but the T domain is exchanged with residues 1-67 of a *Chlamydia trachomatis* DnaJ protein (Chl).
- pCI/StAra-PCL encodes the same sequence as StT-PCL, but the T domain is exchanged with residues 1-75 of a *Arabidopsis thaliana* DnaJ2 protein (Ara).

The following plasmids were generated during this thesis:

- pCI/StT-OVA-G was generated by using pCI/StT-PCL as target vector and exchanging the PCL-coding region with residues 246-353 of the ovalbumin (OVA) and the entire green fluorescent protein. The OVA-coding sequence was codon-optimized, equipped with proper flanking restriction sites and synthesized by GeneArt (Regensburg, Germany). The exchange was accomplished by digesting pCI/StT-PCL and the synthesized insert with KpnI/AgeI. Thereafter, an eGFP-coding region derived of pEGFP/N1 (cat.no. 6085-1, Clontech) was inserted using AgeI/NotI.

- BMGneo/StT-OVA-G containing the complete antigen-coding unit as well as the polyadenylation signal of pCI/StT-OVA-G was generated by digestion of pCI/StT-OVA-G with XhoI/BamHI and ligation of the antigen-containing fragment with SalI/BamHI-digested BMGneo [60].

- pQE-9/StT-OVA-G enabling bacterial expression was generated by cloning a modified antigen-coding unit of pCI/StT-OVA-G into the inducible expression vector pQE-9 (Qiagen). The antigen-coding unit of pCI/StT-OVA-G was altered by PCR mutagenesis with the objective of mutating the start codon of the eGFP-coding part. The front part of the coding unit was amplified using forward primer Strep fow and reverse primer GFPmut rev, while the rear part was amplified using forward primer GFPmut fow and reverse primer GFP rev. The resulting products were fused in a final PCR reaction and the final construct was cloned into pQE-9 using EcoRI/HindIII.

- pCI/StAralong-PCL encodes the same sequence as StAra-PCL, but the J domain was elongated by 163 amino acid residues flanking the C-terminus of J domain of *Arabidopsis thaliana* DnaJ2 protein.

- pCI/StT-MO was generated using the pCI/StT-PCL as target vector already containing residues 131-160 and 791-832 of the hepatitis B polymerase (P) and residues 79-149 of the HBcAg (C). Residues 2-50 of the HBsAg were amplified by PCR from pCI/S [110] using forward primer S2 fow and reverse primer S50 rev, and the PCR product was subsequently cloned into the target vector using KpnI. Residues 10-50 of the HBcAg were amplified from pCI/Core [66] using forward primer C10 fow and reverse primer C50 rev. The resulting PCR product was cloned into the XmaI/NotI-digested target vector using NheI/NotI, thereby replacing residues 81-106 of the *Listeria monocytogenes* listeriolysin-O (L). Residues 140-226 of the HBsAg were amplified from pCI/S using forward primer S140 fow and S226 rev. SIII coding product was cloned into the target vector using XmaI/NotI. Finally, residues 246-353 of the ovalbumin were amplified from pCI/StT-OVA-G using forward primer OVA246 fow and reverse primer pCI rev, and the PCR product was cloned into the target vector using EcoRI/AgeI.

- pCI/St-MO was generated by XhoI digestion of pCI/StT-MO and subsequent ligation of the vector backbone.

- pCI/StT-M was generated using the pCI/StT-PCL as target vector already containing residues 131-160 and 791-832 of the hepatitis B polymerase (P) and residues 79-149 of the HBcAg (C). Residues 2-50 of the HBsAg were amplified by PCR from pCI/S using forward primer S2 fow and reverse primer S50 rev, and the PCR product was subsequently cloned into the target vector using KpnI. Residues 10-50 of the HBcAg were amplified from pCI/Core using forward primer C10 fow and reverse primer C50 rev. The resulting PCR product was cloned into the XmaI/NotI-digested target vector using NheI/NotI, thereby replacing residues 81-106 of the *Listeria monocytogenes* listeriolysin-O (L). Finally, residues 140-226 of the HBsAg were amplified from pCI/S using forward primer S140v2 fow and reverse primer S226v2 rev, and the resulting PCR product was cloned into the target vector using EcoRI/AgeI.

- pCI/St-M was generated by XhoI digestion of pCI/StT-M and subsequent ligation of the vector backbone.

- pCI/StT-SCC encodes the streptavidin-binding tag (St), residues 1-77 of the T-Ag (T), residues 140-226 of the HBsAg (S), residues 79-149 of the HBcAg (C) and residues 10-50 of the HBcAg (C). The vector was generated by cloning the SCC-coding fragment of pCI/StT-M into pCI/R1 [36] using EcoRI/NotI.

2.6. Cell culture techniques

Cell lines and general cell culturing

The Chinese hamster ovary (CHO) cell line (CRL-1772), the human HeLa S3 cell line (CCL-2.2) and the human HEK 293 cell line (CRL-1573) were obtained from the American Tissue Culture Collection (ATCC, Rockville, MD, USA). The RBL-5 derived mutant cell line RMA/S was kindly provided by Dr K. Kärre (Stockholm, Sweden). CHO, HeLa and RMA/S cells were cultured in Clicks/RPMI supplemented with 5% fetal calf serum (FCS), 1% L-glutamine, 1% penicillin/streptomycin and 0.1 M β-mercaptoethanol (β-ME). HEK 293 cells were cultured in DMEM supple-

mented with 10% fetal calf serum (FCS), 1% penicillin/streptomycin and 0.1 M βME. All used cell culture reagents are listed in table 4.

Table 4.: Reagents used for cell culturing

reagent	provider	cat.no.
β-ME	Sigma	M-7522
Clicks/RPMI	Applichem	A2044
DMEM	Gibco	31855-023
FCS	PAA Laboratories	A15-101
G418	PAA Laboratories	P02-12
L-glutamine	PAA Laboratories	M11-004
penicillin/streptomycin	PAA Laboratories	P11-010
RPMI-1640	Gibco	72400-021

Generation of bone marrow-derived dendritic cells (BM-DCs)

BM-DCs were generated as described previously [73]. RPMI-1640 supplemented with 10% FCS, 1% L-glutamine, 1% penicillin/streptomycin and 0.1 M β-mercaptoethanol (β-ME) was used as culture medium. Briefly, femurs and tibiae of 8-12-week-old female C57BL/6J were flushed with culture medium and the obtained bone marrow (BM) was washed twice with culture medium. About 3×10^6 BM cells were seeded per 100 mm petri dish in 10 ml culture medium supplemented with 5% supernatant of a GM-CSF producing cell line. On day four, 5 ml of fresh medium with 5% GM-CSF was added. On day seven, the non-adherent fraction was collected and splitted into two new petri dishes. On day ten, the non-adherent fraction was harvested, analyzed by flow cytometry and used as BM-DCs in further experiments.

Calcium phosphate transfection

HEK 293 cells were transiently transfected with plasmids using the calcium phosphate method. Briefly, HEK 293 cells were grown to 70% confluency and the medium was exchanged about 30 minutes prior transfection. For transfection, 62 µl 2 M Ca_2Cl and 10 µg plasmid DNA were added to total volume of 500 µl ddH_2O and mixed. The solution was added drop by drop to 500 µl of a 2x HBS (280 mM NaCl, 1.5 mM $Na_2HPO_4 \times 2H_2O$, 50 mM Hepes, pH 7.1) under slightly vortexing. Thereafter the

solution is incubated for 90 s at room temperature and added drop by drop to the cells. The medium was exchanged 16 h after transfection to avoid toxic effects of the complexes. The maximum of expression was reached after 36-48 h.

Lipofectamine transfection

Lipofectamine 2000 (cat.no. 11668-027, Invitrogen) was used in accordance with manufacturer's instruction to transiently transfect HeLa cells. In addition, a stably transfected CHO cell line was generated by Lipofectamine 2000 transfection with the episomal vector BMGneo/StT-OVA-G and subsequent selection of stably transfected cells by increasing amounts of G418 (up to 1 mg/ml). The maximum concentration of G418 was added monthly for one week to maintain the episomal construct.

Fluorescence microscopy

To study the intracellular distribution of the constructed antigens, HeLa cells were transfected transiently with the respective plasmid and pCI/Igκ-RFP-SKDEL (a generous gift of Franz Oswald, Internal Medicine I, University of Ulm) as a marker for the endoplasmatic reticulum. 24 h after transfection, the cells were fixed with 2% paraformaldehyde (PFA). Images were aquired using an Olympus IX71 fluorescence microscope.

2.7. Protein analysis

Immunoprecipitation

24 h after transfection, HEK 293 cells were labeled overnight using 100 µCi [^{35}S]-methionine/cysteine (cat.no. IS103, Hartmann Analytic GmbH) in 3 ml methionine/ cysteine-free RPMI-1640 (cat.no. P04-18056, PAN) supplemented with 5% dialyzed FCS, 1% penicillin/streptomycin and 1% L-glutamine. Labeled cells were washed once with PBS and subsequently lysed by the addition of lysis buffer (100 mM TrisHCl pH 8.0, 150 mM NaCl, 0.5% NP40, 0.25% Trasylol, 1 µg/ml leupeptin). Complete lysis of cells was achieved by shaking for 30 min on ice. Extracts were cleared by centrifugation (30 min, 20.000 x g, 4°C) and incubated for 1 h at 4°C with the monoclonal antibody Pab108. Thereafter, the immune complexes were incubated for

1 h at 4°C with protein A sepharose (PAS, cat.no. 17-0780-01, Pharmacia). Strep-tagged antigens lacking the Pab108 recognition site were precipitated by incubating cleared lysates for 2 h at 4°C with StrepTactin sepharose (cat.no. 2-1201-025, IBA). Incubation was followed by five washes with washing buffer (100 mM TrisHCl pH 8.5, 500 mM LiCl, 0.5% NP40), followed by two washes using PBS and 0.1x PBS. Antigens were recovered from sepharose beads by incubation for 1 h at 37°C with elution buffer (7 mM TrisHCl, 1.5% SDS, 5% β-ME). Eluats were frozen at −80°C and lyophilized for SDS-PAGE.

SDS-PAGE

Lyophilized samples derived of immunoprecipitation were dissolved in 30 µl loading buffer (10% glycerol and bromphenol blue, 5% β-ME). Along with the samples 8 µl of [^{14}C]-marker (cat.no. CFA756-1UCI, GE Healthcare) and 22 µl loading buffer were mixed and boiled for 3 min. 10 µl of each sample were loaded onto SDS-polyacrylamide gels and the electrophoresis was performed at 60 V till the samples reached the resolving gel. The voltage was subsequently increased to 120 V. The gel was stained for 15 min using CoomassieBlue staining solution (1.2 g CoomassieBlue, 450 ml methanol, 90 ml acetic acid, 460 ml ddH_2O). Gels were destained for 15 min with destaining solution (10% methanol, 10% isopropanol, 80% ddH_2O). Gels processed for later fluorography were dehydrated for 10 min in acetic acid and subsequently incubated for 10 min in enhancer solution (10% (w/v) PPO in acetic acid). PPO was precipitated by incubating the gel for 15 min in ddH_2O. The gel was subsequently dried by vacuum at 80°C for 1 h. The dried gel was placed in a cassette with a radiography film (cat.no. 28-9068-44, GE Healthcare). Fluorography time depended on the signal intensity.

30 µl of non-lyophilized samples derived of protein purification were mixed with 10 µl loading buffer (30% glycerol and bromphenol blue, 20% β-ME, 4% (w/v) SDS) and boiled for 3 min. SDS-PAGE was performed as described above. The gel was either stained with CoomassieBlue or stained with SyproOrange (cat.no. S-6650, Invitrogen) according to manufacturer's instructions. SyproOrange stained gels were visualized using UV light and analyzed using the GeneGenius system (Syngene).

Western blot

After SDS-PAGE, the gel was incubated for 10 min in equilibration buffer (20 mM Tris acetate pH 8.3, 0.1% SDS). Proteins were blotted onto nitrocellulose membrane at 60 V for 90 min using transfer buffer (20mM Tris acetate pH 8.3, 20% isopropanol, 0.1% SDS) and Mini Trans-blot cell (Biorad). The membrane was subsequently incubated for 30 min in 50% isopropanol, for 10 min in water and for 15 min in TBS (15 mM TrisHCl pH 7.8, 150mM NaCl, 5mM NaN3, 1mM EDTA). To block the remaining available binding sites, the blot was incubated overnight in blocking buffer (TBS, 0.1% gelatine, 100 µg/ml Ig-free BSA). The membrane was washed 30 min using buffer GT (TBS, 0.1% gelatine, 0.1% Tween 20). Afterwards, the nitrocellulose was incubated for 90 min with the primary antibody. Unbound antibody was removed by three washes with buffer GT. In case of mouse- or rat-derived primary antibody, the membrane was incubated for 90 min with a second antibody (developed in rabbit), followed by three washes with buffer GT. Thereafter the nitrocellulose was incubated for 90 min with an HRP-labeled donkey anti-rabbit antibody, followed by three washes with buffer GT and PBS. The membrane was dried and the HRP detection reagent (cat.no. WBKLS0050, Millipore) was applied as recommended by the manufacturer. After drying, the membrane was placed in a cassette with a radiography film. All antibodies used for Western blot analysis are listed in table 5.

Table 5.: Antibodies used for Western Blot

specificity	**type**	**host**	**company**	**cat.no.**
anti-DnaK	monoclonal	mouse	Stressgen	SPA-880
anti-GFP	polyclonal	rabbit	Abcam	AB290
anti-HBcAg	polyclonal	rabbit	gift of Dr. H.-J. Schlicht, Ulm	
anti-Hsp70	monoclonal	mouse	Stressgen	SPA-810
anti-Hsp73	monoclonal	rat	Stressgen	SPA-815
anti-mouse IgG	polyclonal	rabbit	Sigma	M-6024
anti-preS1 (MA18/7)	monoclonal	mouse	gift of Dr. W. H. Gerlich, Giessen	
anti-rat IgG	polyclonal	rabbit	Rockland	612-4102
anti-Strep-tag	monoclonal	mouse	IBA GmbH	2-1507-001
anti-T-Ag	polyclonal	rabbit	self-produced	
HRP-labeled anti-rabbit IgG	polyclonal	donkey	GE Healthcare	NA934V

2.8. Production of native Hsp/antigen complexes

Purification of native Hsp/antigen complexes

Cells were lysed by the addition lysis buffer (100 mM TrisHCl pH 8.0, 150mM NaCl, 0.5% NP40, 0.25% Trasylol, 1 µg/ml leupeptin) and shaking on ice for 30 min. Afterwards, lysates were cleared by centrifugation (30 min, 20.000 x g, 4°C) and passed over StrepTactin sepharose packed polypropylene columns (cat.no. 29922/4, Pierce). Unspecific bound proteins were removed by five column volumes of wash buffer (100 mM TrisHCl pH 8.0, 150 mM NaCl). Hsp-complexed antigen was eluted in 500 µl fractions by elution buffer (PBS, 2.5 mM desthiobiotin).

To purify both complexing Hsp and antigen, bound Hsp/complexed antigens were washed prior antigen elution with an additional column volume Hsp elution buffer (wash buffer, 10 mM ATP). Flow-through containing eluted Hsp was collected in 500 µl fractions, followed by an additional column volume wash buffer. Bound uncomplexed antigen was eluted as described above.

Desthiobiotin and ATP were removed by NAP-5 columns (cat.no. 17-0853-02, GE Healthcare) and antigens were subsequently concentrated by centrifugation in Vivaspin 500 columns (cut off 5.000 MW, cat.no. VS0112, VivaScience).

Adenoviral-based expression system

An adenoviral-based expression system was established in cooperation with the Unit of Gene Therapy, University of Ulm. Briefly, the used adenovirus vector described is an Ad5-based, E1-deleted, first generation vector. pAd/StT-OVA-G is an infectious adenovirus plasmid carrying in place of the deleted E1 region the hCMV-promotor-controlled StT-OVA-G coding unit from the pCI/StT-OVA-G vector. Generation and purification of recombinant Ad virions was performed as described previously [136]. HeLa cells adapted to suspension culture were cultivated in DMEM (supplemented with penicillin/streptomycin, L-glutamine and 7% FCS) under constant stirring. At a cell density of 2×10^6 cells/ml in a total volume of 1 l, cells were centrifuged at 400 x g, resuspended in 500 ml supplemented DMEM, and adenovirus vector was added at a concentration of 50 infectious MOI (50 infectious particles per cell). After 2 h of constant stirring, the medium was filled up to 1 l and cells were cultivated for additional 48 h before processing.

Bacterial expression system

A bacterial inducible expression system was established by cloning a modified StT-OVA-G coding unit from pCI/StT-OVA-G vector into the IPTG inducible bacterial expression vector pQE-9 and transforming *E. coli* Rosetta gami. Transformed *E. col*i Rosetta gami were grown in TB medium (17 mM KH_2PO_4, 72 mM K_2HPO_4, 1.2% (w/v) bactotryptone, 2.4% (w/v) yeast extract, 4% glycerol) in the presence of 50 µg/ml kanamycin, 100 µg/ml ampicillin and 50 µg/ml chloramphenicol. Antigen expression was induced overnight by addition of 1 mM IPTG. Bacteria were harvested by centrifugation, washed, incubated in lysis buffer (100 mM TrisHCl pH 8.0, 150 mM NaCl, 0.5% NP40) containing lysozyme (cat.no. 107255, Boehringer Mannheim) for 30 min at 4°C and finally sonicated. Cleared lysates were processed for Strep-tag purification as described above.

2.9. Vaccination

Unless otherwise noted, mice were immunized into the tibialis anterior muscles (50 µl per muscle) with 100 µl PBS containing 100 µg plasmid DNA. Where indicated, mice were boosted three weeks after first injection with the same dose of plasmid DNA.

In case of vaccination with recombinant proteins, mice were immunized with the indicated amounts of protein and –if indicated– mixed with 25 µl (per mouse) AbISCO-100 adjuvant (cat.no. 20-0100-10, Isconova). In general, a boost vaccination with the same dose of protein and adjuvant was performed three weeks after first immunization.

2.10. DNA isolation and Southern blot analysis

Tissues were frozen, homogenized in a grinder and lysed with buffer containing 100 µg/ml proteinase K (cat.no. 83767023-58, Roche). DNA was extracted with standard procedures and treated for 3 h at 37°C with RNase (cat.no. 109169, Roche). 30 µg DNA were digested with HindIII and separated by agarose gel electrophoresis. DNA was transferred to a nylon membrane by capillar blotting. Plasmid pHBV-1 containing a full-length HBV genome (kindly provided by F. Chisari) was digested with EcoRI and PvuI. The 3.2 kb HBV DNA fragment was isolated and used as tem-

plate for the generation of a HBV-specific probe. α^{32}P-dCTP labelled HBV probe was generated using the High Prime DNA Labeling Kit (cat.no. 11585584001, Roche) according to the manufacturer's instructions. Hybridization was done overnight at 42°C. After washing, the blots were exposed and quantitative analyses of relative abundance of specific DNA molecules were performed using phosphor imaging Fujifilm FLA-3000 and the Aida Image Analyzer v3.52 software (Raytest, Germany).

2.11. Detection of HBsAg, HBeAg and transaminases in serum

Serum HBsAg concentrations were determined using ELISA AUSZYME II (Abbott Laboratories). Serum HBeAg was analyzed by ECLIA (cat.no. 11820583, Roche) using the Elecsys 2010 (Roche). The cut-off is calculated by using a negative and positive sample for calibration. Samples with a cutoff-index (COI) < 1 are negative for HBeAg, and > 1 are positive for HBeAg. Serum alanine aminotransferase (ALT) activity was determined using the Reflotron test (cat.no. 745138, Roche).

2.12. Histology

Thin slides of liver tissue (< 3 mm) were fixed in 4% formalin (pH 7.0) for 24 h and embedded in paraffin. 2 µm thick paraffin sections were stained with hematoxylin-eosin (H&E).

2.13. Determination of antigen-specific antibody response

Blood samples were obtained from immunized mice by tail bleeding at the indicated time points post-vaccination. Serum was derived of blood samples by centrifugation (60 min, 20.000 x g) and collection of supernatant. GFP-specific serum antibodies were detected by end point dilution ELISA. Briefly, MicroELISA plates (cat.no. 442404, Nunc) were coated overnight with 150 ng GFP (a generous gift of Andreas Schreiber, Department of Virology, University of Ulm) per well in 50 µl

coating buffer (0.1 M Na_2CO_3 pH 9.5) at 4°C. The plates were washed twice with washing buffer (PBS, 0.05% Tween 20) and incubated for 2 h at room temperature with blocking buffer (PBS, 3% (w/v) BSA). After five washes using washing buffer, serial dilutions of the sera (prepared in blocking buffer) were added to the coated wells, incubated for 3 h at room temperature and washed five times with washing buffer. Bound serum antibodies were detected using HRP-conjugated rat anti-mouse IgG, IgG1, IgG2a, IgG2b Abs (BD Pharmingen) at a dilution of 1/2000 in blocking buffer. After 1 h incubation with detection antibodies and five washes with washing buffer, each well was incubated with 100 µl o-phenylenediamine x 2 HCl (cat.no. 6172-24, Abbott Laboratories) for 15 min at room temperature in the dark. The reaction was stopped by the addition of 100 µl 1 M H_2SO_4 and the extinction was determined at 492 nm and 620 nm. End point titers were defined as the highest serum dilution resulting in an absorbance value three times greater than control serum (derived of a non-immunized mouse).

2.14. Analysis of surface marker profile

To determine the surface marker profile, cells were washed once with FACS buffer A (PBS, 0.5% (w/v) BSA, 0.1% (w/v) NaN_3) and incubated for 20 min at 4°C with anti-CD16/CD32 mAb to block unspecific binding of detection antibodies to Fc receptors. Cells were washed once using FACS buffer A and incubated for 30 min at 4°C with 0.5 µg/10^6 cells of the respective PE-labeled mAbs. Cells were washed twice using FACS buffer A, fixed in 2% paraformaldehyde (PFA) and analyzed by FCM using FACSCalibur (BD Bioscience) and WinMDI software. All antibodies used for FCM are listed in table 6.

2.15. Determination of antigen-specific CD8 T cells

Preparation of splenocytes

If not indicated otherwise, mice were sacrificed at day 12 post-vaccination and spleens were removed. Splenocyte suspensions were prepared by rubbing spleens in 10 ml PBS + 1% FCS through a sterile mesh. Erythrocytes were removed by lysis buffer (144 mM NH_4Cl, 17 mM Tris, pH 7.2). Splenocytes were washed twice with PBS + 1%

Table 6.: Antibodies/reagents used for FCM. All listed antibodies and reagents were purchased from BD Pharmingen.

antibody/reagent	conjugation	clone	cat.no.
anti-B220	PE	RA3-6B2	553089
anti-CD11b	PE	M1/70	553311
anti-CD11c	PE	HL3	553802
anti-CD16/CD32		2.4G2	553142
anti-CD8	PE	53-6.7	553033
anti-CD8	FITC	53-6.7	553031
anti-CD80 (B7-1)	biotin	16-10A1	553767
anti-CD86 (B7-2)	biotin	GL1	553690
anti-H-2K^b	PE	AF6-88.5	553570
anti-I-A^b	PE	AF6-120.1	553552
anti-IFNγ	FITC	XMG1.2	554411
streptavidin	PerCP		554064

FCS and cell clumps were removed by pipetting. Splenocytes were resuspended in UltraCulture (cat.no. 12-725F, Cambrex) supplemented with 1% L-glutamine and 1% penicillin/streptomycin.

Isolation of liver non-parenchymal cells

To obatin the liver non-parenchymal cell (NPC) population, livers of sacrificed mice were perfused with liver perfusion medium (LPM, cat.no. 17701-038, Gibco) and liver digest medium (LDM, cat.no. 17703-034) in vivo. The livers were removed, cut into pieces and digested for 30 min at 37°C in LDM. Liver suspensions were prepared by rubbing livers through a sterile mesh. NPCs were separated from parenchymal hepatocytes by centrifugation at 500 rpm for 5 min. NPCs were collected, washed with PBS and resuspended in 40% Percoll (cat.no. L6145, Biochrom). The NPC suspension was gently overlaid onto 70% Percoll and centrifuged at 2000 rpm for 20 min. NPCs were collected from the interphase and erythrocytes were removed by lysis buffer. NPCs were washed once with PBS + 1% FCS and subsequently resuspended in supplemented UltraCulture.

Determination of antigen-specific CD8 T cell frequencies

2×10^6 splenocytes were washed once using FACS buffer A (PBS, 0.5% (w/v) BSA, 0.1% (w/v) NaN_3) and incubated for 20 min at 4°C with anti-CD16/CD32 to block unspecific binding of anti-CD8 mAb to Fc receptors. Cells were washed once and incubated for 30 min at 4°C with FITC-conjugated anti-CD8 mAb (diluted 1/200) and PE-conjugated MHC-I:peptide tetramers/pentamers. After three washes, stained cells were fixed with 2% PFA and frequencies of tetramer/pentamer$^+$ CD8 T cells were determined by FCM. Used MHC-I:peptide tetramers/pentamers are listed in table 7.

Table 7.: MHC-I:peptide tetramers/pentamers used for FCM

antigen	designation	conjugation	company	cat.no.
HBcAg	H2-K^b/C_{93-100}	PE	Beckman Coulter	
HBsAg	H2-K^b/$S_{190-197}$	PE	Beckman Coulter	
Influenza A MP	A*0201/Flu-Ma_{58-66}	PE	ProImmune	F007-2A
ovalbumin	H2-K^b/$OVA_{257-264}$	PE	ProImmune	F093-2A

Determination of antigen-specific IFNγ-producing CD8 T cells

Splenocytes (1×10^7/ml) were incubated with 2.5 µg/ml antigenic peptide in supplemented UltraCulture for 4 h at 37°C. Additionally, 5 µg/ml brefeldin A (BFA; cat.no. 15870, Sigma) were added to block anterograde protein transport from the endoplasmatic reticulum (ER) to the Golgi apparatus, thereby leading to intracellular accumulation of produced IFNγ. After the 4 h restimulation, cells were washed once using FACS buffer A and incubated for 20 min at 4°C with anti-CD16/CD32 to block unspecific binding of anti-CD8 mAb to Fc receptors. Cells were washed once and incubated for 30 min at 4°C with PE-conjugated anti-CD8 mAb (diluted 1/200). After three washes, surface stained cells were fixed with 2% PFA for 20 min at room temperature. Thereafter, the fixed cells were washed once and prepared for intracellular staining by incubation with permeabilization buffer (PBS, 0.5% (w/v) BSA, 0.5% (w/v) Saponin, 0.05% (w/v) NaN_3) for 15 min at room temperature. Permeabilized cells were incubated with FITC-conjugated anti-IFNγ mAb (diluted 1/200) for 30 min at room temperature to detect accumulated IFNγ. After three washes with

permeabilization buffer, stained cells were resuspended in FACS buffer A, IFNγ^+ CD8 T cells were determined by FCM. In general, the mean numbers of splenic IFNγ^+ CD8/10^5 CD8 T cells of at least 3 mice are shown.

2.16. Determination of K^b-binding affinities

K^b-binding affinities of epitopes were determined by competition for empty MHC-I molecules with the characterized $K^b/OVA_{257-264}$ peptide and subsequent co-culture of peptide-pulsed cells with $K^b/OVA_{257-264}$-specific CD8 T cells. In order to enhance the amount of empty MHC-I molecules at the cell surface RMA/S were cultured for 24 h at 37°C in serum-free medium (UltraCulture) prior peptide pulsing. 2×10^4 RMA/S were pulsed with titrated amounts of the $K^b/OVA_{257-264}$ peptide in order to generate a dose-response curve. In addition, RMA/S cells were incubated with titrated amounts of the $K^b/S_{190-197}$, the $K^b/S_{208-215}$ or K^b/C_{93-100} peptide in the presence of 5 nM $K^b/OVA_{257-264}$ peptide thus competiting for empty K^b molecules. After two washes with PBS, 2×10^4 pulsed cells were incubated in UltraCulture with 1×10^5 splenic CD8 T cells isolated from OT-I RAG mice using the MACS CD8α^+ T cell isolation kit (cat.no. 130-090-859, Milenyi Biotec) according to the manufacturer's protocol. Supernatants were collected after 20 h of co-culturing at 37°C and analyzed for IFNγ.

2.17. Detection of IFNγ by ELISA

INFγ was detected by conventional double-sandwich enzyme-linked immunosorbent assay (ELISA). MicroELISA plates (cat.no. 442404, Nunc) were coated overnight with 50 ng anti-IFNγ antibody (cat.no. 551216, BD Biosciences) diluted in coating buffer (1 M $Na_2HPO_4 \times 2H_2O$ pH 9.0) at 4°C. The plates were blocked for 1 h at room temperature with blocking buffer (PBS, 3% (w/v) BSA) in order to avoid unspecific binding. After two washes using washing buffer (PBS, 0.05% Tween 20), samples and IFNγ standards (cat.no. 554587, BD Biosciences) were added to the wells, incubated for 3 h at room temperature and washed four times with washing buffer. Bound IFNγ was detected by addtion of 50 ng biotinylated anti-IFN antibody (cat.no. 554410, BD Biosciences) diluted in blocking buffer and incubation for 1 h at room

temperature. After six washes with washing buffer, 50 ng streptavidin-conjugated alkaline phosphatase (SAP) (cat.no. 016-050-084, Jackson ImmunoResearch) were added for 30 min at room temperature. After eight washes with wash buffer, the SAP substrate nitrophenyl phosphated disodium salt (cat.no. 71768, Fluka) disolved in diethanolamine buffer (10.3% (v/v) diethanolamine, 3.9 mM $MgCl_2 \times 6H_2O$, 3 mM NaN_3) was added to the plates. The enzymatic reaction was stopped after 5-15 min by addition of 0.5 mM EDTA (pH 8.0). Extinction was analyzed at 405/490 nm using a TECAN micro plate reader (TECAN, Crailsheim, Germany) and EasyWin software (TECAN).

2.18. Statistics

Statistic analyses were performed using GraphPad Prism (Version 4, GraphPad Software Inc.). Figures show mean values and SEM (standard error of the mean). Significant differences are indicated with the P value determined by an unpaired t test, whereas a $P < 0.05$ is considered significantly different. If not indicated otherwise, figures show data of one representative experiment (of at least three independent replicates).

3. Results

3.1. Characterization of Hsp-complexed antigens

3.1.1. Construction and expression of Hsp-capturing antigens

We developed a system in which the Hsp-capturing J domain of the SV40 virus is N-terminally fused to different antigenic domains. The Hsp-binding T_{1-77} J domain of the T-Ag contains four α-helices forming a finger-like structure with an exposed conserved HPD motif on the tip of a loop (figure 3a). A chimeric model antigen pCI/T_{77}-SFG was designed consisting of residues 1-77 of the T-Ag (T), residues 140-226 of the HBsAg, residues 58-66 of the influenza A matrix protein and the entire sequence of eGFP (figure 3b).

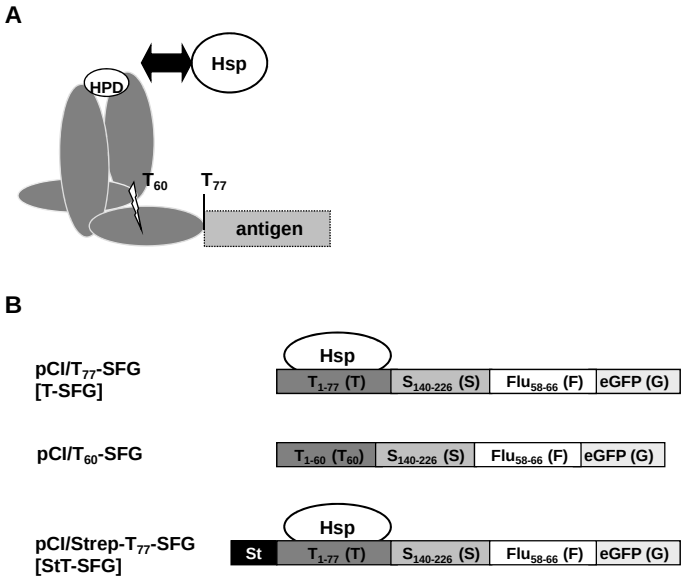

Figure 3.: Hsp-mediated antigen expression system. **a** Schematic presentation of the finger-like structure with the exposed HPD motif and the C-terminally fused antigen. **b** Designation and schematic presentation of the cloned chimeric antigens.

Transient transfection of HEK 293 cells with pCI/T_{77}-SFG and subsequent immunoprecipitation with an anti-T-Ag mAb revealed that a product of the expected size of about 40 kDa was efficiently expressed. An additional band representing the captured Hsp was efficiently co-precipitated (figure 4, lane b). When the correct formation of the helical loop structure of the J domain was impaired (by shortening the N-terminal J domain from 77 residues to 60 residues, T_{1-60}), the chimeric protein lost its ability to capture Hsp in situ. The loss of the Hsp-binding capability resulted also in a non-detectable expression level of the antigen (figure 4, lane c). The N-terminal addition of a Strep-tag used for purification altered neither the Hsp-binding capability of the J domain, nor the recognition of the J domain by the anti-T-Ag mAb, nor the overall expression level of the chimeric antigen (figure 4, lane d). Despite the accumulation of high steady-state levels of Hsp/antigen complexes, no secretion of the chimeric proteins was detected.

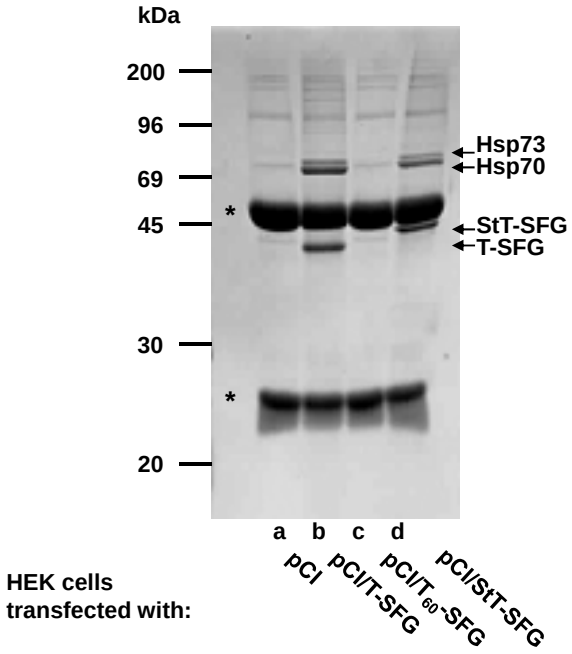

Figure 4.: Hsp-facilitated antigen expression system. HEK 293 cells were transiently transfected with pCI (lane a), pCI/T-SFG (lane b), pCI/T60-SFG (lane c), or with pCI/StT-SFG (lane d). Cells were immunoprecipitated with anti-T-Ag mAb and analyzed by SDS-PAGE and Coomassie Blue staining. The positions of the T-SFG and StT-SFG fusion proteins and the Hsp70/73 are indicated. The IgG/HC or IgG/LC of the anti-T-Ag mAb is indicated by an asterik.

The N-terminal Strep-tag could thus be used for purification of chimeric antigens. HEK 293 cells were transiently transfected with pCI/StT-SFG and the chimeric protein was purified with the StrepTactin system from cell lysates. Affinity purification using the N-terminal Strep-tag resulted in ($\geq$ 90% purity) native Hsp/antigen complexes (figure 5a). Therefore, the N-terminal Strep-tag offers the novel possibility to purify in vivo pre-formed Hsp/antigen complexes in a native form. SDS-PAGE analyses of purified Hsp/antigen complexes produced in the human HEK 293 cell line revealed two distinct protein bands of apparent 70 kDa (figure 5a). Western Blot analyses of purified Hsp/StT-SFG complexes identified two different human Hsp molecules complexed with StT-SFG: a major band representing inducible Hsp70, and a minor band representing constitutively expressed Hsp73 (figure 4, figure 5b). Thus, the viral J domain is able to capture different human Hsp70 molecules.

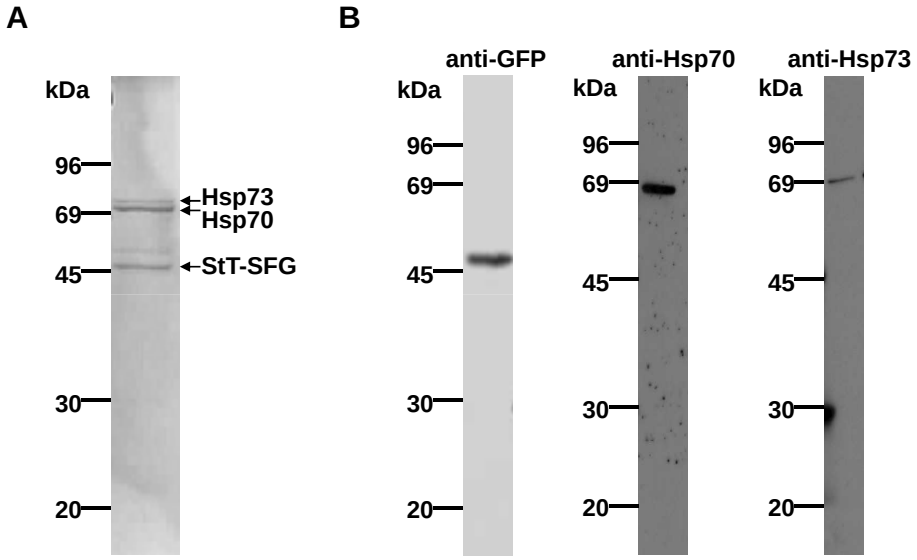

Figure 5.: Purification of in vivo preformed Hsp/antigen complexes. **a** HEK 293 cells were transiently transfected with pCI/StT-SFG, lysed and immunopurified with a StrepTactin column followed by release of complexes with desthiobiotin. Purified Hsp/antigen complexes were denatured and analyzed by SDS-PAGE and Coomassie Blue staining. The positions of the ST-SFG fusion proteins and the Hsp70/73 are indicated. **b** Purified Hsp/antigen complexes were denatured, analyzed by SDS-PAGE and GFP-, Hsp70- and Hsp73-specific Western blotting.

The intracellular localization of Hsp/StT-SFG complexes was analyzed using fluorescence microscopy of transiently transfected HeLa cells. Hsp/StT-SFG complexes showed cytoplasmatic localization and no colocalization with the ER (figure 6), sup-

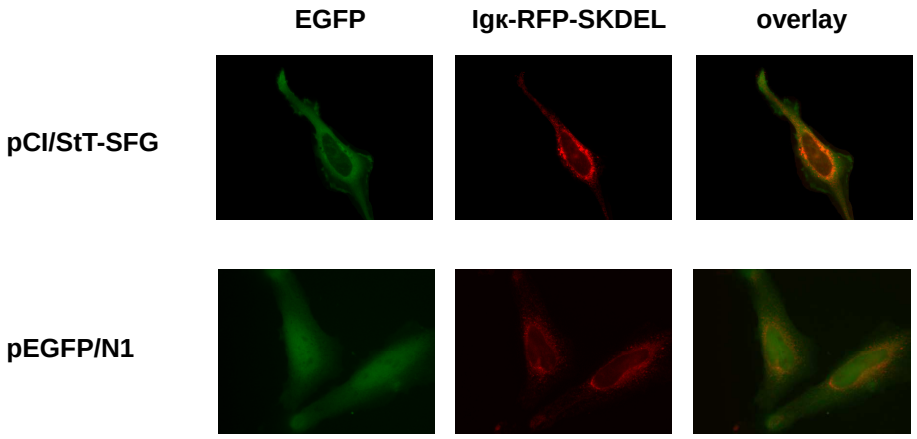

Figure 6.: Intracellular localization of Hsp/antigen complexes. HeLa cells were transiently transfected with the ER-marker pCI/Igκ-RFP-SKDEL and pEGFP/N1 or pCI/StT-SFG and fixed. Images were aquired using an Olympus IX71 fluorescence microscope.

porting the observation of non detectable secretion of Hsp-complexed antigens. In contrast, eGFP (pEGP/N1) showed an ubiquitous localization pattern with cytosolic and nuclear accumulation. Therefore, the Hsp-association retains complexed antigens in the cytoplasm and prevents their shuttling into other cellular compartments (e.g. nucleus, ER). In addition, the fluorescence intensity of eGFP was dramatically lowered by complex formation with Hsp. Spectra analysis of purified eGFP protein and Hsp/StT-SFG complexes revealed a significantly quenched fluorescence intensity of Hsp-complexed StT-SFG (figure 7).

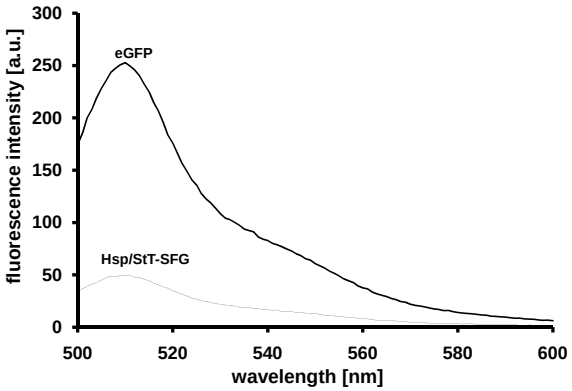

Figure 7.: Quenching of fluorescence by Hsp-association. Spectra of the purified Hsp/StT-SFG complexes and bacterial-derived recombinant eGFP proteins were determined using the ND-3300 Fluororspectrometer Nanodrop according to the manufacturer's instructions.

3.1.2. Immunogenicity of recombinant Hsp-complexed antigens

To explore the immunogenicity of recombinant Hsp-complexed antigens, a chimeric model antigen pCI/StT_{77}-OVA-G was designed consisting of a N-terminal Strep-tag, residues 1-77 of the T-Ag, residues 246-353 of ovalbumin (OVA) and eGFP(figure 8). For large scale production of Hsp/StT-OVA-G, an adenoviral expression systems was

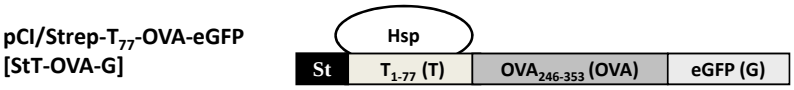

Figure 8.: Schematic presentation of the Hsp-binding StT-OVA-G protein

developed. Therefore, human HeLa spinner cell cultures were transduced with a recombinant adenovirus encoding the StT-OVA-G fusion protein (Ad/StT-OVA-G). Lysates of infected cells were purified using the StrepTactin system. Combination of the adenoviral expression system and the StrepTactin-based purification resulted in the production of high amounts of pure ($\geq$ 95% purity) Hsp-complexed recombinant proteins (figure 9). About 1-2 µg StT-OVA-G protein complexed with Hsp70/73 could be purified from 1×10^6 HeLa cells. The Hsp-facilitated expression system can thus be used to selectively purify either native Hsp/antigen complexes (figure 9, fractions 1-6), or its isolated components (figure 9, right panel). The complexed Hsp70/73 could be gently and quantitatively released from StrepTactin-bound antigen by treatment with ATP (figure 9, fractions 1*-4*). The uncomplexed StT-OVA-G protein was then released from the column by desthiobiotin (figure 9, fractions 1#-4#).

Purified, HeLa cell-derived Hsp/St-OVA-G complexes were used as protein-based vaccine to prime $K^b/OVA_{257-264}$-specific CD8 T cell in B6 mice. Two injections of a low dose (2 µg per mouse) of purified, recombinant Hsp/StT-OVA-G complexes without further adjuvants efficiently induced $K^b/OVA_{257-264}$-specific CD8 T cells readily detectable by either $K^b/OVA_{257-264}$ pentamers or 4 h ex vivo restimulation of primed splenocytes with the $K^b/OVA_{257-264}$ peptide (figure 10, group 1). Vaccination of mice with either purified StT-OVA-G fusion protein (not associated with Hsp), or equimolar amounts of purified StT-OVA-G fusion protein and purified Hsp didn't induce CD8 T cell responses (figure 10, group 2 and 3). Thus, immunization of mice with Hsp/StT-OVA-G complexes efficiently induced antigen-specific CD8 T cell responses demonstrating that Hsp-association of antigens is essential for CD8 T cell priming.

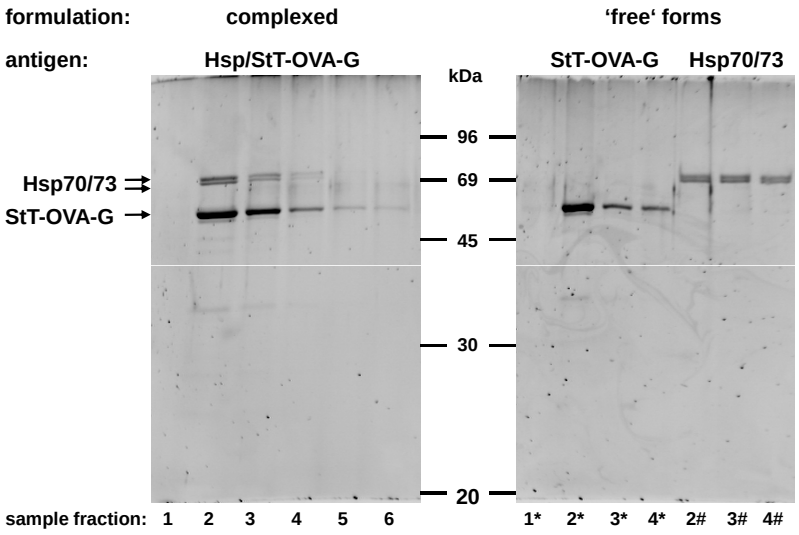

Figure 9.: Production of Hsp-complexed antigen or single antigen. HeLa spinner cells were transduced with Ad/St-OVA-G virus and cleared lysates were purified using StrepTactin system. StrepTactin bound Hsp/StT-OVA-G complexes were either directly eluted with elution buffer (fractions 1-6), or Hsp was eluted with an ATP-containing buffer (fraction 1*-4*) prior elution of single StT-OVA-G with elution buffer (fractions2#-4#). Samples were prepared for SDS-PAGE and gels were stained with SyproOrange. The positions of the StT-OVA-G protein and the Hsp70/73 are indicated.

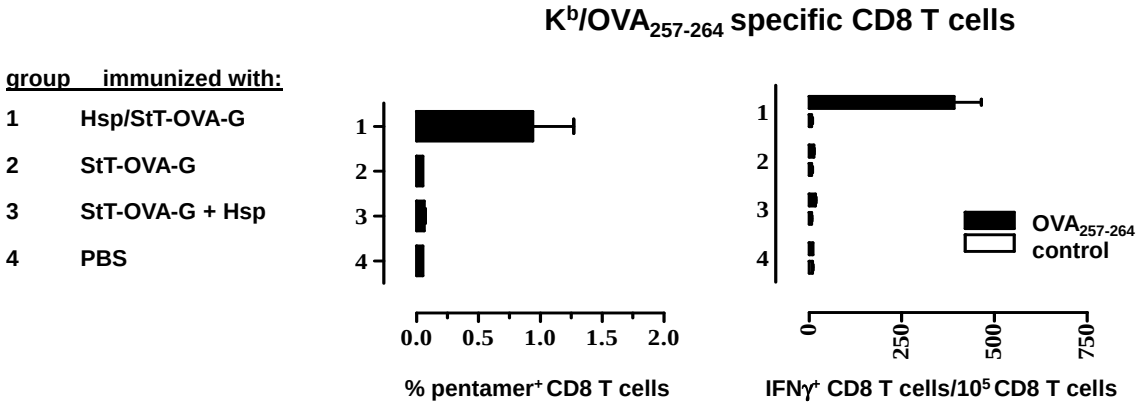

Figure 10.: Induction of $K^b/OVA_{257-264}$-specific CD8 T cell responses by recombinant Hsp/antigen complexes. B6 mice (five mice per group) were immunized with 2 µg HeLa-derived StT-OVA-G protein either complexed with Hsp70/73 (group 1) or not (group 2), a mixture of 2 µg StT-OVA-G protein and equimolar amounts of purified Hsp70/73 (group 3), or injected with PBS as control (group 4). Mice were boosted after three weeks by intramuscular injection of the same dose of the same vaccine. Twelve days after boost, $K^b/OVA_{257-264}$-specific CD8 T cells were determined by $K^b/OVA_{257-264}$-specific pentamer staining of splenic CD8 T cells(left panel) or by 4 h ex vivo stimulation with $K^b/OVA_{257-264}$ peptide, followed by determination of IFNγ^+ CD8 T cell frequencies.

To test whether the Hsp-facilitated priming of CD8 T cells is independent of CD4 T cells, MHC-II deficient mice ($A\alpha^{-/-}$) were immunized by two injections of a low dose (2 µg per mouse) of purified, recombinant Hsp/StT-OVA-G complexes or ovalbumin. Immunization of $A\alpha^{-/-}$ with Hsp/StT-OVA-G complexes induced $K^b/OVA_{257-264}$-pentamer specific CD8 T cells (figure 11, group 2). Thus, the general priming of $K^b/OVA_{257-264}$-specific CD8 T cells after immunization with Hsp/StT-OVA-G complexes was independent of CD4 T cells. However, immunization with Hsp/StT-OVA-G complexes in the absence of CD4 T cells induced reduced numbers of $K^b/OVA_{257-264}$-pentamer specific CD8 T cells compared to B6 mice (figure 11, group 2). Neither B6 nor $A\alpha^{-/-}$ mice were able to generate detectable levels of $K^b/OVA_{257-264}$-specific CD8 T cell in response to ovalbumin (figure 11, group 3).

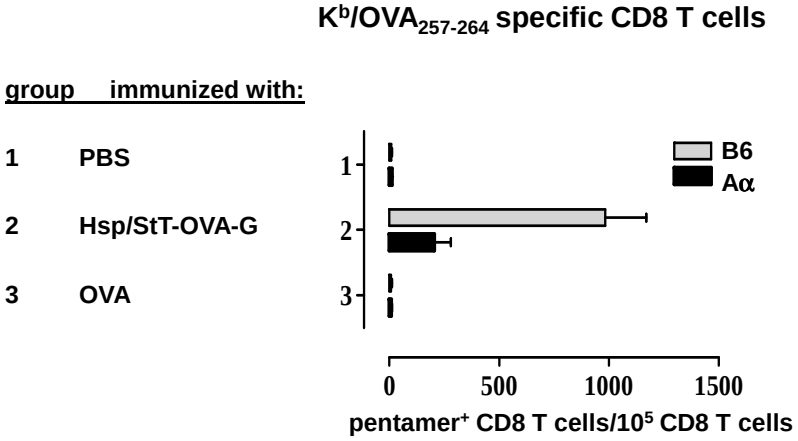

Figure 11.: CD4 T cell independent priming of CD8 T cells by Hsp/antigen complexes. B6 or $A\alpha^{-/-}$ mice (three mice per group) were immunized with PBS (group 1), 2 µg HeLa-derived Hsp/StT-OVA-G complexes (group 2) or 2 µg ovalbumin (group 3). Mice were boosted after three weeks by intramuscular injection of the same dose of the same vaccine. Twelve days after boost, $K^b/OVA_{257-264}$-specific CD8 T cells were determined by $K^b/OVA_{257-264}$-specific pentamer staining of splenic CD8 T cells.

Immunization with Hsp/StT-OVA-G complexes efficiently induced antigen-specific antibodies against the StT-OVA-G fusion protein and recombinant eGFP in a Western blot assay (figure 12b). However, antibodies against Hsp70/73 couldn't be detected (figure 12b). Uncomplexed StT-OVA-G fusion protein induced only a weak eGFP-specific antibody response, which could be hardly detected by Western blotting. Thus, Hsp/antigen complexes efficiently induced antigen-specific antibodies demonstrating that Hsp-association also facilitates humoral immune responses.

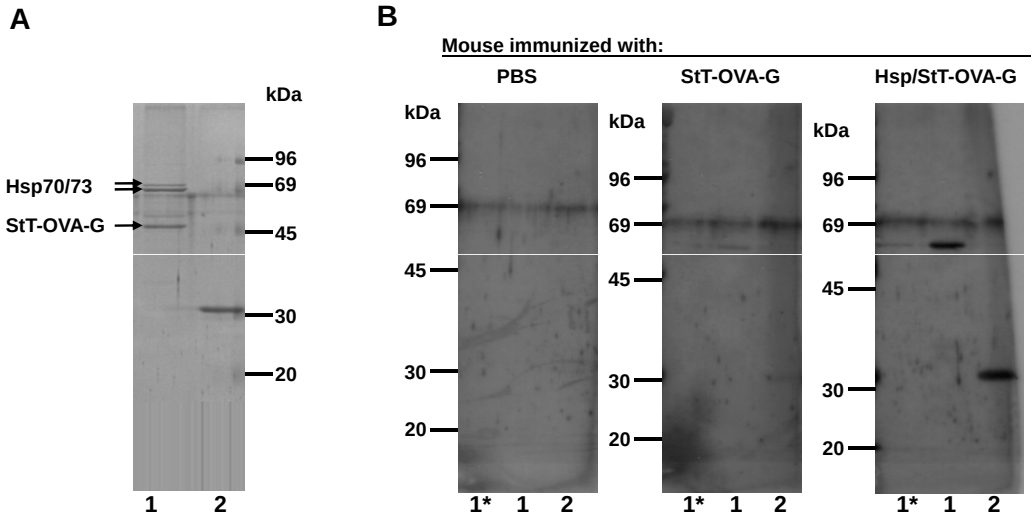

Figure 12.: Hsp/antigen complexes efficiently induced antigen-specific antibodies. **a** 0.5 µg HeLa-derived Hsp/StT-OVA-G complexes (lane 1)and 1 µg bacterial-derived recombinant eGFP (lane 2) were analyzed by SDS-PAGE and Coomassie Blue staining. **b** 0.05 µg (lanes 1*), 0.5 µg HeLa-derived Hsp/StT-OVA-G complexes (lanes 1)and 1 µg bacterial-derived recombinant eGFP (lane 2) were analyzed by SDS-PAGE and Western blotting. Blotted proteins were detected by using sera obtained from B6 mice immunized twice with PBS, 2 µg StT-OVA-G or 2 µg Hsp/StT-OVA-G. Sera were collected twelve days after boost.

To further characterize the Hsp-mediated adjuvant effect on the cellular (figure 10) as well as humoral immune response (figure 12), the isotype profile of eGFP-specific IgG antibodies was analyzed by ELISA. The bulk of the eGFP-specific antibody response consisted of IgG1 antibodies, whereas only a minor IgG2 subset was detectable. Immunization with Hsp/StT-OVA-G complexes thus shifted the immune responses towards a Th2 profile characterized by a high IgG1/IgG2 ratio (figure 13). The Th2 profile induced by Hsp/StT-OVA-G complexes thus demonstrates that Hsp70/73 has no intrinsic, innate adjuvant activity.

Immunization with low doses of Hsp/antigen complexes without further adjuvants efficiently induced CD8 T cell responses (figure 10, group 1). It was therefore explored if priming of CD8 T cells by Hsp-complexed antigens could be further enhanced by co-administration of a defined adjuvant (AbISCO). Priming of $K^b/OVA_{257-264}$-specific CD8 T cells by Hsp/StT-OVA-G complexes was significantly enhanced by co-delivery with AbISCO (figure 14). Thus, the immunogenicity of Hsp/antigen complexes could be efficiently enhanced by co-delivering them with the adjuvant AbISCO.

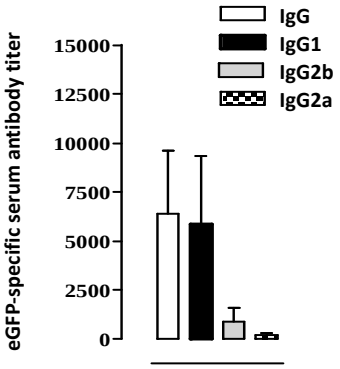

Figure 13.: Hsp/antigen complexes induced a Th2-directed immune response. Sera of three B6 mice immunized twice with 2 µg HeLa-derived Hsp/StT-OVA-G complexes were collected twelve days after boost and analyzed for eGFP-specific IgG isotypes by ELISA.

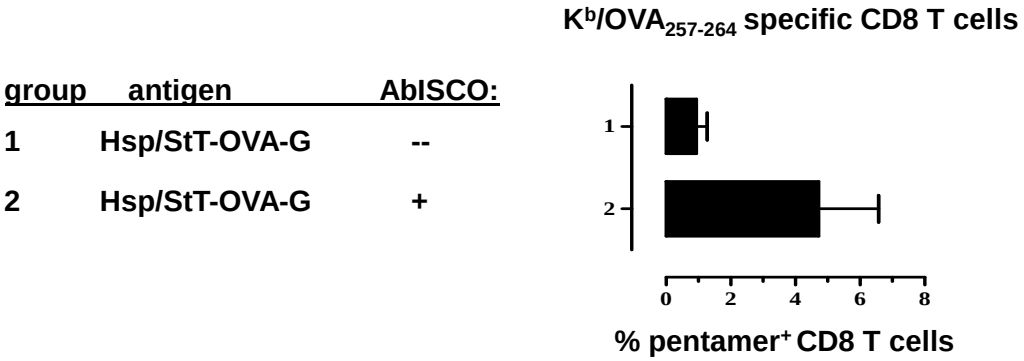

Figure 14.: Immunogenicity of Hsp/antigen complexes could be enhanced by AbISCO co-administration. B6 mice (four mice per group) were immunized with 2 µg HeLa-derived Hsp/StT-OVA-G complexes either without further adjuvant (group 1) or co-delivered with AbISCO (group 2). Mice were boosted after three weeks by an intramuscular injection of the same dose of the same vaccine and adjuvant. Twelve days after boost, $K^b/OVA_{257-264}$-specific CD8 T cells were determined by OVA-specific pentamer staining of splenic CD8 T cells.

3.1.3. The viral J domain efficiently binds bacterial Hsp70

Hsp-binding by the viral J domain facilitated the expression of chimeric antigens in transiently transfected HEK 293 cells (figure 4) or adenovirally transduced HeLa cells (figure 9). In order to produce antigens in a commercial setting, the well established CHO cell line was used. Therefore, a stably transfected CHO cell line expressing the StT-OVA-G fusion protein was generated by transfection with BMGneo/StT-OVA-G and selection with G418. Purification of the StT-OVA-G fusion protein from cleared CHO lysates co-precipitated Hsp73 (figure 15a). Notably, Hsp/StT-OVA-G complexes derived of stably transfected CHO cells lacked the inducible Hsp70 protein and contained only the larger constitutively expressed Hsp73 (figure 15b). In transiently transfected murine and chicken cell lines the viral J domain captured only the Hsp73 isoform. Thus, the viral J domain efficiently captures different Hsp70 molecules in different eukaryotic producer cell lines of different species origin. B6 mice with low doses of CHO-derived Hsp/StT-OVA-G complexes efficiently induced $K^b/OVA_{257-264}$-specific CD8 T cells (figure 15c). This response was comparable to HEK-derived StT-OVA-G complexed with Hsp70/73. Thus, priming of CD8 T cells by eukaryotic Hsp/antigen complexes was independent of the origin and isoform of the complexed Hsp70.

In order to determine if the viral J domain of the T-Ag of SV40 is also able to bind prokaryotic Hsp70, a bacterial expression system consisting of an IPTG inducible promotor and the StT-OVA-G encoding sequence. *E. coli* Rosetta gami were transformed and expression of the StT-OVA-G fusion protein was induced by addition of IPTG. SDS-PAGE analysis of StrepTactin-purified bacterial lysates revealed different protein band patterns dependent on the purification process. Addition of ATP during the purification resulted in the purification of two proteins of about 42 and 52 kDa (figure 16a, lane b), whereas an additional protein of about 70 kDa was co-purified in the absence of ATP (figure 16a, lane a). Western blot analysis identified the full-length StT-OVA-G protein (figure 16b). In addition, the co-precipitated protein of about 70 kDa was identified as DnaK (the bacterial homolog of Hsp70). Western blot analysis confirmed that the binding of DnaK to the viral J domain was sensitive to ATP as DnaK could be quantitatively removed from the StT-OVA-G fusion protein by ATP treatment (figure 16b, lane b). Thus, fusion proteins containing

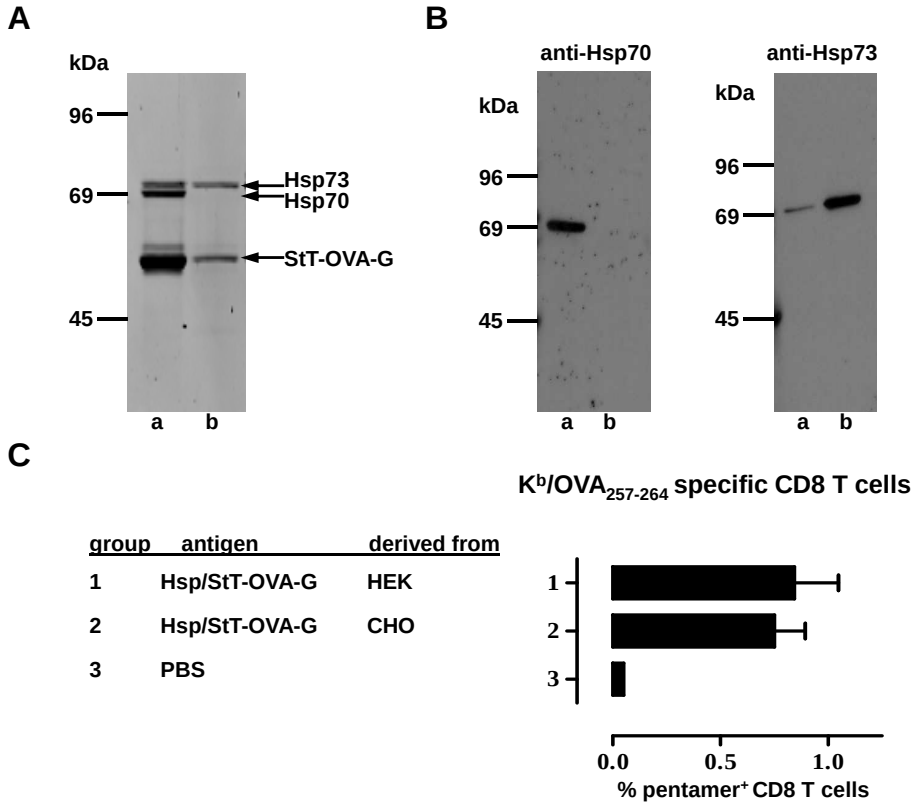

Figure 15.: Immunogenicity of Hsp/antigen complexes expressed in different eukaryotic cells. **a, b** Hsp/StT-OVA-G complexes were purified from transiently transfected HEK 293 cells (lanes a) or stably transfected CHO cells (lanes b) and analyzed by SDS-PAGE and SyproOrange staining. The positions of the StT-OVA-G protein, Hsp70 and Hsp73 are indicated. **b** Samples were analyzed by SDS-PAGE followed by Hsp70 and Hsp73-specific Western blotting. **c** B6 mice (four per group) were immunized with 2 µg HEK 293-derived (lane 1) or CHO-derived (lane 2) Hsp/StT-OVA-G complexes, or injected with PBS (lane 3). Mice were boosted after three weeks by an intramuscular injection of the same dose of the same vaccine. Twelve days after boost, $K^b/OVA_{257-264}$-specific CD8 T cells were determined by $K^b/OVA_{257-264}$-specific pentamer staining of splenic CD8 T cells.

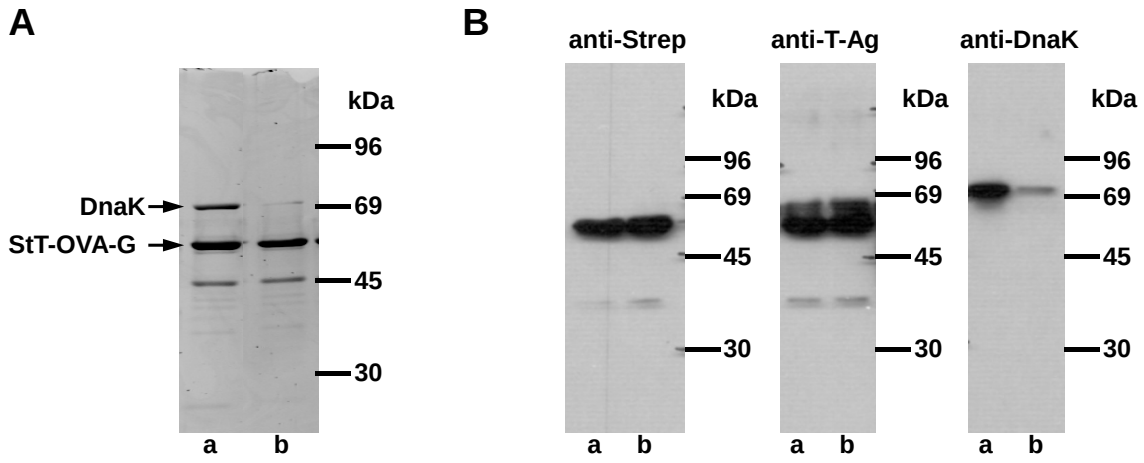

Figure 16.: Expression of recombinant Hsp/antigen complexes in bacterial expression host. **a,b** *E. coli* Rosetta gami were transformed with pQE-9/StT-OVA-G and antigen expression was induced overnight by addition of IPTG. Bacterial lysates were purified using StrepTactin columns followed by release of Hsp/antigen complexes with desthiobiotin (lanes a) or by sequential elution of Hsp (in an ATP-containing buffer) and the StT-OVA-G protein (with desthiobiotin, lanes b). Samples were analyzed by SDS-PAGE and SyproOrange staining. The positions of the StT-OVA-G protein and the bacterial DnaK are indicated. **b** Samples were analyzed by SDS-PAGE followed by Western blotting using Strep-tag-, T-Ag-, and DnaK-specific antibodies.

the viral J domain can be efficiently expressed in bacterial expression systems and form complexes with bacterial Hsp70/DnaK.

In addition, the immunogenicity of the purified DnaK/StT-OVA-G complexes was explored. Vaccination with bacterial DnaK/StT-OVA-G complexes showed significantly increased priming of $K^b/OVA_{257-264}$-specific CD8 T cells compared to immunization with eukaryotic Hsp/StT-OVA-G complexes. DnaK/StT-OVA-G complexes induced five-fold higher $K^b/OVA_{257-264}$-specific CD 8 T cell frequencies (figure 17). Therefore, the bacterial expression of antigens with the viral J domain results in DnaK/antigen complexes, which efficiently induce CD8 T cell responses.

To explore the enhanced immunogenicity of antigens bound to Hsp70/73 and especially the bacterial DnaK, BM-DCs (figure 18a) were stimulated with Hsp/StT-OVA-G complexes and analyzed for the up-regulation of activation markers. Pulsing of BM-DCs with HEK 293-derived StT-OVA-G protein or Hsp/StT-OVA-G complexes didn't up-regulate the activation markers CD80 and CD86 (figure 18b). In contrast, bacterial-derived DnaK/StT-OVA-G complexes efficiently activated BM-DCs,

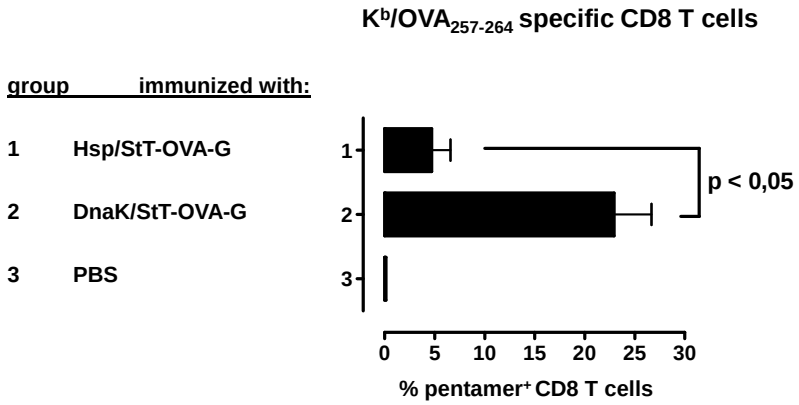

Figure 17.: Enhanced immunogenicity of bacteria-derived Hsp/antigen complexes. B6 mice (four per group) were immunized with 5 µg HEK 293-derived Hsp/StT-OVA-G complexes and AbISCO (lane 1), 5 µg *E. coli*-derived DnaK/StT-OVA-G complexes and AbISCO (lane 2), or injected with PBS (lane 3). Mice were boosted after three weeks by an intramuscular injection of the same dose of the same vaccine. Twelve days after boost, $K^b/OVA_{257-264}$-specific CD8 T cells were determined by $K^b/OVA_{257-264}$-specific pentamer staining of splenic CD8 T cells.

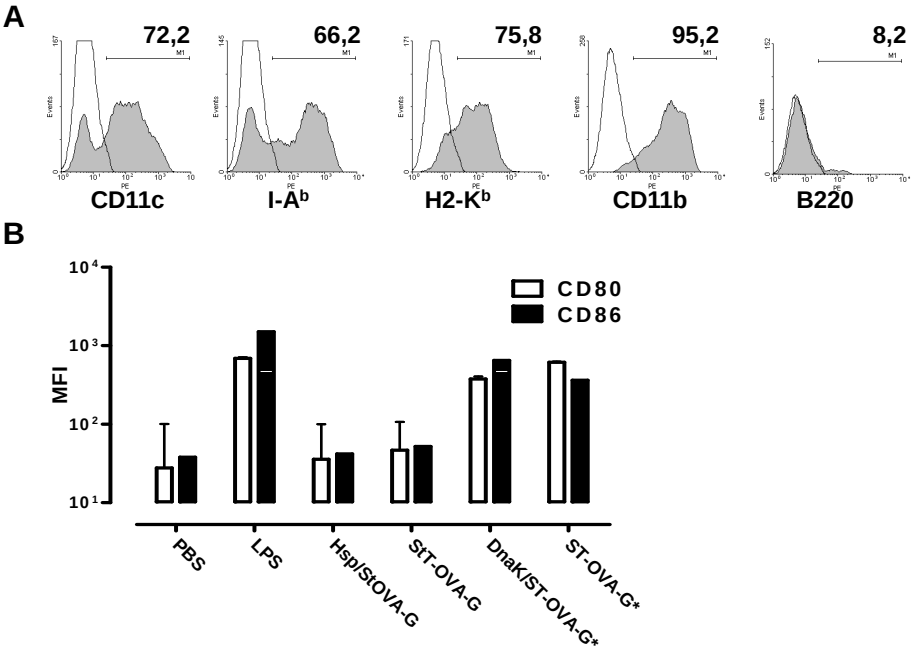

Figure 18.: Innate immune system isn't activated by mammalian-derived Hsp/antigen complexes. **a** BM-DCs were generated as described and surface-stained for CD11c, CD11b, I-A^b, H2-K^b and B220. **b** 2x10^5 BM-DCs were stimulated for 16 h with PBS, 500 ng LPS or 5 µ mammalian or bacterial-derived StT-OVA-G protein either complexed by Hsp/DnaK or not. BM-DCs were analyzed for surface expression of CD80 and CD86. The mean fluorescence intensity (MFI) is shown. Bacterial-derived proteins are indicated by an asterik.

which showed significantly up-regulated surface expression of the activation markers CD80 and CD86 (figure 18b). The activation of BM-DCs by bacterial-derived DnaK/StT-OVA-G complexes was independent of the complexation status as uncomplexed StT-OVA-G proteins activated BM-DCs as well. Up-regulation of CD80 and CD86 was also observed with 500 ng LPS suggesting that a major LPS contamination of bacterial-derived proteins is responsible for the BM-DC activation. Therefore, the enhanced immunogenicity of bacterial-derived DnaK/StT-OVA-G compared to mammalian-derived Hsp/StT-OVA-G complexes is rather based on the contaminating LPS than on enhanced intrinsic features of bacterial DnaK.

3.1.4. Fusion proteins containing different J domains bind Hsp70/73

The J domain of the T-Ag of SV40 differs from J domains found in DnaJ-like proteins of other species but shares conserved features such as the four α-helices forming a finger-like structure and the exposed, conserved HPD motif on the tip of it. A comparison of the viral J domain with J domains of bacterial (*Chlamydia trachomatis*) or plant (*Arabidopsis thaliana*) origin revealed major differences in the sequence surrounding the central HPD motif as well as in the overall amino acid composition (figure 19a). Chimeric antigens N-terminally fused to J domains of different origin (viral, bacterial, plant) were designed to address the question if stable Hsp70/73-binding is restricted to the viral J domain, or in fact, a general feature of J domains independent of their species origin (figure 19b). Expression studies showed that comparable levels of chimeric antigens were expressed in transiently transfected HEK 293 cells and that Hsp70/73 molecules were captured with comparable efficiency by the three different J domains tested (figure 20a). In addition to comparable expression efficiencies of the constructs containing J domains of either viral, bacterial or plant origin, DNA vaccination induced comparable $K^d/Pol_{140-148}$- and K^d/LLO_{91-98}-specific CD8 T cell responses irrespective of the origin of the fused J domain (figure 20b). However, no K^d/C_{87-95}-specific CD8 T cells were primed. Thus, the $K^d/Pol_{140-148}$- and K^d/LLO_{91-98}-specific CD8 T cell responses seemed to suppress the priming of CD8 T cell directed against the K^d/C_{87-95} epitope.

Unexpected stable binding of Hsp70/73 by J domains of viral, bacterial and plant origin could be caused by the lack of regulatory elements thus impairing the dissoci-

A

origin	protein	organism	Swissprot	Swissprot acc.no.	J-domain
SV 40	T-Antigen	virus	TALA_SV40	P03070	aa 12-75
Chlamydia trachomatis	Chaperon DnaJ	bacterium	DNAJ_CHLTR	O84345	aa 2-67
Arabidopsis thaliana	Chaperon DnaJ2	plant	DNAJ2_ARATH	P42825	aa 14-75

Constructs:

#1 SV 40 T-Antigen (MDKVLNREES L) QLMDLLGLE RSAWGNIPLM RKAYLKKCKE F**HPD**KGGDEE KMKKMNTLYK KMEDGVKYAH QPDFGGF

#2 *Chlamydia trachomatis* (M)DYYTILG VAKTATPEEI KKAYRKLAVK Y**HPD**KNPGDA EAERRFKEVS EAYEVLGDAQ KRESYDRYG

#3 *Arabidopsis thaliana* (MFGRGPSKKS DNT) KFYEILG VPKTAAPEDL KKAYKKAAIK N**HPD**KGGDPE KFKELAQAYE VLSDPEKREI YDQYG

B

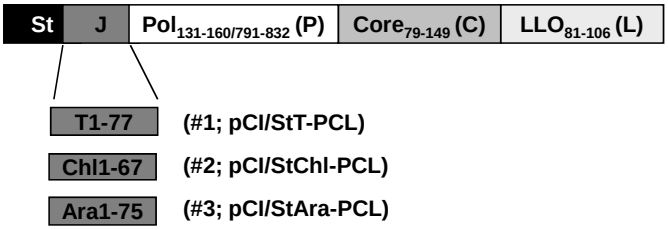

Figure 19.: Construction of Hsp-capturing chimeric antigen constructs using J domains of different species origin. **a** Alignment of amino acid sequences of SV40- (#1), *Chlamydia trachomatis*- (#2) and *Arabidopsis thaliana*- (#3) derived J domains. Species origin, designation and accession number (Swissprot) as well as the amino acid residues forming the J domain of the respective protein are indicated. The central, conserved HPD motif is emphasized. **b** pCI-based expression vectors were generated containing a N-terminal Strep-tag sequence, followed by either the SV40 T_{1-77} domain (construct #1), the *Chlamydia trachomatis* $DnaJ_{1-67}$ domain (construct #2), or the *Arabidopsis thaliana* $DnaJ2_{14-75}$ domain (construct #3) and a C-terminal chimeric antigen sequence composed of the HBV-derived $Pol_{131-160}$ and $Pol_{781-832}$ (P), $Core_{79-149}$ (C), and the *Listeria monocytogenes*-derived LLO_{81-106} (L).

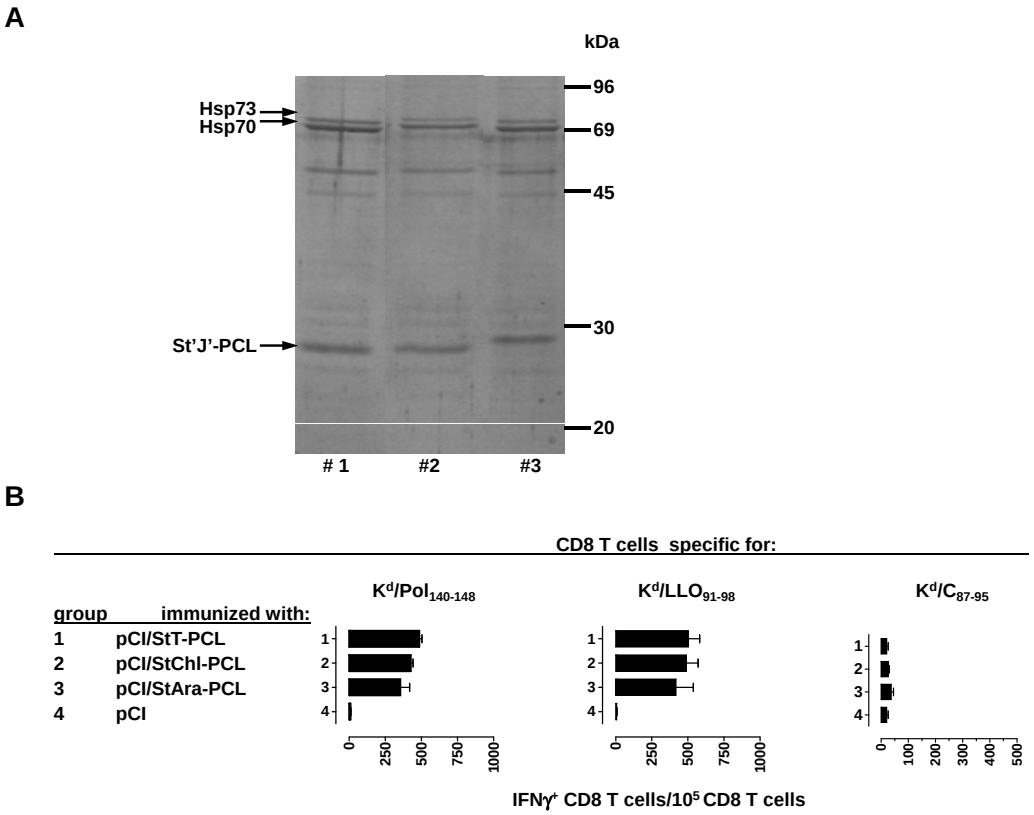

Figure 20.: J domains of different species origin captured Hsp, facilitated expression of chimeric antigen and efficiently induced antigen-specific CD8 T cells. (a) HEK 293 cells were transiently transfected with vectors encoding a N-terminal Strep-tag sequence, followed by either the SV40 T_{1-77} domain (construct #1), the *Chlamydia trachomatis* $DnaJ_{1-67}$ domain (construct #2), or the *Arabidopsis thaliana* $DnaJ2_{14-75}$ domain (construct #3) and a C-terminal chimeric antigen sequence composed of the HBV-derived $Pol_{131-160}$ and $Pol_{781-832}$ (P), $Core_{79-149}$ (C), and the *Listeria monocytogenes*-derived LLO_{81-106} (L). Cells were lysed, chimeric proteins were immunoprecipitated using Strep-Tactin sepharose and analyzed by SDS-PAGE and Coomassie Blue staining. The positions of the respective chimeric antigens (#1-3) and the co-precipitated Hsp70/73 are indicated. **b** BALB/c mice (four per group) were immunized with 100 µg pCI/StT-PCL (lanes 1), pCI/StChl-PCL (lanes 2), pCI/StAra-PCL (lanes 3), or non-coding pCI DNA (lanes 4). Specific CD8 T cell responses were analyzed twelve days after injection by 4 h ex vivo restimulation with the $K^d/Pol_{140-148}$, the K^d/LLO_{91-98} or with the K^d/C_{87-95} peptide, followed by determination of IFNγ^+ CD8 T cell frequencies.

ation of Hsp/antigen complexes. To explore the effect of J domain flanking regions on the stable Hsp-assocation the J domain derived of *Arabidopsis thaliana* DnaJ2 protein the J domain of pCI/StAra-PCL was C-terminally elongated by incorporation of about 160 amino acid residues. This region is composed of a 30 residues encompassing glycine-rich domain and about 130 amino acid residues representing a zinc finger domain containing four repeats of a CXXCXGXG motif. Transient transfection of HEK 293 followed by immunoprecipitation using StrepTactin showed efficient expression of the fusion protein StAralong-PCL containing an elongated J domain derived of *Arabidopsis thaliana*. In addition, Hsp70/73 was efficiently co-precipitated with StAralong-PCL demonstrating that the C-terminal flanking region of the J domain derived of *Arabidopsis thaliana* DnaJ2 protein exerts no influence on stable Hsp-binding mediated by the J domain. Accompaning efficient expression in a Hsp-bound form vaccination of BALB/c mice with pCI/StAralong-PCL induced $K^d/Pol_{140-148}$- and K^d/LLO_{91-98}-specific CD8 T cell responses comparable to pCI/StAra-PCL (figure 21). In addition, C-terminal elongation of the J domain of *Arabidopsis thaliana* DnaJ2 protein didn't circumvent the suppression of K^d/C_{87-95}-specific CD8 T cells. Thus, C-terminal flanking region of the J domain derived of *Arabidopsis thaliana* DnaJ2 protein had no effect on vaccine efficacy.

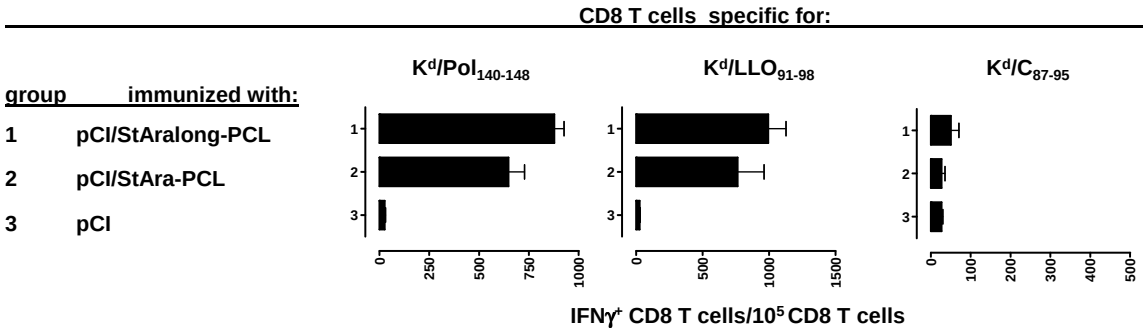

Figure 21.: C-terminal flanking region of *Arabidopsis thaliana*-derived J domain had no effect on immunogenicity. BALB/c mice (four per group) were immunized with 100 µg pCI/StAralong-PCL (lanes 1), pCI/StAra-PCL (lanes 2), or non-coding pCI DNA (lanes 3). Specific CD8 T cell responses were analyzed twelve days after injection by 4 h ex vivo restimulation of splenic T cells with the $K^d/Pol_{140-148}$, the K^d/LLO_{91-98}, or with the K^d/C_{87-95} peptide, followed by determination of IFNγ^+ CD8 T cell frequencies.

3.1.5. Hsp/antigen complexes efficiently induce CD8 T cell responses in HLA-A*0201-tg mice

In order to explore the potential of Hsp-complexed antigens to induce human relevant CD8 T cell responses, HLA-A*0201-tg mice were immunized with purified Hsp/StT-SFG complexes. Hsp/StT-SFG complexes (figure 3) were used for vaccination as StT-SFG contains the immunodominant, HLA-A*0201-restricted Flu-Ma_{58-66} epitope of the influenza A matrix protein, which has often been used to characterize CD8 T cell responses. A single vaccination with Hsp/StT-SFG complexes induced a detectable Flu-Ma_{58-66}-specific CD8 T cell response in HLA-A*0201-tg mice. The specific CD8 T cell response could further be enhanced by boost administration of Hsp/StT-SFG complexes (figure 22a). Furthermore, StT-SFG protein without complexing Hsp70/73 was not able to prime Flu-Ma_{58-66}-specific CD8 T cells (figure 22b). Co-administration of Hsp/StT-SFG complexes with AbISCO elicited higher Flu-Ma_{58-66}-specific CD8 T cell frequencies than Hsp/StT-SFG complexes (figure 22c), demonstrating that improved priming of CD8 T cells mediated by AbISCO co-administration is also independent of the MHC-I restriction.

3.1.6. Hsp/antigen complexes are able to induce multispecific CD8 T cell responses

Hsp-binding vaccines are an attractive strategy to induce multispecific CD8 T cell responses. Hsp-association facilitated the expression of chimeric antigens allowing incorporation of a lot of antigenic information (figure 4, figure 20a). Hsp-association also increased the immunogenicity of recombinant fusion proteins (figure 10, figure 22b). The StT-SFG construct was used as model vaccine for induction of multispecific CD8 T cell responses in a humanized mouse model (HLA-A*0201-tg mice). In addition to the HLA-A*0201-restricted Flu-Ma_{58-66} epitope, the StT-SFG construct also bears two recently characterized HLA-A*0201-restricted epitopes of the HBsAg ($S_{185-194}$ and $S_{208-216}$). Vaccination of HLA-A*0201-tg mice with purified Hsp/StT-SFG complexes efficiently induced Flu-Ma_{58-66}-specific CD8 T cells but neither $S_{185-194}$- nor $S_{208-216}$-specific CD8 T cells (figure 23, groups 2). The corresponding pCI/T-SFG DNA vaccine elicited the same pattern of CD8 T cells (figure 23, groups 3) demonstrating that different vaccination protocols don't alter the

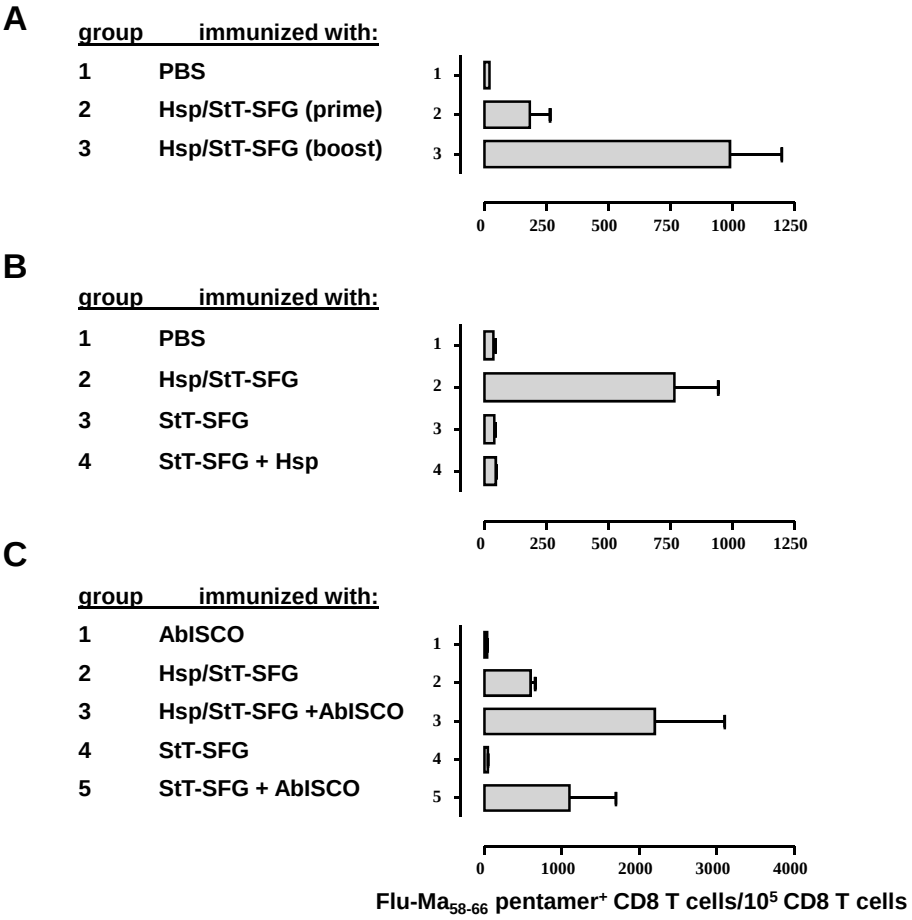

Figure 22.: Hsp/StT-SFG complexes efficiently induce HLA-A*0201/Flu-Ma$_{58-66}$-specific CD8 T cells. **a** HLA-A*0201-tg mice (four per group) were immunized once (group 2) or in a prime-boost regimen (group 3) with 2 µg HEK 293-derived Hsp/StT-SFG complexes, or injected with PBS (group 1). Mice were boosted after three weeks by an intramuscular injection of the same dose of the same vaccine. Twelve days after final injection, Flu-Ma$_{58-66}$ specific CD8 T cells were determined by Flu-Ma$_{58-66}$-specific pentamer staining of splenic CD8 T cells. **b** HLA-A*0201-tg mice (four per group) were immunized with 2 µg HEK 293-derived StT-SFG protein either complexed with Hsp70/73 (group 2) or not (group 3), a mixture of 2 µg StT-SFG protein and equimolar amounts of purified Hsp70/73 (group 4), or injected with PBS as control (group 1). Twelve days after final injection, Flu-Ma$_{58-66}$ specific CD8 T cells were determined as described above. **c** HLA-A*0201-tg mice (four per group) were immunized with 2 µg HEK 293-derived StT-SFG complexes (groups 2 and 3), or 2 µg StT-SFG protein (groups 4 and 5), either without further adjuvant (groups 2 and 4) or co-delivered with AbISCO (groups 3 and 5), or injected with AbISCO a control (group 1). Mice were boosted after three weeks by an intramuscular injection of the same dose of the same vaccine and adjuvant. Twelve days after final injection, Flu-Ma$_{58-66}$ specific CD8 T cells were determined as described above.

pattern of primed CD8 T cells. In order to explore if the Flu-Ma_{58-66} epitope induced an immunodominant CD8 T cell response and thus suppressed the priming of CD8 T cells of other specificity, the Flu epitope was deleted from the pCI/T-SFG construct (figure 23a). The resulting pCI/T-SG could efficiently prime $S_{185-194}$- as well as $S_{208-216}$-specific CD8 T cells (figure 23, groups 4) thus demonstrating that the presence of the immunodominant Flu-Ma_{58-66} epitope efficiently suppresses CD8 T cell responses of other specificity. Hsp-binding vaccines can incorporate large amounts of antigenic information and are thus able to induce multispecific CD8 T cell responses, which are nevertheless subjected to immunodominance effects.

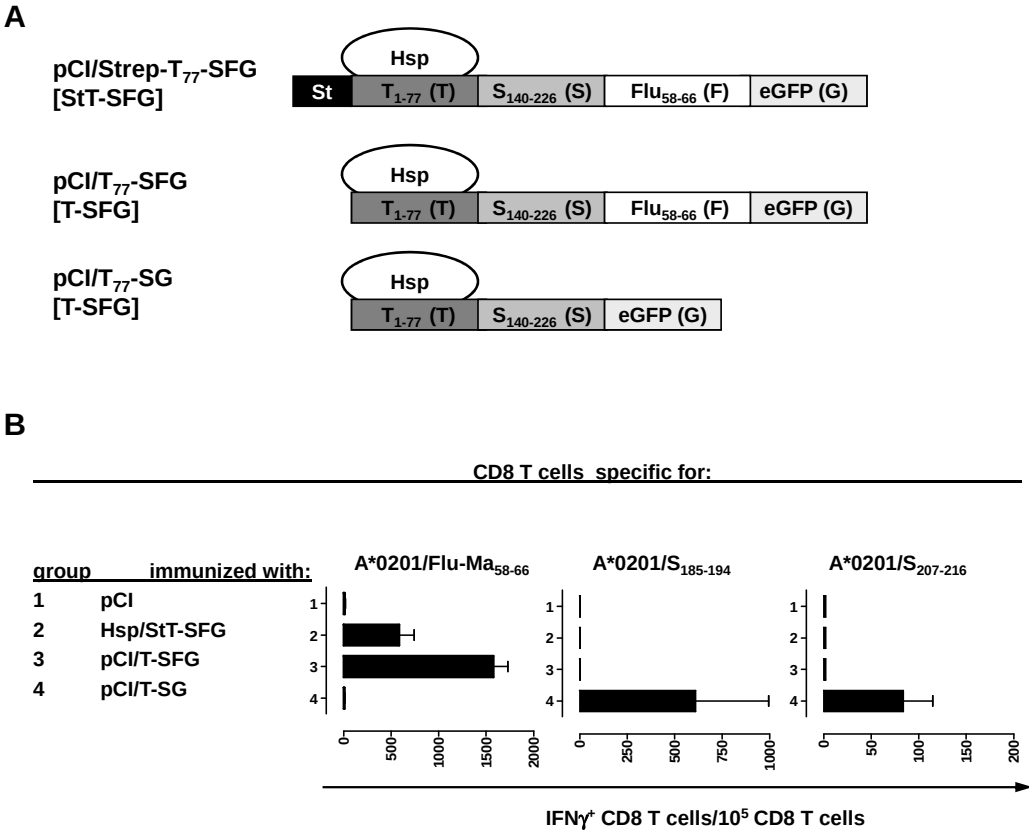

Figure 23.: Hsp/StT-SFG complexes induced immunodominant CD8 T cells specific for HLA-A*0201/Flu-Ma_{58-66}. **a** Schematic presentation and designation of Hsp-binding constructs used to evaluate induction of multispecific CD 8 T cell responses. **b** HLA-A*0201-tg mice (four mice per group) were immunized with 100 µg pCI (groups 1), 2 µg HEK 293-derived StT-SFG complexes (groups 2), 100 µg pCI/T-SFG (groups 3), or 100 µg pCI/T-SG (groups 4). Specific CD8 T cell responses were analyzed twelve days after injection by 4 h ex vivo restimulation of splenic T cells with the A*0201/Flu-Ma_{58-66}, the A*0201/$S_{185-194}$, or the A*0201/$S_{208-216}$ peptide, followed by determination of IFNγ^+ CD8 T cell frequencies.

3.2. Hsp-binding HBV multidomain vaccines are affected by immunodominance phenomenons

3.2.1. Design of a Hsp-binding HBV-specific multidomain vaccine

Immunization with Hsp-binding vaccines demonstrated their ability to induce multispecific CD8 T cells (figure 20b, figure 23b), although priming of subdominant CD8 T cell responses depended on the lack of immunodominant epitopes (figure 23). In order to explore the full potential of Hsp-binding vaccines to induce multispecific CD8 T cell responses, a vaccine consisting of multiple epitope-bearing domains of different HBV antigens was designed (figure 24a). The composition of incorporated antigenic domains was based on characterized CD8 T cell epitopes (table 8) and the size of the single domains was adjusted to allow natural processing of the explored epitopes by incorporation of natural flanking sequences. The HBV multidomain vaccine StT-MO (figure 24a) contained a N-terminal Strep-tag and the J domain of the T-Ag fused to residues 2-50 of HBsAg, residues 131-160 and 791-832 of HBV-derived polymerase, residues 246-353 of ovalbumin, residues 79-149 and 10-50 of HBcAg, and residues 140-226 of HBsAg. In addition to HBV-derived antigenic domains, the vaccine thus incorporated an ovalbumin fragment containing the $K^b/OVA_{257-264}$ epitope widely used to characterize CD8 T cell responses.

Expression analyses showed that the fusion protein StT-MO was able to bind Hsp70/73 by its J domain and thus accumulated to steady state levels (figure 24b), whereas the expression of the fusion protein St-MO –lacking the J domain– was strikingly decreased. Therefore, Hsp-binding mediated by the viral J domain efficiently facilitated the expression of the highly chimeric HBV multidomain vaccine StT-MO.

3.2.2. Induction of multispecific, murine CD8 T cell responses

Using HLA-A*0201 transgenic HHD mice CD8 T cell responses to five well defined HLA-A*0201-restricted HBV epitopes (table 8) were analyzed. A single immunization with pCI/C or pCI/Pol elicited CD8 T cell responses to either the $A*0201/C_{18-27}$ (figure 25, groups 2) or the $A*0201/Pol_{803-811}$ epitope (figure 25, groups 3). Immunization of mice with pCI/StT-MO induced CD8 T cell responses to both epitopes

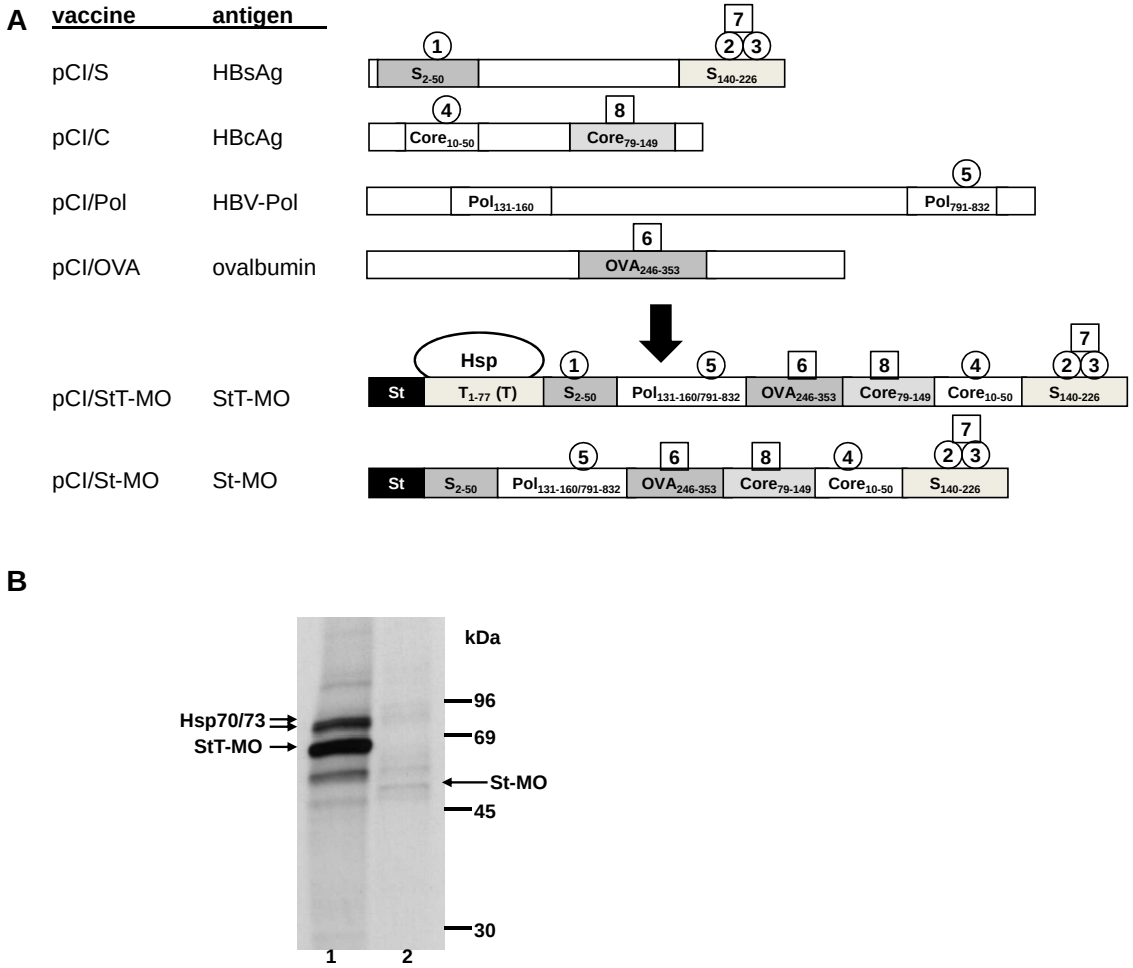

Figure 24.: Expression of HBV multidomain vaccine StT-MO. **a** Schematic presentation of expression vectors encoding single (pCI/S, pCI/C, pCI/Pol and pCI/OVA) or multidomain (pCI/StT-MO and pCI/St-MO) vaccines. The multidomain vaccine consists of the following antigen fragments: S_{2-50}, $Pol_{131-160}$, $Pol_{791-832}$, $OVA_{257-264}$, C_{79-149}, C_{10-50} and $S_{140-226}$. The Strep-Tag, the Hsp-binding SV40-T_{77}-derived DnaJ sequence and the MHC-I-restricted epitopes (◯ HLA-A*0201; □ H2-K^b; for detail see table 8) are indicated. **b** HEK 293 cells were transiently transfected with pCI/StT-MO (lane 1) or pCI/St-MO (lane 2). Cells were labeled with [^{35}S]-methionine/cysteine, immunoprecipitated with StrepTactin sepharose and analyzed by SDS-PAGE followed by fluorography. The positions of the StT-MO and St-MO proteins and Hsp70/73 are indicated.

Table 8.: List of MHC-I restricted epitopes of HBV multidomain including the antigenic origin, localization, amino acid sequence, MHC-I restriction and the binding affinity to the respective MHC-I.

#	antigen	epitope	sequence	restriction	IC 50% [nM]
1	HBsAg	S_{20-28}	FLLTRILTI	HLA-A*0201	10
2	HBsAg	$S_{185-194}$	GLSPTVWLSV	HLA-A*0201	18
3	HBsAg	$S_{208-216}$	ILSPFLPLL	HLA-A*0201	nd
4	HBcAg	C_{18-27}	FLPSDFFPSV	HLA-A*0201	3
5	HBV-Pol	$Pol_{803-811}$	SLYADSPSV	HLA-A*0201	14
6	OVA	$OVA_{257-264}$	SIINFEKL	K^b	4
7	HBsAg	$S_{190-197}$	VWLSVIWM	K^b	13
8	HBcAg	C_{93-100}	MGLKFRQL	K^b	4
8*	HBcAg		MGLKIRQL		nd

(figure 25, groups 5) but CD8 T cell frequencies were lower than in mice vaccinated with pCI/C or pCI/pol (figure 25, groups 2 and 3). Injection of pCI/S primed CD8 T cell responses to all three HBsAg derived epitopes (figure 25, groups 1), whereas pCI/StT-MO vaccination only induced CD8 T cell responses to the A*0201/S_{20-28} epitope but not to the A*0201/$S_{185-194}$ and A*0201/$S_{208-216}$ epitopes (figure 25, groups 5). A*0201/S_{20-28}-specific CD8 T cell responses were comparable in pCI/S and pCI/StT-Mo immunized mice. Only a fraction of the HLA-A*0201-restricted epitope repertoire of HBsAg could thus specifically prime CD8 T cells if delivered as multidomain vaccine (pCI/StT-MO), while the pCI/S vaccine supported efficient priming of a multispecific CD8 T cell response. Thus, the diversity of the CD8 T cell responses to HBV antigens differed in mice vaccinated with either the pCI/StT-MO, or the pCI/S, pCI/C or pCI/Pol DNA vaccines.

The designed multidomain vaccine pCI/StT-MO also contained three well defined H2-K^b-restricted epitopes in the surface ($S_{140-226}$), core (C_{79-149}) and OVA domains (table 8). B6 mice were immunized with the single antigen encoding plasmids pCI/S, pCI/C or pCI/OVA, or with the multidomain vaccine pCI/StT-MO and CD8 T cell frequencies were determined 12 days after injection. While K^b/$OVA_{257-264}$-specific CD8 T cells were efficiently induced in B6 mice by vaccination with pCI/StT-MO, neither K^b/$S_{190-197}$- nor K^b/C_{93-100}-specific CD8 T cells were primed in these animals by immunization with this vaccine (figure 26, groups 4). Immunization with pCI/OVA and pCI/StT-MO induced comparable K^b/$OVA_{257-264}$-specific CD8 T cell

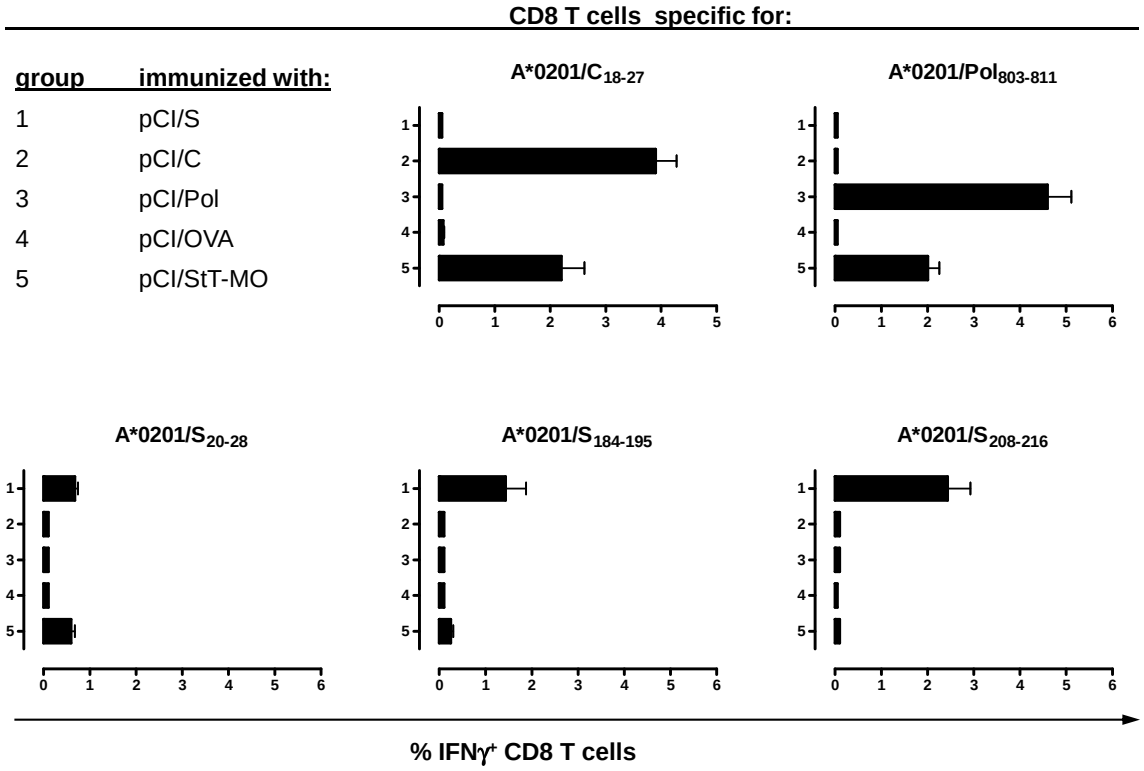

Figure 25.: Immunodominance limited the induction of multispecific CD8 T cells specific for HLA-A*0201-restricted epitopes. HLA-A*0201 tg mice (four mice per group) were immunized with 100 µg pCI/S (groups 1), pCI/C (groups 2), pCI/Pol (groups 3), pCI/OVA (groups 4), or with pCI/StT-MO (groups 5). The specific CD8 T cell responses were analyzed twelve days after injection by 4 h ex vivo restimulation of splenic T cells with the A*0201/C_{18-27}, the A*0201/$Pol_{803-811}$, the A*0201/S_{20-28}, the A*0201/$S_{185-194}$, or with the the A*0201/$S_{208-216}$ peptide, followed by determination of IFNγ^+ CD8 T cell frequencies.

responses (figure 26, groups 3 and 4). Mice immunized with the single antigen encoding plasmids pCI/S or pCI/C efficiently generated CD8 T cell responses specific for the $K^b/S_{190-197}$ or the K^b/C_{93-100} epitope (figure 26, groups 1 and 2). CD8 T cells responses to the $K^b/S_{190-197}$ and K^b/C_{93-100} epitope were thus suppressed in the presence of a $K^b/OVA_{257-264}$-specific CD8 T cell response. This was further supported by immunization experiments using vaccines that encode the epitope-containing $S_{140-226}$ or C_{79-149} fragment as Hsp-binding fusion antigen. The fusion antigen vectors pCI/T-$S_{140-226}$ and pCI/T-C_{79-149} efficiently induced CD8 T cell responses directed against the $K^b/S_{190-197}$ or K^b/C_{93-100} epitope (figure 26, groups 5 and 6). Therefore, $K^b/S_{190-197}$- and K^b/C_{93-100}-specific CD8 T cells could efficiently be primed by Hsp-binding fusion antigens but only in the abscence of $K^b/OVA_{257-264}$-specific CD8 T cell responses.

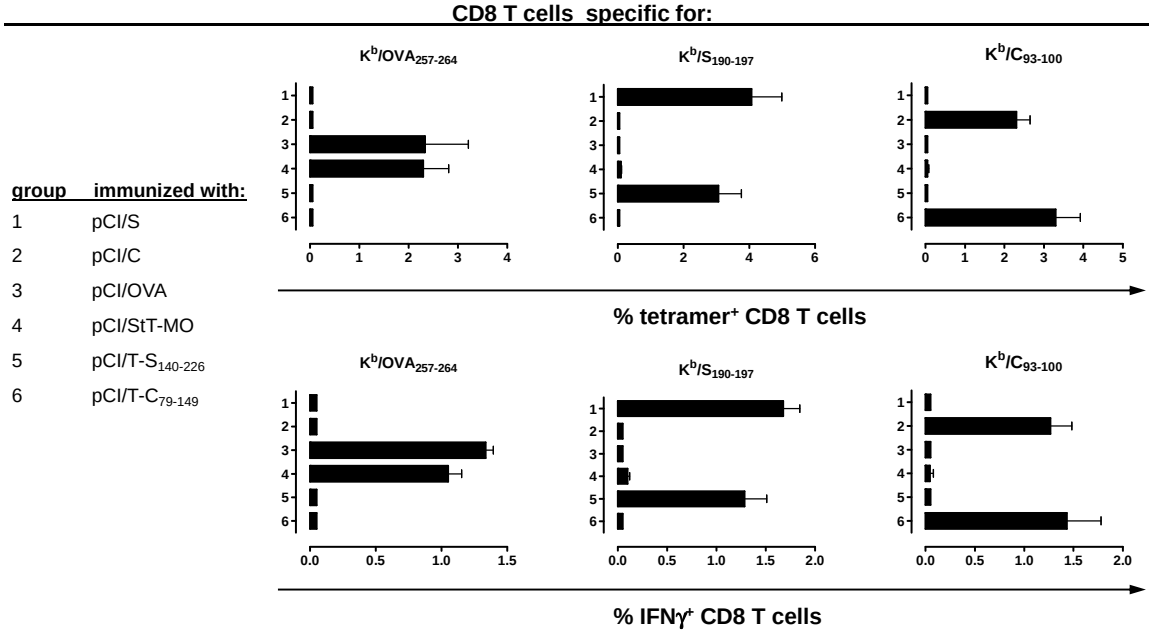

Figure 26.: HBV multidomain vaccine StT-MO efficiently induced OVA-specific CD8 T cells. B6 mice (four mice per group) were immunized with 100 µg pCI/S (groups 1), pCI/C (groups 2), pCI/OVA (groups 3), pCI/StT-MO (groups 4), pCI/T-$S_{140-226}$ (groups 5), or with pCI/T-C_{79-149} (groups 6). The specific CD8 T cell responses were analyzed twelve days after injection by $K^b/OVA_{257-264}$-, $K^b/S_{190-197}$-, or K^b/C_{93-100}-specific tetramer staining of splenic T cells (upper panels), or by 4 h ex vivo restimulation of splenic T cells with the $K^b/OVA_{257-264}$, the $K^b/S_{190-197}$, or with the the K^b/C_{93-100} peptide, followed by determination of IFNγ^+ CD8 T cell frequencies (lower panels).

Furthermore, the suppression of CD8 T cell responses to the $K^b/S_{190-197}$ and K^b/C_{93-100} epitopes was also evident in mice immunized with the pCI/St-MO vaccine (figure 27). This construct (figure 24a) contained all antigenic features of pCI/StT-MO, but lacked the J domain and thus the ability to capture Hsp70/73. In accordance with the lacking capability to capture Hsp70/73, the expression level of the St-MO antigen was significantly lower than its Hsp-binding form (figure 24b). Immunization with pCI/St-MO elicited lower $K^b/OVA_{257-264}$-specific CD8 T cell responses than immunization with the Hsp-binding form pCI/StT-MO (figure 27, groups 2 and 3). However, neither $K^b/S_{190-197}$- nor K^b/C_{93-100}-specific CD8 T cell responses were primed by immunization with pCI/St-MO. Thus, Hsp-capturing mediated by the viral J domain enhanced the expression of the fusion antigen (figure 24b) and also the immunogenicity of the construct (figure 27) but didn't alter the immunodominance hierarchy of the CD8 T cell responses.

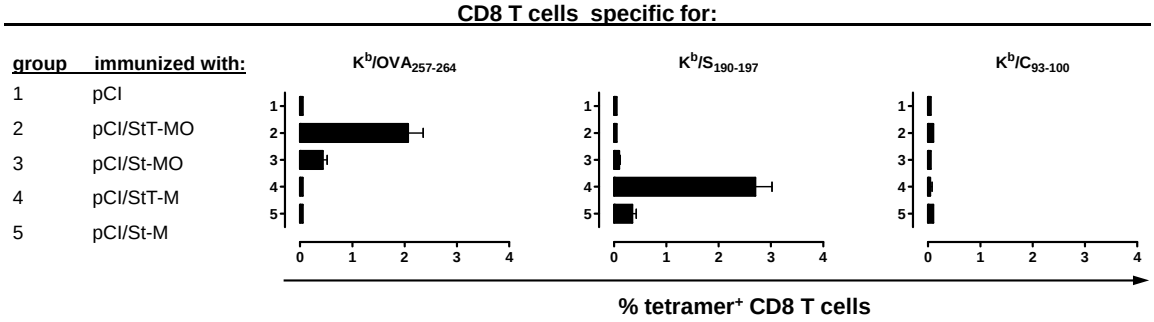

Figure 27.: Hsp-binding capability didn't alter immunodominance hierarchy. B6 mice (four mice per group) were immunized with 100 µg pCI (groups 1), pCI/StT-MO (groups 2), pCI/St-MO (groups 3), pCI/StT-M (groups 4), or with pCI/St-M (groups 5). Twelve days after injection specific CD8 T cell responses were analyzed by $K^b/OVA_{257-264}$-, $K^b/S_{190-197}$-, or K^b/C_{93-100}-specific tetramer staining of splenic T cells.

Immunization with the HBV multidomain vaccine containing an ovalbumin fragment (pCI/StT-MO) efficiently induced $K^b/OVA_{257-264}$-specific CD8 T cells, whereas other K^b-restricted CD8 T cell responses were completely suppressed. To check if $K^b/OVA_{257-264}$-specific CD8 T cells were responsible for the suppression of other K^b-restricted epitopes, a HBV multidomain vaccine lacking the ovalbumin fragment (pCI/StT-M) was designed. Expression analyses emphasized the need of J domain mediated Hsp-binding to stably express chimeric antigens as only the Hsp-bound form pCI/StT-M was efficiently expressed (figure 28).

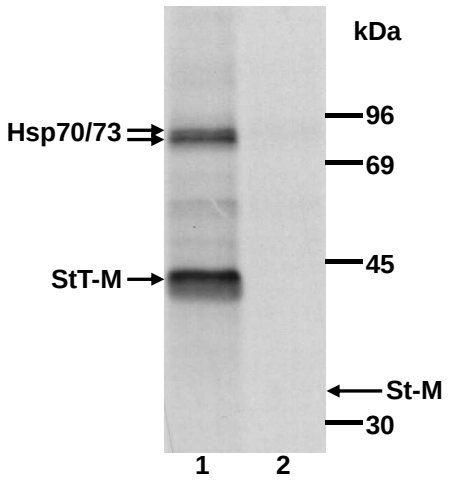

Figure 28.: Expression of HBV multidomain vaccine StT-M. HEK 293 cells were transiently transfected with pCI/StT-M (lane 1) or pCI/St-M (lane 2). Cells were labeled with [^{35}S]-methionine/cysteine, immunoprecipitated with StrepTactin sepharose and analyzed by SDS-PAGE followed by fluorography. The positions of the StT-M and St-M proteins and Hsp70/73 are indicated.

Immunization of B6 mice with pCI/StT-M efficiently induced $K^b/S_{190-197}$- but no K^b/C_{93-100}- specific CD8 T cells (figure 27, groups 4). Thus, deletion of the ovalbumin fragment bearing the immunodominant $K^b/OVA_{257-264}$ epitope gave rise to priming of $K^b/S_{190-197}$-specific CD8 T cells but not to CD8 T cells specific for the K^b/C_{93-100} epitope. Immunization with the Hsp-binding multidomain vaccine pCI/StT-M elicited significantly higher $K^b/S_{190-197}$-specific CD8 T cells than immunization with the multidomain vaccine pCI/St-M lacking the viral J domain and thus the ability to capture Hsp70/73 (figure 27, groups 4 and 5). Hsp70/73-association thus enhanced the immunogenicity of complexed antigens but didn't change the intrinsic immunodominance hierarchy of incorporated epitopes confirming previous findings concerning immunodominant $K^b/OVA_{257-264}$-specific CD8 T cell responses (figure 27, groups 2 and 3).

3.2.3. Characterization of immunodominance hierachies

An additional HBV oligodomain vaccine pCI/StT-SCC (figure 29a) was designed to investigate the observed immunodominance hierarchy between $K^b/S_{190-197}$- and K^b/C_{93-100}- specific CD8 T cell responses. The oligodomain vaccine pCI/StT-SCC

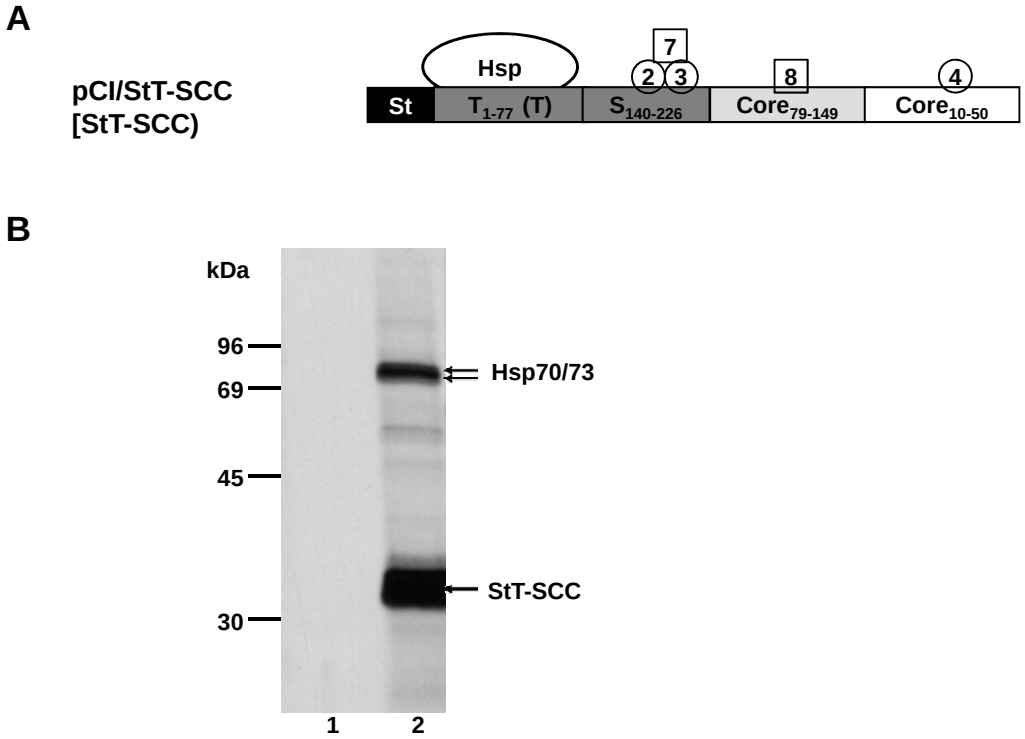

Figure 29.: Expression of the HBV oligodomain vaccine StT-SCC. **a** Schematic presentation of HBV oligodomain vaccine StT-SCC. The HBV oligodomain vaccine StT-SCC consists of the following antigen fragments: $S_{140-226}$, C_{79-149} and C_{10-50}. The Strep-Tag, the Hsp-binding SV40-T_{77}-derived DnaJ sequence and the MHC-I-restricted epitopes (◯ HLA-A*0201; □ H2-K^b; for detail see table 8) are indicated. **b** HEK 293 cells were transiently transfected with pCI (lane 1) or pCI/StT-SCC (lane 2). Cells were labeled with [^{35}S]-methionine/cysteine, immunoprecipitated with StrepTactin sepharose and analyzed by SDS-PAGE followed by fluorography. The positions of the StT-SCC protein and Hsp70/73 are indicated.

incorporated the residues 140-226 of the HBsAg and residues 79-149 and 10-50 of the HBcAg C-terminally fused in-frame to the Strep-Tag and J domain of the T-Ag of SV40. The absence of other HBV-derived antigenic domains was intended to avoid potential side effects on the observed immunodominance between $K^b/S_{190-197}$- and K^b/C_{93-100}-specific CD8 T cells. Expression analyses of transiently transfected HEK 293 cells showed a high expression level of the Hsp-binding StT-SCC fusion protein (figure 29b).

Similarly to the immunization with the HBV multidomain vaccine pCI/StT-M (figure 27, groups 4), the pCI/StT-SCC DNA vaccine efficiently induced $K^b/S_{190-197}$- but no K^b/C_{93-100}-specific CD8 T cell responses in vaccinated B6 mice (figure 30, groups

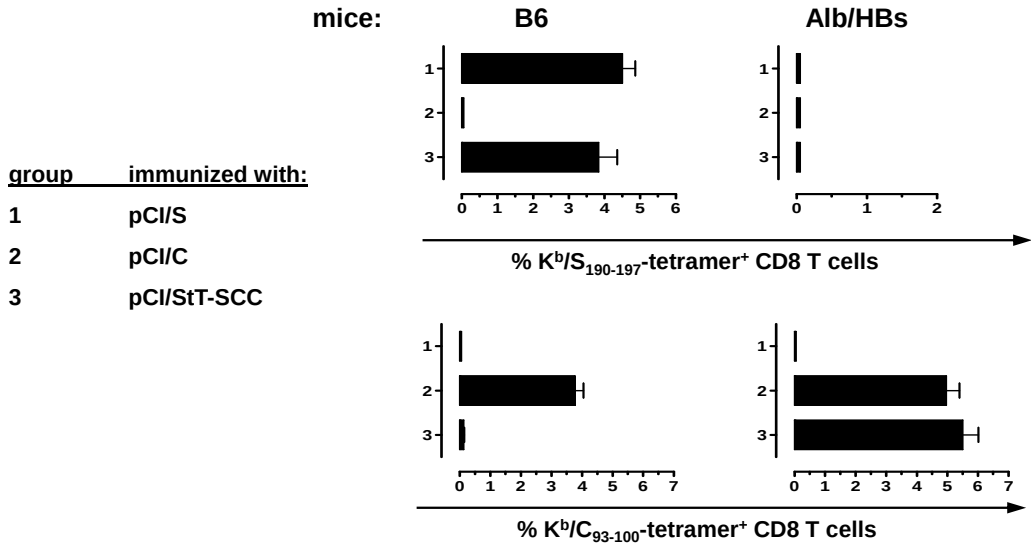

Figure 30.: $K^b/S_{190-197}$-specific CD8 T cells suppressed K^b/C_{93-100}-specific CD8 T cell responses. B6 and Alb/HBs tg mice (four mice per group) were immunized with pCI/S (groups 1), pCI/C (groups 2), or with pCI/StT-SCC (groups 3). The specific CD8 T cell responses were analyzed twelve days after injection by $K^b/S_{190-197}$- (upper panels) and K^b/C_{93-100}-specific (lower panels) tetramer staining of splenic CD8 T cells.

2). Thus, distinct immunodominance mechanisms were detected in the K^b-restricted CD8 T cell response to multidomain antigens: while the $K^b/OVA_{257-264}$-specific CD8 T cell response efficiently suppressed the $K^b/S_{190-197}$- and K^b/C_{93-100}-specific CD8 T cell responses, the $K^b/S_{190-197}$-specific CD8 T cell response suppressed the priming of K^b/C_{93-100}-specific CD8 T cells. Regarding the designed multidomain antigens the K^b/C_{93-100}-specific CD8 T cell response was subdominant, because it was readily suppressed by CD8 T cell responses to the $K^b/OVA_{257-264}$ or the $K^b/S_{190-197}$ epitope. The subdominant CD8 T cell response to the K^b/C_{93-100} epitope was unexpected as it contains the optimal anchor motifs at positions F5 and L8. Using a competition assay for empty surface K^b-molecules, no major differences between the binding affinities of the K^b/C_{93-100} and $K^b/S_{190-197}$ epitope for the K^b-molecule were observed (figure 31b). In collaboration with Søren Buus and Kasper Lamberth (University of Copenhagen, Denmark) it was shown that the K^b-binding affinitiy of the K^b/C_{93-100} epitope was comparable to those of the $K^b/OVA_{257-264}$ and $K^b/S_{190-197}$ epitopes (table 8). Thus, a simple epitope competition model for K^b-molecules couldn't account for the observed immunodominance hierarchy.

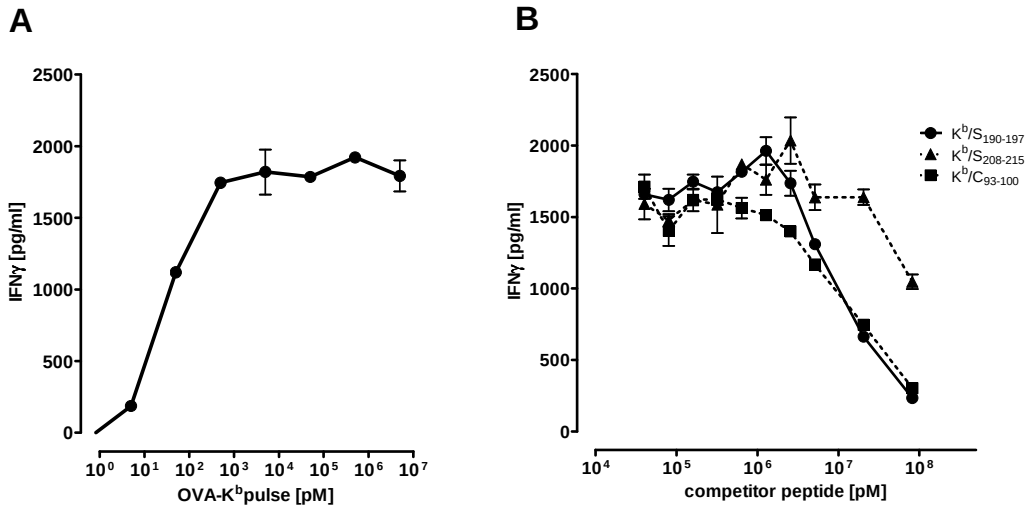

Figure 31.: Determination of K^b-binding affinity of epitopes. **a** 2×10^4 RMA/S were pulsed with titrated amounts of the $K^b/OVA_{257-264}$ peptide, followed by 20 h co-cultivation with 1×10^5 $K^b/OVA_{257-264}$-specific CD8 T cells. Supernatants were analyzed for IFNγ by ELISA. **b** 2×10^4 RMA/S were pulsed with a mix of 5 nM $K^b/OVA_{257-264}$ peptide and titrated amounts of competitor petides K^b/C_{93-100} (■), $K^b/S_{190-197}$ (•), or $K^b/S_{208-215}$ (▲). Pulsed cells were co-cultured for 20 h with 1×10^5 $K^b/OVA_{257-264}$-specific CD8 T cells. Supernatants were analyzed for IFNγ by ELISA.

To further characterize the $K^b/S_{190-197}$-mediated suppression mechanism we used Alb/HBs tg mice. These mice overexpress the large surface (LS) antigen in the liver under heterologous albumin promotor control. Western blot analyses showed high level expression of the glycosylated and non-glycosylated 42 and 39 kDa isoforms of the LS in the liver of Alb/HBs tg mice (figure 34a, lane 3). Due to internal translation start codons of the LS transgene, Alb/HBs tg mice also expressed the middle surface (MS) antigen as well as the secreted HBsAg readily detectable in the sera (figure 34b). In contrast to B6 mice, DNA immunization with the HBsAg-encoding vector pCI/S didn't induce $K^b/S_{190-197}$-specific CD8 T cell responses in Alb/HBs tg mice (figure 30, groups 1) demonstrating that Alb/HBs tg mice are tolerant to this $K^b/S_{190-197}$-specific CD8 T cell response due to their liver-associated expression of the LS. Similarly, the pCI/StT-SCC efficiently inducing $K^b/S_{190-197}$-specific CD8 T cells in B6 mice failed to induce $K^b/S_{190-197}$-specific CD8 T cell responses in Alb/HBs tg mice (figure 30, groups 3). However, in contrast to the vaccination studies in non-tg B6 mice, the absence of $K^b/S_{190-197}$-specific CD8 T cells allowed priming of K^b/C_{93-100}-specific CD8 T cells in Alb/HBs tg mice (figure 30, groups

2). Immunization of Alb/HBs tg mice with the oligodomain vaccine pCI/StT-SCC primed comparable amounts of K^b/C_{93-100}-specific CD8 T cells as immunization of mice (non-tg B6 or Alb/HBs tg) with the HBcAg-encoding vector pCI/C (figure 30, groups 2 and 3). Thus, pCI/StT-SCC transduced APCs displayed sufficient K^b/C_{93-100} complexes on their surface to efficiently induce K^b/C_{93-100}-specific CD8 T cell responses. As antigen processing and presentation are likely to be identical in pCI/StT-SCC transduced APCs from B6 and Alb/HBs tg mice, antigen processing and epitope competition for K^b-molecules weren't involved in the $K^b/S_{190-197}$-mediated suppression of the K^b/C_{93-100} CD8 T cell response. Thus, the absence of (simultaneously primed) $K^b/S_{190-197}$-specific CD8 T cells facilitated efficient priming of K^b/C_{93-100}-specific CD8 T cell responses.

3.2.4. Spatial separation of antigen-encoding vaccines circumvented immunodominance

Immunization of B6 mice with vaccines containing the K^b/C_{93-100} epitope as well as the immunodominant $K^b/S_{190-197}$ epitope (e.g. pCI/StT-SCC) failed to induce K^b/C_{93-100}-specific CD8 T cells (figure 30, groups 2). It was thus investigated if the suppression of K^b/C_{93-100}-specific CD8 T cells depended on the co-localization of immunodominant and subdominant epitopes on a single antigen molecule. B6 mice were therefore immunized either with a mix of 50 µg pCI/S and 50 µg pCI/C, or with 50 µg pCI/S or pCI/C mixed with 50 µg (empty) pCI in order to adjust the injected DNA amount. Immunization with 50 µg antigen encoding plasmid mixed with 50 µg pCI efficiently induced either $K^b/S_{190-197}$-specific CD8 T cells or K^b/C_{93-100}-specific CD8 T cells (figure 32, groups 2 and 3). Injection of a mix of plasmids encoding HBsAg and HBcAg efficiently primed $K^b/S_{190-197}$-specific CD8 T responses comparable to the vaccination with pCI/S (figure 32), whereas only a minor K^b/C_{93-100}-specific CD8 T cell response was induced. The plasmid mix consisting of pCI/C and pCI/S primed a significantly reduced K^b/C_{93-100}-specific CD8 T cell response (figure 32, groups 1 and 3) compared to immunization with pCI/C . These data demonstrate that immunodominant epitopes can suppress subdominant epitopes in trans and thus don't have to be located on the same antigen as the subdominant epitope.

The immunodominant $K^b/S_{190-197}$ epitope significantly impaired the priming of subdominant K^b/C_{93-100}-specific CD8 T cells even without being co-localized on the

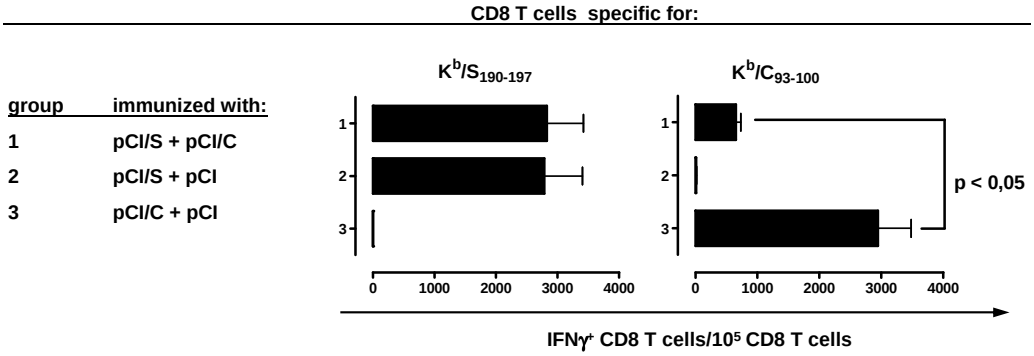

Figure 32.: Priming of subdominant K^b/C_{93-100}-specific CD8 T cells is hampered by spatial co-priming of dominant $K^b/S_{190-197}$-specific CD8 T cells. B6 mice (four mice per group) were immunized with 50 µg pCI/S and 50 µg pCI/C (groups 1), 50 µg pCI/S and 50 µg pCI (groups 2), or with 50 µg pCI/C and 50 µg pCI (groups 3). The specific CD8 T cell responses were analyzed twelve days after injection by 4 h ex vivo restimulation of splenic T cells with the $K^b/S_{190-197}$ or the K^b/C_{93-100} peptide followed by determination of IFNγ^+ CD8 T cell frequencies.

same antigen (figure 32, groups 1). It was thus explored if the observed immunodominance of $K^b/S_{190-197}$-specific CD8 T cells was a systemic or locally restricted effect. Therefore, B6 mice were simultaneously vaccinated with 50 µg pCI/S and 50 µg pCI/C, whereas the vaccines were spatially separated. This kind of vaccine administration induced comparable $K^b/S_{190-197}$- and K^b/C_{93-100}-specific CD8 T cell responses as vaccination with 50 µg of the respective single antigen encoding plasmid (figure 33). These data demonstrate that although the $K^b/S_{190-197}$ epitope was able to suppress the priming of K^b/C_{93-100}-specific CD8 T cells in trans (figure 32), that the immunodominance phenomenon just occurred if the priming sites of $K^b/S_{190-197}$- and K^b/C_{93-100}-specific CD8 T cells co-localized. The observed immunodominance of $K^b/S_{190-197}$-specific CD8 T cells was thus restricted to their own priming sites as spatially divided administration of vaccines could easily circumvent suppression of K^b/C_{93-100}-specific CD8 T cell responses.

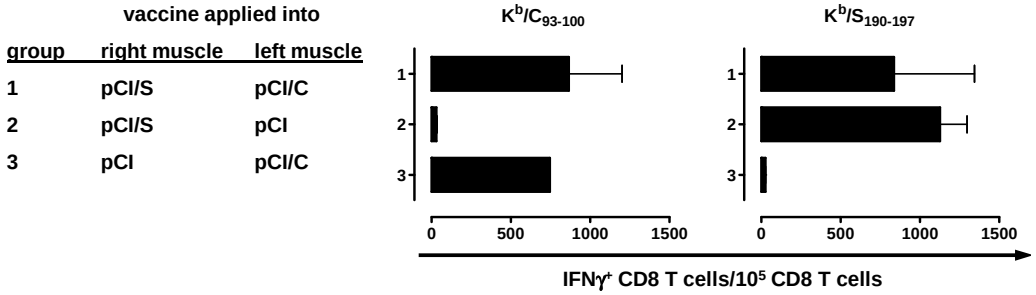

Figure 33.: Spatially divided administration of vaccines circumvents immunodominance. B6 mice (four mice per group) were immunized with 50 µg pCI/S (into the right muscle) and 50 µg pCI/C (into the left muscle) (groups 1), 50 µg pCI/S (into the right muscle) and 50 µg pCI (into the left muscle) (groups 2), or with 50 µg pCI/C (into the left muscle) and 50 µg pCI (into the right muscle)(groups 3). The specific CD8 T cell responses were analyzed twelve days after injection by 4 h ex vivo restimulation of splenic T cells with the $K^b/S_{190-197}$ or the K^b/C_{93-100} peptide, followed by determination of IFNγ^+ CD8 T cell frequencies.

3.3. Subdominant, K^b/C_{93-100}-specific CD8 T cells showed enhanced anti-viral activity

The above analysis identified the K^b/C_{93-100} epitope of HBV as a subdominant epitope, that was easily suppressed by various CD8 T cell responses ($K^b/OVA_{257-264}$ and $K^b/S_{190-197}$) in the model systems used. As subdominant epitopes have previously been shown to break T cell tolerance, it was investigated if the identified, K^b/C_{93-100}-specific CD8 T cell response was able to break CD8 T cell tolerance in 1.4 HBV-S^{mut} tg B6 mice. This line contains a terminally redundant 1.4 viral HBV construct driving the expression of all HBV-derived proteins (LS, MS, Pol, HBeAg, HBcAg, X) except the HBsAg, which is not translated due to a mutation introduced at the translation start codon of the HBsAg gene. Immunoprecipitation followed by Western blot analysis showed expression of the non-glycosylated and glycosylated LS isoforms in the liver of 1.4 HBV-S^{mut} tg B6 mice (figure 34a, lane 2). In contrast to Alb/HBs tg mice, no HBsAg was found in sera of 1.4 HBV-S^{mut} tg B6 mice (figure 34b). However, HBeAg was readily detected in the sera of 1.4 HBV-S^{mut} tg B6 mice (figure 34c). Western blot analyses also confirmed the expression of HBcAg in the liver (figure 34d).

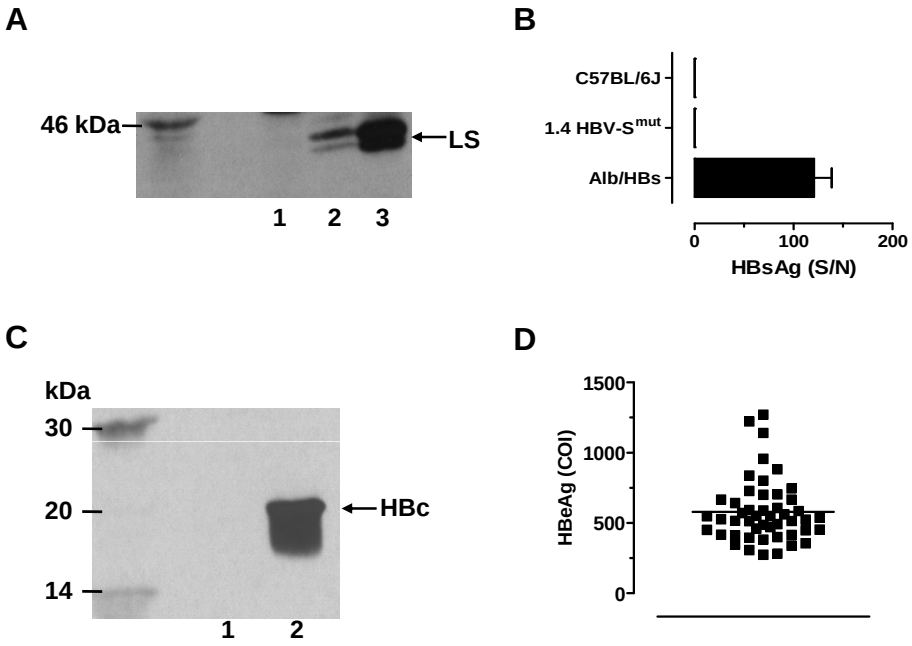

Figure 34.: Characterization of 1.4 HBV-S^{mut} tg B6 mice. **a** Expression of the large surface (LS) antigen. Liver lysates from C57BL6/J (lane 1), 1.4 HBV-S^{mut} tg B6 (lane 2) and Alb/HBs tg (lane 3) mice were immunoprecipitated using a polyclonal rabbit anti-HBsAg serum to capture all HBV envelope. The LS antigen was detected with the preS1-specific antibody mAb MA18/7 by western blotting. **b** HBsAg concentration in the serum of C57BL/6J, 1.4 HBV-S^{mut} tg B6 and Alb/HBs tg mice was determined by the commercial ELISA AUSZYME II. **c** HBeAg levels in sera of 1.4 HBV-S^{mut} tg B6 mice (n=48) were determined by using ElectroChemiLuminescence ImmunoAssay (COI, cutoff-index). **d** HBcAg expression in the liver of 1.4 HBV-S^{mut} tg B6 mice was determined by western blotting using a HBcAg-specific antibody. Equal amounts of liver lysates from C57BL/6J (lane 1) and 1.4 HBV-S^{mut} tg B6 mice (lane 2) were analyzed.

1.4 HBV-S^{mut} tg B6 mice were immunized with either the pCI/S or the pCI/C vaccine and analyzed for induction of specific CD8 T cells. Single or repeated injections of pCI/S into 1.4 HBV-S^{mut} tg B6 mice didn't elicit K^b/S$_{190-197}$-specific CD8 T cell immunity in spleen or liver (figure 35a, groups 1). In contrast, a single injection of pCI/C primed K^b/C$_{93-100}$-specific CD8 T cell responses in 1.4 HBV-S^{mut} tg B6 mice (figure 35a, groups 2). K^b/C$_{93-100}$-specific CD8 T cells were readily detectable in the transgene-expressing liver (figure 35a, groups 2) but only barely detectable in the spleen. The kinetic of K^b/C$_{93-100}$-specific CD8 T cells in the liver of 1.4 HBV-S^{mut} tg B6 mice upon vaccination with pCI/C was analyzed (figure 35b). Between day 7 and 11 after immunization, a massive expansion of K^b/C$_{93-100}$-specific CD8 T cells in the liver was observed resulting in a peak of about 10% K^b/C$_{93-100}$-specific intrahepatic CD8 T cells at day 11 post-vaccination. However, K^b/C$_{93-100}$-specific CD8 T cells in the liver rapidly declined thereafter (figure 35b). Therefore, vaccination with pCI/C bearing the subdominant K^b/C$_{93-100}$ epitope but not vaccination with pCI/S bearing the immunodominant K^b/S$_{190-197}$ epitope was able to break the T cell tolerance in 1.4 HBV-S^{mut} tg B6 mice demonstrating that subdominant epitopes can show improved tolerance-breaking features.

The functionality of K^b/C$_{93-100}$-specific CD8 T cells accumulated in the liver of 1.4 HBV-S^{mut} tg B6 mice upon vaccination with pCI/C (figure 35a, groups 2) was analyzed by determination of HBV replication levels. Southern blot analyses of liver DNA obtained from non-immunized or pCI-injected 1.4 HBV-S^{mut} tg B6 mice showed three prominent bands corresponding to the expected sizes of the relaxed circular (RC) DNA, the double-stranded (DS) DNA and the single stranded (SS) DNA species of HBV (figure 36a). The analysis didn't reveal a covalently closed circular (ccc) DNA species. Reduced HBV replication in the liver of 1.4 HBV-S^{mut} tg B6 mice was observed 11 days after immunization with pCI/C (figure 36a) but not after immunization with the pCI/S vaccine. In addition to reduced HBV replication, focal T cell infiltrates in the liver of pCI/C-immunized 1.4 HBV-S^{mut} tg B6 mice could be detected by immunohistology (figure 36b). Although infiltrating the liver and reducing the HBV replication level, the Core-specific, anti-viral CD8 T cells didn't elicit a rise in serum transaminase levels (figure 36c). Anti-viral CD8 T cells could thus deliver their inhibitory effect on viral replication without the destruction of hepatocytes. However, the reduction in HBV replication was transient as it rebounded

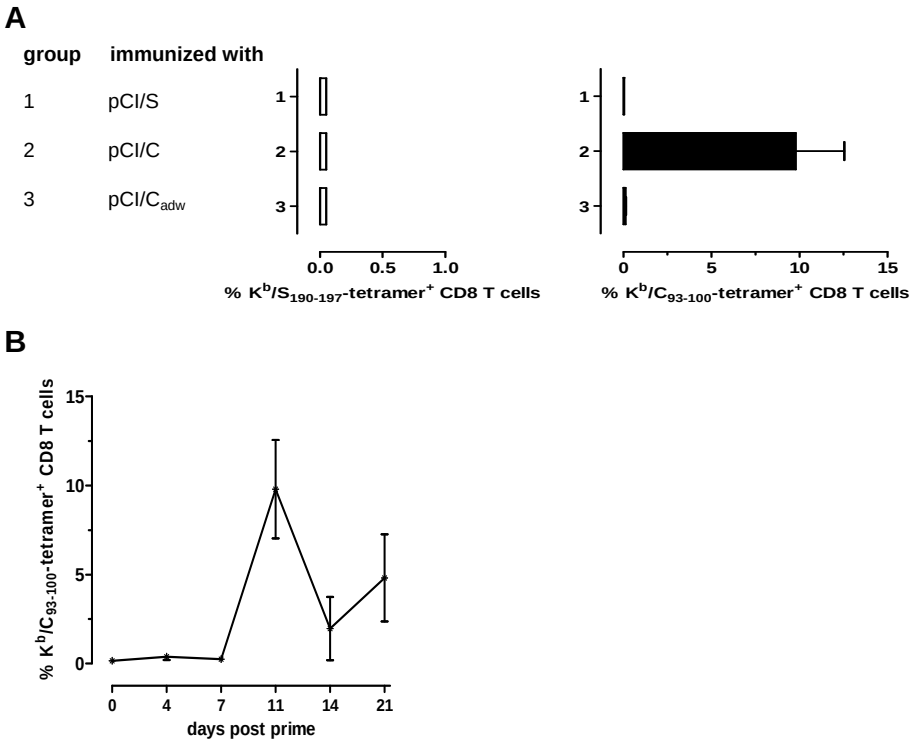

Figure 35.: Subdominant CD8 T cells could break T cell tolerance. **a** 1.4 HBV-S^{mut} tg B6 mice (three mice per group) were immunized with pCI/S (groups 1), pCI/C (groups 2), or with pCI/C$_{adw}$ (groups 3). The specific CD8 T cell responses were determined eleven days after injection by K^b/S$_{190-197}$- and K^b/C$_{93-100}$-specific tetramer staining of liver T cells. **b** 1.4 HBV-S^{mut} tg B6 mice (three mice per group) were immunized with pCI/C. K^b/C$_{93-100}$-specific CD8 T cells in the liver were determined by tetramer staining at the indicated time points post-vaccination.

at day 21 post-immunization, i.e. at a time point at which most K^b/C_{93-100}-specific CD8 T cells had disappeared from the liver (figure 35b).

Immunization studies were performed using the pCI/C vaccine that encoded the HBcAg of the D genotype identical to that expressed by the 1.4 HBV-S^{mut} tg B6 mouse). A pCI/C_{adw} vaccine encoding the HBcAg of the A genotype didn't induce K^b/C_{93-100}-specific CD8 T cells in B6 as well as 1.4 HBV-S^{mut} tg B6 mice (figure 35a, groups 3). The pCI/C_{adw} vaccine also failed to reduce the HBV replication in 1.4 HBV-S^{mut} tg B6 mice (figure 36a). An exchange of the central anchor motif at position 5 from a F to an I (table 8) is likely to destroy the antigenicity of the K^b/C_{93-100} epitope of the A genotype. These findings thus confirmed that CD8 T cell responses to the subdominant K^b/C_{93-100} epitope play a central role in the inhibition of HBV replication in this model. Therefore, a single vaccination with pCI/C transiently induced a functional but non-cytotoxic K^b/C_{93-100}-specific CD8 T cell immunity in this model.

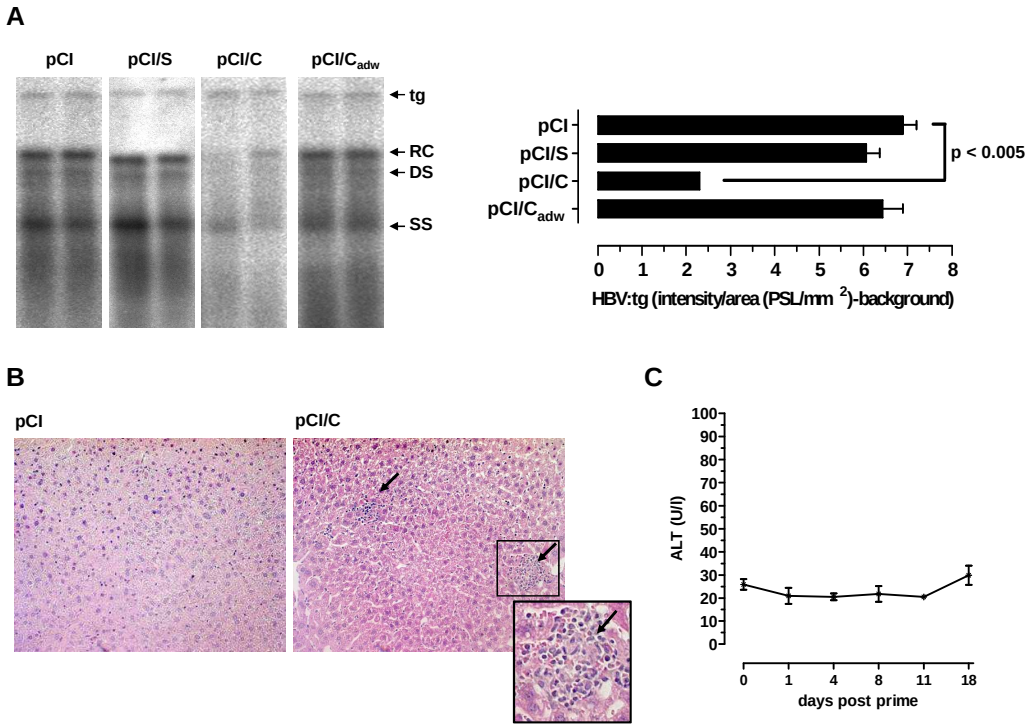

Figure 36.: pCI/Core-induced K^b/C_{93-100}-specific CD8 T cells inhibit viral replication in the liver of 1.4 HBV-S^{mut} tg B6 mice. **a** 1.4 HBV-S^{mut} tg B6 mice were immunized with pCI, pCI/S, pCI/C, or with pCI/C_{adw}. Eleven days after injection HBV replication in the livers of immunized mice was determined by Southern blot analysis. (tg) integrated transgene, (RC) relaxed circular, (DS) double-stranded linear and (SS) single-stranded linear DNA species are indicated. Two representative mice per group are shown. Bands for the integrated transgene are used for normalization of the amount of HBV specific DNA bound to the membrane. Quantification of HBV replication (in 3-6 mice) is demonstrated as ratio of HBV replicates/transgene. **b** Eleven days after vaccination with pCI (left panel) or pCI/C (right panel) livers of 1.4 HBV-S^{mut} tg B6 mice were analyzed by histology (H&E staining). Focal T cell infiltrates are indicated by arrows. **c** Sera of pCI/C-immunized 1.4 HBV-S^{mut} tg B6 mice were analyzed for serum alanine aminotransferase (ALT) activity at the indicated time points post-vaccination.

4. Discussion

4.1. Recombinant complexes of antigen with Hsp are potent CD8 T cell stimulating immunogens

In the present study a Hsp-binding chimeric antigen construct pCI/T_{1-77}-SFG (figure 3) was designed and expressed in transiently transfected HEK 293 cells. Expression analyses revealed that for efficient expression the functional J domain of the SV40 T-Ag (T_{1-77}) and thus expression in a Hsp-bound form was essential (figure 4, lane c). This confirmed previous reports that expression of chimeric antigens is facilitated by Hsp-association [98, 107, 109, 111]. The N-terminal addition of a Strep-tag (pCI/StT-SFG) altered neither the Hsp-binding capability of the J domain nor the recognition by the anti-T-Ag mAb used for immunoprecipitation (figure 4, lane d). Therefore, the N-terminal Strep-tag didn't influence the structure and function of the viral J domain but was accessible and thus allowed the purification of native Hsp/antigen complexes of high purity for the first time (figure 5a). In contrast, other purification strategies involving anti-T-Ag antibodies or incorporation of histidine- or calmodulin-tags into the chimeric antigen T-SFG failed due to rigid extraction and purification conditions.

Hsp-association of chimeric antigens resulted in cytosolic accumulation and prevented their translocation into the ER and subsequent secretion (figure 6) supporting previous reports that Hsp-binding to the J domain prevents secretion of fusion proteins [37,98]. In addition, Hsp-association markedly affected the structural properties of the fused antigens as demonstrated by the significantly quenched fluorescence intensity of the Hsp-complexed StT-SFG (figure 6, figure 7). Small but significant changes in the antigen-structure could also explain the efficient expression of toxic proteins in a Hsp-bound form [97, 99].

Chimeric antigens expressed in transiently transfected human HEK 293 efficiently captured the constitutively (Hsp73) as well as the inducible (Hsp70) Hsp isoform (figure 5b). A similar pattern was observed in adenoviral-transduced human HeLa cells (figure 9). However, Hsp/antigen complexes purified from stably transfected CHO cells contained only the constitutively expressed Hsp73 isoform (figure 15a,b). This was in accordance with previous reports that analyzed the expression of chimeric T-Ag fusion proteins in cell lines derived of rodent, monkey or avian origin and demonstrated the accumulation of Hsp73/antigen complexes [109,111]. It is unknown if HEK 293 and HeLa cells constitutively express the inducible Hsp70 isoform or if its induced by transfection/transduction-mediated stress. As capturing of Hsp70 by the viral J domain seemed to be restricted to human cell lines, this could also reflect a intrinsic, species-specific feature of human Hsp70. Although differing in composition of associated Hsp isoforms, chimeric antigens containing the J domain of the SV40 T-Ag were efficiently expressed as Hsp/antigen complexes in all tested eukaryotic cells demonstrating that Hsp-binding exerted by the viral J domain is species independent.

Hsp/antigen complexes derived of stably transfected CHO as well as transiently transfected HEK 293 differed in the complexed Hsp isoforms as well as the species origin (figure 15a,b). Despite these differences, CHO-derived Hsp70/antigen complexes as well as HEK 293-derived Hsp70/73 complexed antigen efficiently primed comparable amounts of antigen-specific CD8 T cells (figure 15c) suggesting that immunogenicity of Hsp/antigen complexes is independent of the complexed Hsp isoform as well as of the species origin of Hsp. Because of the binding of Hsp to the viral J domain as well as the immunogenicity of Hsp/antigen complexes is species independent, effective vaccines based on Hsp/antigen complexes can be produced in a large panel of cell lines. This enables vaccine production in the same species as the vaccine recipient thereby minimizing the potential to induce autoimmune responses.

Because of possible concerns due to the viral origin of the used J domain of the SV40 T-Ag, it was investigated if J domains derived of bacterial (*Chlamydia trachomatis*) or plant (*Arabidopsis thaliana*) origin are able to bind human Hsp70/73. Despite significant differences in their amino acid composition (figure 19a), bacterial -as well as plant-derived J domains were able to efficiently capture human Hsp70/73 and thus facilitated the expression of chimeric antigens comparable to the viral J domain of the SV40 T-Ag (figure 20a). In accordance with facilitated expression and Hsp-association, DNA vaccination with chimeric antigen constructs fused to the

investigated J domains elicited comparable CD8 T cell responses (figure 20b). In addition, it was also possible to design a chimeric J domain consisting of the 33 N-terminal residues of the T_{77} domain and the 46 C-terminal residues of the *Chlamydia trachomatis*-derived J domain that was able to capture Hsp and showed enhanced immunogenicity upon DNA vaccination. The Hsp-facilitated antigen expression system is thus exceptionally flexible because it can exploit a large variety of natural or chimeric J domains from different sources and, in addition, can be transferred to a large panel of cell lines. Another benefit of the developed system is that, in addition to Hsp/antigen complexes, Hsp as well as the antigen can be separately purified due to the ATP-dependent binding of the J domain to Hsp [109]. Thus, Hsp could be gently removed from StrepTactin-bound antigen by ATP-treatment (figure 9).

Hsp/StT-OVA-G complexes efficiently induced $K^b/OVA_{257-264}$-specific CD8 T cells in immunized B6 mice, whereas uncomplexed antigen as well as in vitro mixed Hsp and antigen failed to prime $K^b/OVA_{257-264}$-specific CD8 T cell responses (figure 10) indicating that immunogenic Hsp/antigen complexes were only formed in vivo and that Hsp-association was required to facilitate priming of CD8 T cells. This suggests that the enhanced cross-priming abilitiy of Hsp rather relies on specific delivery than on general immuno-stimulatory features [13, 14, 19]. Tested in vitro over a broad dose range, recombinant Hsp/antigen complexes purified from eukaryotic cell extracts didn't stimulate IFNα/β, IFNγ, IL-6 and IL-12 release from BM-DCs and didn't up-regulate the activation markers CD80 and CD86 (figure 18b). These complexes thus seem to contain only limited if any intrinsic adjuvant activity. This is in contrast to multiple reports that Hsp preparations efficiently activate the innate immune system [6, 7, 77, 92, 115, 122, 127, 128]. However, Hsp-stimulated activation of innate immunity may be triggered by agents contaminating Hsp preparations [11, 13, 14, 75, 130, 138] as the majority of Hsp preparations was produced by recombinant expression in bacteria. StT-OVA-G proteins expressed in bacteria efficiently complexed bacterial DnaK (i.e. the bacterial Hsp70 homolog). Bacterial DnaK/StT-OVA-G complexes showed significantly enhanced immunogenicity compared to Hsp/StT-OVA-G complexes derived of eukaryotic cells (figure 17). In addition, bacterial-derived DnaK/StT-OVA-G complexes efficiently stimulated BM-DCs to produce IL-6 as well as TNFα and to up-regulate the activation markers CD80 and CD86 (figure 18b) due to LPS contaminations. Thus, bacterial but not eukary-

otic Hsp/antigen complexes purified by the Strep-tag affinity purification system contained immuno-stimulating contaminants.

The immunogenicity of recombinant Hsp/antigen complexes could be significantly enhanced by co-delivery of defined adjunvants (such as AbISCO or CpG-containing ODN) (figure 14). Vaccines that enhance immune responses triggered by Hsp/antigen complexes can thus be designed using standard technologies. The Hsp-mediated effect of CD8 T cell priming is CD4 T cell independent as MHC-II deficient ($A\alpha^{-/-}$) B6 mice immunized with Hsp/antigen complexes (without further adjuvant) efficiently primed CD8 T cells (figure 11). However, CD4 T cells seemed to be able to enhance Hsp-mediated priming of CD8 T cells. Thus, enhanced immunogenicity of Hsp-complexed antigens is rather based on specific delivery (including uptake, intracellular traffic and antigen processing) [14, 19] than on innate immuno-stimulating activity and CD4 T cell help. The lack of an intrinsic, innate adjuvant activity of Hsp was further supported by analyses of IgG isotype profiles of Hsp/StT-OVA-G immunized B6 mice that showed a Th2 directed immune response (figure 13).

Enhanced immunogenicity of Hsp/antigen complexes wasn't restricted to the cellular immune response as Hsp/StT-OVA-G complexes also efficiently induced a GFP-specific serum antibody response (figure 12b) that was markedly increased compared to vaccination with uncomplexed StT-OVA-G fusion protein. Despite efficient induction of GFP-specific antibodies, no Hsp-specific antibodies were produced upon vaccination with human-derived Hsp/StT-OVA-G complexes supporting previous findings that human Hsp70/73 delivered as recombinant protein exhibits only low if any immunogenicity for murine B cells [108]. Hsp-complexed antigens thus efficiently primed humoral as well as cellular immune responses in mice without inducing Hsp-specific antibodies that could potentially lead to autoimmune responses.

Hsp/antigen complexes were also able to induce human relevant Flu-Ma_{58-66}-specific CD8 T cell responses in a HLA-A*0201-tg mouse model demonstrating that Hsp-mediated priming of CD8 T cells is independent of MHC-I restriction (figure 22b) but strictly dependent on Hsp-association. In addition, prime/boost regimens showed that Flu-Ma_{58-66}-specific CD8 T cell responses primed by Hsp/StT-SFG complexes can be efficiently boosted by a second injection of Hsp/StT-SFG complexes (figure 22a). Although recombinant Hsp/StT-SFG complexes efficiently stimulated CD8 T cell responses in mice, the respective DNA-based vaccine pCI/StT-SFG encoding the same antigen complexed to endogenous murine Hsp of transduced APCs induced

three- to fourfold higher Flu-Ma_{58-66}-specific CD8 T cell responses (figure 23b). This demonstrates the exceptional efficacy of DNA vaccination in priming murine CD8 T cell responses [49] as DNA vaccines allow expression of antigens and generation of their antigenic peptides in the conventional 'endogenous' antigen processing and presentation pathway [33]. Although DNA vaccines have demonstrated high immunogenicity and the ability to induce protective immunity in multiple preclinical disease models, their application in humans is limited because of inefficient DNA delivery techniques [49]. Although the involved processing and presentation mechanism are mainly unknown [18, 23, 33, 97] protein-based vaccines delivered in a Hsp-bound form are a promising approach that allows induction of humoral as well as cellular immune responses.

Immunodominance is a well-documented but ill-defined phenomenon [139] limiting the efficacy of multivalent vaccines to induce multispecific CD8 T cell responses. This was demonstrated by vaccination of BALB/c mice with vaccines encoding a chimeric antigen construct (pCI/St-X-PCL). $K^d/Pol_{140-148}$- as well as K^d/LLO_{91-98}-specific CD8 T cell responses were efficiently primed but seemed to suppress the induction of K^d/C_{87-95}-specific CD8 T cells (figure 20b). In addition, immunodominance of the well characterized Flu-Ma_{58-66} epitope and its cognate CD8 T cell response was observed upon vaccination of HLA-A*0201-tg mice with vaccines bearing the immunodominant Flu-Ma_{58-66} epitope (figure 23b). Although DNA vaccination with pCI/T-SFG induced significantly higher Flu-Ma_{58-66}-specific CD8 T cell responses compared to immunization with Hsp/StT-SFG complexes, both vaccination protocols resulted in the striking suppression of HBsAg-specific CD8 T cell responses. This demonstrates that the observed immunodominance is independent of the applied vaccination protocol allowing to skip the time-consuming production of Hsp-complexed antigens and analyze the impact of vaccine modifications by DNA vaccination. A DNA vaccine lacking the Flu-Ma_{58-66} epitope (pCI/T-SG) efficiently primed subdominant HBsAg-specific CD8 T cell responses in HLA*0201-tg mice (figure 23b) indicating that the Flu-Ma_{58-66}-specific CD8 T cell response solely suppresses the HBsAg-specific immunity. Therefore, deletion of immunodominant epitopes seems to be a way to circumvent immunodominance hierarchies [70] that are not attenuated by delivering the antigens in Hsp-bound form [107].

4.2. Hsp-binding multidomain vaccines are subjected to immunodominance

Immunodominance was shown to have massive effects on priming of multispecific CD8 T cell responses upon vaccination [113] as well as during infection [104] potentially avoiding complete pathogen elimination and thus favoring chronic infections [126]. However, little is known about how immunodominant and subdominant determinants are distinguished by the CD8 T cell system. Immunodominance has been observed between epitopes from viruses [24, 47, 88, 94, 105, 123], minor histocompatibility antigens [135] and model antigens [25]. Several factors have been proposed to contribute to immunodominance including factors on the APC side, e.g., kinetics of viral protein expression [94], efficiency of antigen processing [9, 24, 26, 90], binding affinity of peptides to MHC-I molecules [25, 64, 139], stability of the MHC-I:peptide complexes [129] and competition between MHC-I alleles for cell surface expression [123], as well as factors on the responding T cell side, e.g., competition [102,105] or interference [135] between responding T cells, or T cells and APCs [61, 133], kinetics of T cell responses to Ag [69], TCR avidity [61, 124], variations in the naive T cell repertoire [29, 39, 47, 64, 87] and regulatory T cells selectively suppressing certain responses [8, 50]. Antigen processing efficiency and MHC-I-restricted epitope presentation unlikely caused the observed immunodominance of $K^b/OVA_{257-264}$- or $K^b/S_{190-197}$-specific CD8 T cell in B6 mice (figure 27) as well as 'co-immunodominance' of A*0201/C_{18-27}- and A*0201/$Pol_{803-811}$- CD8 T cell responses in HLA-A*0201-tg mice (figure 25) as epitope-bearing domains were incorporated into the HBV multidomain vaccines including sufficient epitope-flanking sequences to ensure proper processing. In accordance with studies circumventing immunodominance by epitope modifications [70], elimination of antigenic domains bearing immunodominant epitopes efficiently induced previously suppressed (subdominant) CD8 T cell specifities and thus successfully altered immunodominance hierarchy. Vaccination studies analyzing the effect of endogenous Hsp-association of antigen revealed that Hsp-binding significantly increased CD8 T cell responses but didn't support priming of subdominant CD8 T cell specificities (figure 27). In contrast to the previously reported circumvention of L^d-mediated 'inter-restrictional' immunodominance [107], Hsp association couldn't overcome the observed immuno-

dominance phenomenon suggesting that in this setting another immunodominance mechanism is active. A simple epitope competition model for K^b-molecules also couldn't account for the observed immunodominance hierarchy as the investigated epitopes showed comparable binding affinities (table 8). Moreover, immunization of Alb/HBs tg mice with pCI/StT-SCC demonstrated that the K^b/C_{93-100} epitope was correctly processed and sufficiently presented on the surface of APCs to prime K^b/C_{93-100}-specific CD8 T cell responses (figure 30). However, priming of subdominant K^b/C_{93-100}-specific CD8 T cell responses was dependent on the absence of immunodominant $K^b/S_{190-197}$-specific CD8 T cells suggesting that differences in the precursor frequency or intrinsic features of naive CD8 T cells specific for dominant versus subdominant epitopes play a role in the described immunodominance hierarchy [64, 87]. Partial suppression of K^b/C_{93-100}-specific CD8 T cell responses was also observed by immunization with a mix of HBcAg- and HBsAg-encoding plasmids (figure 32) supporting an immunodominance mechanism independent of general antigen processing. In accordance with other reports [70], spatially separated injection of DNA vaccines containing either an immunodominant epitope (HBsAg) or a subdominant epitope (HBcAg) primed subdominant as well as immunodominant CD8 T cell responses at the same time (figure 33). These data suggest a 'local regulator model' in which differential recruitment of CD8 T cells with different recognition specificities, differential efficiencies in synapse formation with APCs, different relative efficiencies in the commitment for the priming program or the clonal expansion may operate.

The data have practical implications for understanding anti-viral CD8 T cell responses and for the rational design of T cell-stimulating vaccines. Escape mutations in an immunodominant epitope eliminating its antigenicity don't necessarily lead to an inability to clear the infection but may pave the way for a broad range of subdominant T cell responses. Delivery of multiple polytope vaccines with a limited number of epitopes to different sites at different times may be more efficient in stimulating multispecific T cell responses than delivery of many epitopes at the same time to the same site. This may be even more important in clinical settings in which unpredictable immunodominance hierarchies could develop due to the MHC heterogeneity of man. Thus, less may be more.

4.3. Priming of subdominant, K^b/C_{93-100}-specific CD8 T cells breaks tolerance and exerts anti-viral activity in a HBV-tg mouse model

A distinct immunodominance hierarchy was revealed by vaccination with HBV multidomain vaccines. As CD8 T cell responses directed against subdominant epitopes are able to break tolerance [114] it was investigated whether the identified, subdominant, K^b/C_{93-100}-specific CD8 T cell response is also able to break tolerance in a HBV tg mouse model. The 1.4HBV-S^{mut} tg line –a variant of the well-established 1.3HBV model [48]– was used to detect anti-viral CD8 T cells.

The immunodominant $K^b/S_{190-197}$ epitope efficiently suppressed the priming of K^b/C_{93-100}-specific CD8 T cell responses in B6 mice (figure 30) but failed to prime $K^b/S_{190-197}$-specific CD8 T cells in 1.4HBV-S^{mut} tg mice (figure 35a). In contrast, K^b/C_{93-100}-specific CD8 T cells were readily primed in 1.4HBV-S^{mut} tg mice and showed anti-viral activity. This was unexpectedly as 1.4HBV-S^{mut} tg mice expressed only low amounts of LS and MS in the liver without secretion of HBsAg into the circulation (figure 34) and were expected to allow peripheral priming of HBsAg-specific CD8 T cells. This assumption was obviously wrong. High levels of HBsAg in the circulation (as found in HBsAg-tolerant Alb/HBs tg mice) are thus not critical for establishing tolerance to HBsAg. In contrast, the tolerance could be broken by vaccination with the pCI/C vaccine which efficiently primed subdominant, K^b/C_{93-100}-specific CD8 T cells even in the presence of large amounts of HBeAg (the secreted HBcAg 'variant'). The presence of an antigen in the serum thus doesn't exclude (HBeAg in 1.4HBV-S^{mut} tg mice) nor imply (HBsAg in Alb/HBs tg mice) its ability to break T cell tolerance. It rather seems that subdominant CD8 T cell epitopes/responses are the major player in this game. These autoreactive CD8 T cells accumulated in the liver of 1.4HBV-S^{mut} tg mice and exerted anti-viral, non-cytotoxic functions (figure 36) upon immunization with the pCI/C vaccine. However, the accumulation of K^b/C_{93-100}-specific CD8 T cells and their inhibitory effect on viral replication in the liver was transiently and down regulated by unknown mechanisms. This suggests that efforts to induce protective as well as therapeutic anti-viral T cell immunity should include a consideration of the cryptic repertoire of subdominant epitopes.

5. Summary

Heat shock proteins (Hsp) of the Hsp70/90 families facilitate cellular immune responses to antigenic peptides or proteins bound to them and have therefore been used as vaccine vehicles. We have developed an expression system in which chimeric proteins with a Hsp-capturing, viral J domain fused to diverse antigen-encoding sequences form stable complexes with eukaryotic (Hsp70, Hsp73) stress proteins and accumulate to high steady state levels.

In the first part of the thesis, the molecular interaction of different J domains with cellular Hsp70/73 was characterized. Chimeric model antigens were fused C-terminally to J domains from different species (viruses/SV40, bacteria/*Chlamydia trachomatis* or plants/*Arabidopsis thaliana*) and tested if they bind cellular Hsp70/73. These J domains differ significantly in their amino acid composition but efficiently captured murine or human Hsp70/73 proteins and facilitated antigen expression equally well. Furthermore, the different J domains were able to capture eukaryotic Hsp70/73 as well as bacterial Hsp70 (DnaK) thus enabling vaccine production in a large panel of cell lines. We tested different tags to isolate complexes of chimeric antigens with Hsp70/73 and were successful to purify native Hsp/antigen complexes using a streptavidin-binding tag 'Strep-tag' cloned N-terminally in frame to the Hsp-binding J domain. This allowed us to establish a method to efficiently purify Hsp/antigen complexes as well as its isolated components with high purity. Hsp/antigen complexes efficiently elicited antigen-specific CD8 T cell responses in mice when delivered as vaccines without adjuvants. The described expression system thus supports the flexible design of multivalent, CD8 T cell-stimulating vaccines.

In the second part of the thesis, we investigated whether immunodominance hierarchies between CD8 T cell epitopes limit the potential of multivalent, Hsp-binding vaccines. Immunodominance is a well documented but ill-defined feature of many T cell responses. We demonstrated that incorporation of an immunodominant, Flu-specific epitope (HLA-A*0201/Flu-Ma_{58-66}) into recombinant Hsp-capturing vac-

cines resulted in a striking suppression of HBsAg-specific CD8 T cell responses (i.e. HLA-A*0201/$S_{185-194}$ and HLA-A*0201/$S_{208-216}$). Immunodominance was independent of MHC-I restriction as comparable effects were observed analyzing murine H2-K^b-restricted epitopes. K^b/$OVA_{257-264}$- and K^b/$S_{190-197}$-specific CD8 T cell responses didn't allow priming of a K^b/C_{93-100}-specific CD8 T cell response in mice immunized with multidomain vaccines. These distinct immunodominance hierarchies weren't due to general antigen processing efficiency and epitope competition as tolerance to the HBsAg in transgenic (tg) Alb/HBs mice (that express large amounts of transgene-encoded HBsAg in the liver) facilitated priming of subdominant, K^b/C_{93-100}-specific CD8 T cell immunity by multidomain antigens. The 'weak' (i.e. easily suppressed) K^b/C_{93-100}-specific CD8 T cell response was efficiently elicited by a HBcAg-encoding vector in 1.4 HBV-S^{mut} tg mice mice (that harbor a replicating HBV genome producing HBV antigens in the liver). K^b/C_{93-100}-specific CD8 T cells accumulated in the liver of vaccinated 1.4 HBV-S^{mut} tg mice mice and suppressed HBV replication. Subdominant epitopes in vaccines can hence prime specific CD8 T cell immunity in a tolerogenic milieu and deliver specific anti-viral effects to HBV-expressing hepatocytes.

6. Bibliography

[1] Akbari, O., Panjwani, N., Garcia, S., Tascon, R., Lowrie, D., Stockinger, B. *DNA vaccination: transfection and activation of dendritic cells as key events for immunity.* J Exp Med 1999; 189:169–178.

[2] Albert, M.L., Pearce, S.F., Francisco, L.M., Sauter, B., Roy, P., Silverstein, R.L., Bhardwaj, N. *Immature dendritic cells phagocytose apoptotic cells via alphavbeta5 and CD36, and cross-present antigens to cytotoxic T lymphocytes.* J Exp Med 1998; 188:1359–1368.

[3] Albert, M.L., Sauter, B., Bhardwaj, N. *Dendritic cells acquire antigen from apoptotic cells and induce class I-restricted CTLs.* Nature 1998; 392:86–89.

[4] Arnold-Schild, D., Kleist, C., Welschof, M., Opelz, G., Rammensee, H.G., Schild, H., Terness, P. *One-step single-chain Fv recombinant antibody-based purification of gp96 for vaccine development.* Cancer Res 2000; 60:4175–4178.

[5] Asea, A. *Stress proteins and initiation of immune response: chaperokine activity of hsp72* Exerc.Immunol.Rev. 2005; 11:34–45.

[6] Asea, A., Kraeft, S., Kurt-Jones, E., Stevenson, M., Chen, L., Finberg, R., Koo, G., Calderwood, S. *HSP70 stimulates cytokine production through a CD14-dependant pathway, demonstrating its dual role as a chaperone and cytokine* Nat.Med. 2000; 6:435–442.

[7] Asea, A., Rehli, M., Kabingu, E., Boch, J.A., Bare, O., Auron, P.E., Stevenson, M.A., Calderwood, S.K. *Novel signal transduction pathway utilized by extracellular HSP70: role of toll-like receptor (TLR) 2 and TLR4.* J Biol Chem 2002; 277:15028–15034.

[8] Assarsson, E., Sidney, J., Oseroff, C., Pasquetto, V., Bui, H.H., Frahm, N., Brander, C., Peters, B., Grey, H., Sette, A. *A quantitative analysis of the variables affecting the repertoire of T cell specificities recognized after vaccinia virus infection.* J Immunol 2007; 178:7890–7901.

[9] Basler, M., Youhnovski, N., Broek, M.V.D., Przybylski, M., Groettrup, M. *Immunoproteasomes down-regulate presentation of a subdominant T cell epitope from lymphocytic choriomeningitis virus.* J Immunol 2004; 173:3925–3934.

[10] Basu, S., Binder, R.J., Ramalingam, T., Srivastava, P.K. *CD91 is a common receptor for heat shock proteins gp96, hsp90, hsp70, and calreticulin.* Immunity 2001; 14:303–313.

[11] Bausinger, H., Lipsker, D., Ziylan, U., Manie, S., Briand, J., Cazenave, J., Muller, S., Haeuw, J., Ravanat, C., de la, S.H., Hanau, D. *Endotoxin-free heat-shock protein 70 fails to induce APC activation* Eur.J.Immunol. 2002; 32:3708–3713.

[12] Becker, T., Hartl, F.U., Wieland, F. *CD40, an extracellular receptor for binding and uptake of Hsp70-peptide complexes.* J Cell Biol 2002; 158:1277–1285.

[13] Bendz, H., Marincek, B.C., Momburg, F., Ellwart, J.W., Issels, R.D., Nelson, P.J., Noessner, E. *Calcium signaling in dendritic cells by human or mycobacterial Hsp70 is caused by contamination and is not required for Hsp70-mediated enhancement of cross-presentation.* J Biol Chem 2008; 283:26477–26483.

[14] Bendz, H., Ruhland, S.C., Pandya, M.J., Hainzl, O., Riegelsberger, S., Braüchle, C., Mayer, M.P., Buchner, J., Issels, R.D., Noessner, E. *Human heat shock protein 70 enhances tumor antigen presentation through complex formation and intracellular antigen delivery without innate immune signaling.* J Biol Chem 2007; 282:31688–31702.

[15] Berwin, B., Rosser, M.F.N., Brinker, K.G., Nicchitta, C.V. *Transfer of GRP94 (Gp96)-associated peptides onto endosomal MHC class I molecules.* Traffic 2002; 3:358–366.

[16] Berwin, B., Hart, J.P., Rice, S., Gass, C., Pizzo, S.V., Post, S.R., Nicchitta, C.V. *Scavenger receptor-A mediates gp96/GRP94 and calreticulin internalization by antigen-presenting cells.* EMBO J 2003; 22:6127–6136.

[17] Binder, R.J., Han, D.K., Srivastava, P.K. *CD91: a receptor for heat shock protein gp96.* Nat Immunol 2000; 1:151–155.

[18] Binder, R. *Heat shock protein vaccines: from bench to bedside* Int.Rev.Immunol. 2006; 25:353–375.

[19] Binder, R., Blachere, N., Srivastava, P. *Heat shock protein-chaperoned peptides but not free peptides introduced into the cytosol are presented efficiently by major histocompatibility complex I molecules* J.Biol.Chem. 2001; 276:17163–17171.

[20] Binder, R., Srivastava, P. *Peptides chaperoned by heat-shock proteins are a necessary and sufficient source of antigen in the cross-priming of CD8+ T cells* Nat.Immunol. 2005; 6:593–599.

[21] Binder, R.J., Kelly, J.B., Vatner, R.E., Srivastava, P.K. *Specific immunogenicity of heat shock protein gp96 derives from chaperoned antigenic peptides and not from contaminating proteins.* J Immunol 2007; 179:7254–7261.

[22] Brodsky, J., Pipas, J. *Polyomavirus T antigens: molecular chaperones for multiprotein complexes* J.Virol. 1998; 72:5329–5334.

[23] Castellino, F., Boucher, P., Eichelberg, K., Mayhew, M., Rothman, J., Houghton, A., Germain, R. *Receptor-mediated uptake of antigen/heat shock protein complexes results in major histocompatibility complex class I antigen presentation via two distinct processing pathways* J.Exp.Med. 2000; 191:1957–1964.

[24] Chen, W., Anton, L., Bennink, J., Yewdell, J. *Dissecting the multifactorial causes of immunodominance in class I-restricted T cell responses to viruses* Immunity. 2000; 12:83–93.

[25] Chen, W., Khilko, S., Fecondo, J., Margulies, D.H., McCluskey, J. *Determinant selection of major histocompatibility complex class I-restricted antigenic peptides is explained by class I-peptide affinity and is strongly influenced by nondominant anchor residues.* J Exp Med 1994; 180:1471–1483.

[26] Chen, W., Norbury, C., Cho, Y., Yewdell, J., Bennink, J. *Immunoproteasomes shape immunodominance hierarchies of antiviral CD8(+) T cells at the levels of T cell repertoire and presentation of viral antigens* J.Exp.Med. 2001; 193:1319–1326.

[27] Chisari, F.V., Pinkert, C.A., Milich, D.R., Filippi, P., McLachlan, A., Palmiter, R.D., Brinster, R.L. *A transgenic mouse model of the chronic hepatitis B surface antigen carrier state.* Science 1985; 230:1157–1160.

[28] Cho, B., Palliser, D., Guillen, E., Wisniewski, J., Young, R., Chen, J., Eisen, H. *A proposed mechanism for the induction of cytotoxic T lymphocyte production by heat shock fusion proteins* Immunity. 2000; 12:263–272.

[29] Choi, E.Y., Christianson, G.J., Yoshimura, Y., Sproule, T.J., Jung, N., Joyce, S., Roopenian, D.C. *Immunodominance of H60 is caused by an abnormally high precursor T cell pool directed against its unique minor histocompatibility antigen peptide.* Immunity 2002; 17:593–603.

[30] Ciupitu, A.M., Petersson, M., O'Donnell, C.L., Williams, K., Jindal, S., Kiessling, R., Welsh, R.M. *Immunization with a lymphocytic choriomeningitis virus peptide mixed with heat shock protein 70 results in protective antiviral immunity and specific cytotoxic T lymphocytes.* J Exp Med 1998; 187:685–691.

[31] Ciupitu, A., Petersson, M., Kono, K., Charo, J., Kiessling, R. *Immunization with heat shock protein 70 from methylcholanthrene-induced sarcomas induces tumor protection correlating with in vitro T cell responses* Cancer Immunol.Immunother. 2002; 51:163–170.

[32] Clarke, S.R., Barnden, M., Kurts, C., Carbone, F.R., Miller, J.F., Heath, W.R. *Characterization of the ovalbumin-specific TCR transgenic line OT-I: MHC elements for positive and negative selection.* Immunol Cell Biol 2000; 78:110–117.

[33] Cresswell, P., Ackerman, A., Giodini, A., Peaper, D., Wearsch, P. *Mechanisms of MHC class I-restricted antigen processing and cross-presentation* Immunol.Rev. 2005; 207:145–157.

[34] Davis, H., Schirmbeck, R., Reimann, J., Whalen, R. *DNA-mediated immunization in mice induces a potent MHC class I-restricted cytotoxic T lymphocyte response to the hepatitis B envelope protein* Hum.Gene Ther. 1995; 6:1447–1456.

[35] Delneste, Y., Magistrelli, G., Gauchat, J., Haeuw, J., Aubry, J., Nakamura, K., Kawakami-Honda, N., Goetsch, L., Sawamura, T., Bonnefoy, J., Jeannin, P. *Involvement of LOX-1 in dendritic cell-mediated antigen cross-presentation.* Immunity 2002; 17:353–362.

[36] Denzel, M. *Entwicklung und Validierung einer neuen Immunisierungsstrategie: Induktion von Antikörper- und T-Zellantworten mit Stressprotein-komplexierten Antigenen.* Diplomarbeit, Universität Ulm 2006.

[37] El Kholy, S., Riedl, P., Kwissa, M., Reimann, J., Schirmbeck, R. *Selective expression of immunogenic, virus-like particle-derived antibody-binding epitopes* Intervirology 2002; 45:251–259.

[38] Enomoto, Y., Bharti, A., Khaleque, A., Song, B., Liu, C., Apostolopoulos, V., Xing, P., Calderwood, S., Gong, J. *Enhanced immunogenicity of heat shock protein 70 peptide complexes from dendritic cell-tumor fusion cells* J.Immunol. 2006; 177:5946–5955.

[39] Facchinetti, A., Santa, S.D., Mezzalira, S., Rosato, A., Biasi, G. *A large number of T lymphocytes recognize Moloney-murine leukemia virus-induced antigens, but a few mediate long-lasting tumor immunosurveillance.* J Immunol 2005; 174:5398–5406.

[40] Feltquate, D.M., Heaney, S., Webster, R.G., Robinson, H.L. *Different T helper cell types and antibody isotypes generated by saline and gene gun DNA immunization.* J Immunol 1997; 158:2278–2284.

[41] Firat, H., Tourdot, S., Ureta-Vidal, A., Scardino, A., Suhrbier, A., Buseyne, F., Rivière, Y., Danos, O., Michel, M.L., Kosmatopoulos, K., Lemonnier, F.A. *Design of a polyepitope construct for the induction of HLA-A0201-restricted HIV 1-specific CTL responses using HLA-A*0201 transgenic, H-2 class I KO mice.* Eur J Immunol 2001; 31:3064–3074.

[42] Fissolo, N., Riedl, P., Reimann, J., Schirmbeck, R. *DNA vaccines prime CD8+ T cell responses to epitopes of viral antigens produced from overlapping reading frames of a single coding sequence* Eur.J.Immunol. 2005; 35:117–127.

[43] Flechtner, J., Cohane, K., Mehta, S., Slusarewicz, P., Leonard, A., Barber, B., Levey, D., Andjelic, S. *High-affinity interactions between peptides and heat shock protein 70 augment CD8+ T lymphocyte immune responses* J.Immunol. 2006; 177:1017–1027.

[44] Flynn, G.C., Pohl, J., Flocco, M.T., Rothman, J.E. *Peptide-binding specificity of the molecular chaperone BiP.* Nature 1991; 353:726–730.

[45] Fynan, E.F., Webster, R.G., Fuller, D.H., Haynes, J.R., Santoro, J.C., Robinson, H.L. *DNA vaccines: protective immunizations by parenteral, mucosal, and gene-gun inoculations.* Proc Natl Acad Sci U S A 1993; 90:11478–11482.

[46] Gilkeson, G.S., Pippen, A.M., Pisetsky, D.S. *Induction of cross-reactive anti-dsDNA antibodies in preautoimmune NZB/NZW mice by immunization with bacterial DNA.* J Clin Invest 1995; 95:1398–1402.

[47] Gruta, N.L.L., Kedzierska, K., Pang, K., Webby, R., Davenport, M., Chen, W., Turner, S.J., Doherty, P.C. *A virus-specific CD8+ T cell immunodominance hierarchy determined by antigen dose and precursor frequencies.* Proc Natl Acad Sci U S A 2006; 103:994–999.

[48] Guidotti, L.G., Matzke, B., Schaller, H., Chisari, F.V. *High-level hepatitis B virus replication in transgenic mice.* J Virol 1995; 69:6158–6169.

[49] Gurunathan, S., Klinman, D., Seder, R. *DNA vaccines: immunology, application, and optimization** Annu.Rev.Immunol. 2000; 18:927–974.

[50] Haeryfar, S., DiPaolo, R., Tscharke, D., Bennink, J., Yewdell, J. *Regulatory T cells suppress CD8+ T cell responses induced by direct priming and cross-priming and moderate immunodominance disparities* J.Immunol. 2005; 174:3344–3351.

[51] Halpern, M.D., Kurlander, R.J., Pisetsky, D.S. *Bacterial DNA induces murine interferon-gamma production by stimulation of interleukin-12 and tumor necrosis factor-alpha.* Cell Immunol 1996; 167:72–78.

[52] Halverscheid, L., Mannes, N.K., Weth, R., Kleinschmidt, M., Schultz, U., Reifenberg, K., Schirmbeck, R., Nassal, M., Blum, H.E., Reimann, J., Geissler, M. *Transgenic mice replicating hepatitis B virus but lacking expression of the major HBsAg.* J Med Virol 2008; 80:583–590.

[53] Harmala, L.A.E., Ingulli, E.G., Curtsinger, J.M., Lucido, M.M., Schmidt, C.S., Weigel, B.J., Blazar, B.R., Mescher, M.F., Pennell, C.A. *The adjuvant effects of Mycobacterium tuberculosis heat shock protein 70 result from the rapid and prolonged activation of antigen-specific CD8+ T cells in vivo.* J Immunol 2002; 169:5622–5629.

[54] Hogquist, K.A., Jameson, S.C., Heath, W.R., Howard, J.L., Bevan, M.J., Carbone, F.R. *T cell receptor antagonist peptides induce positive selection.* Cell 1994; 76:17–27.

[55] Huang, Q., Richmond, J., Suzue, K., Eisen, H., Young, R. *In vivo cytotoxic T lymphocyte elicitation by mycobacterial heat shock protein 70 fusion proteins maps to a discrete domain and is CD4(+) T cell independent* J.Exp.Med. 2000; 191:403–408.

[56] Ichino, M., Mor, G., Conover, J., Weiss, W.R., Takeno, M., Ishii, K.J., Klinman, D.M. *Factors associated with the development of neonatal tolerance after the administration of a plasmid DNA vaccine.* J Immunol 1999; 162:3814–3818.

[57] Ishioka, G.Y., Fikes, J., Hermanson, G., Livingston, B., Crimi, C., Qin, M., del Guercio, M.F., Oseroff, C., Dahlberg, C., Alexander, J., Chesnut, R.W., Sette, A. *Utilization of MHC class I transgenic mice for development of minigene DNA vaccines encoding multiple HLA-restricted CTL epitopes.* J Immunol 1999; 162:3915–3925.

[58] Jiao, S., Williams, P., Berg, R.K., Hodgeman, B.A., Liu, L., Repetto, G., Wolff, J.A. *Direct gene transfer into nonhuman primate myofibers in vivo.* Hum Gene Ther 1992; 3:21–33.

[59] Jones, D.H., Partidos, C.D., Steward, M.W., Farrar, G.H. *Oral delivery of poly(lactide-co-glycolide) encapsulated vaccines.* Behring Inst Mitt 1997; 220–228.

[60] Karasuyama, H., Melchers, F. *Establishment of mouse cell lines which constitutively secrete large quantities of interleukin 2, 3, 4 or 5, using modified cDNA expression vectors.* Eur J Immunol 1988; 18:97–104.

[61] Kedl, R., Schaefer, B., Kappler, J., Marrack, P. *T cells down-modulate peptide-MHC complexes on APCs in vivo* Nat.Immunol. 2002; 3:27–32.

[62] Klinman, D.M., Yi, A.K., Beaucage, S.L., Conover, J., Krieg, A.M. *CpG motifs present in bacteria DNA rapidly induce lymphocytes to secrete interleukin 6, interleukin 12, and interferon gamma.* Proc Natl Acad Sci U S A 1996; 93:2879–2883.

[63] Köntgen, F., Süss, G., Stewart, C., Steinmetz, M., Bluethmann, H. *Targeted disruption of the MHC class II Aa gene in C57BL/6 mice.* Int Immunol 1993; 5:957–964.

[64] Kotturi, M.F., Scott, I., Wolfe, T., Peters, B., Sidney, J., Cheroutre, H., von Herrath, M.G., Buchmeier, M.J., Grey, H., Sette, A. *Naive precursor frequencies and MHC binding rather than the degree of epitope diversity shape CD8+ T cell immunodominance.* J Immunol 2008; 181:2124–2133.

[65] Krieg, A.M., Yi, A.K., Matson, S., Waldschmidt, T.J., Bishop, G.A., Teasdale, R., Koretzky, G.A., Klinman, D.M. *CpG motifs in bacterial DNA trigger direct B-cell activation.* Nature 1995; 374:546–549.

[66] Kuhröber, A., Pudollek, H., Reifenberg, K., Chisari, F., Schlicht, H., Reimann, J., Schirmbeck, R. *DNA immunization induces antibody and cytotoxic T cell responses to hepatitis B core antigen in H-2b mice* J.Immunol. 1996; 156:3687–3695.

[67] Kurotaki, T., Tamura, Y., Ueda, G., Oura, J., Kutomi, G., Hirohashi, Y., Sahara, H., Torigoe, T., Hiratsuka, H., Sunakawa, H., Hirata, K., Sato, N. *Efficient cross-presentation by heat shock protein 90-peptide complex-loaded dendritic cells via an endosomal pathway.* J Immunol 2007; 179:1803–1813.

[68] Lew, D., Parker, S.E., Latimer, T., Abai, A.M., Kuwahara-Rundell, A., Doh, S.G., Yang, Z.Y., Laface, D., Gromkowski, S.H., Nabel, G.J. *Cancer gene therapy using plasmid DNA: pharmacokinetic study of DNA following injection in mice.* Hum Gene Ther 1995; 6:553–564.

[69] Liu, F., Whitton, J.L., Slifka, M.K. *The rapidity with which virus-specific CD8+ T cells initiate IFN-gamma synthesis increases markedly over the course of infection and correlates with immunodominance.* J Immunol 2004; 173:456–462.

[70] Liu, J., Ewald, B.A., Lynch, D.M., Nanda, A., Sumida, S.M., Barouch, D.H. *Modulation of DNA vaccine-elicited CD8+ T-lymphocyte epitope immunodominance hierarchies.* J Virol 2006; 80:11991–11997.

[71] Liu, M.A. *DNA vaccines: a review.* J Intern Med 2003; 253:402–410.

[72] Livingston, J.B., Lu, S., Robinson, H., Anderson, D.J. *Immunization of the female genital tract with a DNA-based vaccine.* Infect Immun 1998; 66:322–329.

[73] Lutz, M.B., Kukutsch, N., Ogilvie, A.L., Rössner, S., Koch, F., Romani, N., Schuler, G. *An advanced culture method for generating large quantities of highly pure dendritic cells from mouse bone marrow.* J Immunol Methods 1999; 223:77–92.

[74] Mahnke, K., Qian, Y., Fondel, S., Brueck, J., Becker, C., Enk, A.H. *Targeting of antigens to activated dendritic cells in vivo cures metastatic melanoma in mice.* Cancer Res 2005; 65:7007–7012.

[75] Marincek, B.C., Kühnle, M.C., Srokowski, C., Schild, H., Hämmerling, G., Momburg, F. *Heat shock protein-antigen fusions lose their enhanced immunostimulatory capacity after endotoxin depletion.* Mol Immunol 2008; 46:181–191.

[76] Martin, T., Parker, S.E., Hedstrom, R., Le, T., Hoffman, S.L., Norman, J., Hobart, P., Lew, D. *Plasmid DNA malaria vaccine: the potential for genomic integration after intramuscular injection.* Hum Gene Ther 1999; 10:759–768.

[77] Massa, C., Melani, C., Colombo, M.P. *Chaperon and adjuvant activity of hsp70: different natural killer requirement for cross-priming of chaperoned and bystander antigens.* Cancer Res 2005; 65:7942–7949.

[78] Mattner, F., Fleitmann, J., Lingnau, K., Schmidt, W., Egyed, A., Fritz, J., Zauner, W., Wittmann, B., Gorny, I., Berger, M., Kirlappos, H., Otava, A., Birnstiel, M., Buschle, M. *Vaccination with poly-L-arginine as immunostimulant for peptide vaccines: induction of potent and long-lasting T-cell responses against cancer antigens* Cancer Res. 2002; 62:1477–1480.

[79] Mayer, M., Bukau, B. *Hsp70 chaperones: cellular functions and molecular mechanism* Cell Mol.Life Sci. 2005; 62:670–684.

[80] Mizukami, S., Kajiwara, C., Ishikawa, H., Katayama, I., Yui, K., Udono, H. *Both CD4+ and CD8+ T cell epitopes fused to heat shock cognate protein 70 (hsc70) can function to eradicate tumors.* Cancer Sci 2008; 99:1008–1015.

[81] Mombaerts, P., Iacomini, J., Johnson, R.S., Herrup, K., Tonegawa, S., Papaioannou, V.E. *RAG-1-deficient mice have no mature B and T lymphocytes.* Cell 1992; 68:869–877.

[82] Monaco, J.J. *A molecular model of MHC class-I-restricted antigen processing.* Immunol Today 1992; 13:173–179.

[83] Mor, G., Yamshchikov, G., Sedegah, M., Takeno, M., Wang, R., Houghten, R.A., Hoffman, S., Klinman, D.M. *Induction of neonatal tolerance by plasmid DNA vaccination of mice.* J Clin Invest 1996; 98:2700–2705.

[84] Moroi, Y., Mayhew, M., Trcka, J., Hoe, M., Takechi, Y., Hartl, F., Rothman, J., Houghton, A. *Induction of cellular immunity by immunization with novel hybrid peptides complexed to heat shock protein 70* Proc.Natl.Acad.Sci.U.S.A 2000; 97:3485–3490.

[85] Noessner, E., Gastpar, R., Milani, V., Brandl, A., Hutzler, P.J.S., Kuppner, M.C., Roos, M., Kremmer, E., Asea, A., Calderwood, S.K., Issels, R.D. *Tumor-derived heat shock protein 70 peptide complexes are cross-presented by human dendritic cells.* J Immunol 2002; 169:5424–5432.

[86] Norbury, C.C., Basta, S., Donohue, K.B., Tscharke, D.C., Princiotta, M.F., Berglund, P., Gibbs, J., Bennink, J.R., Yewdell, J.W. *CD8+ T cell cross-priming via transfer of proteasome substrates.* Science 2004; 304:1318–1321.

[87] Obar, J.J., Khanna, K.M., Lefrançois, L. *Endogenous naive CD8+ T cell precursor frequency regulates primary and memory responses to infection.* Immunity 2008; 28:859–869.

[88] Oseroff, C., Peters, B., Pasquetto, V., Moutaftsi, M., Sidney, J., Panchanathan, V., Tscharke, D.C., Maillere, B., Grey, H., Sette, A. *Dissociation between epitope hierarchy and immunoprevalence in CD8 responses to vaccinia virus western reserve.* J Immunol 2008; 180:7193–7202.

[89] Palliser, D., Guillen, E., Ju, M., Eisen, H. *Multiple intracellular routes in the cross-presentation of a soluble protein by murine dendritic cells* J.Immunol. 2005; 174:1879–1887.

[90] Pang, K.C., Sanders, M.T., Monaco, J.J., Doherty, P.C., Turner, S.J., Chen, W. *Immunoproteasome subunit deficiencies impact differentially on two immunodominant influenza virus-specific CD8+ T cell responses.* J Immunol 2006; 177:7680–7688.

[91] Pascolo, S., Bervas, N., Ure, J.M., Smith, A.G., Lemonnier, F.A., Pérarnau, B. *HLA-A2.1-restricted education and cytolytic activity of CD8(+) T lymphocytes from beta2 microglobulin (beta2m) HLA-A2.1 monochain transgenic H-2Db beta2m double knockout mice.* J Exp Med 1997; 185:2043–2051.

[92] Paul, A.G., van Kooten, P.J., van Eden, W., van der Zee, R. *Highly autoproliferative T cells specific for 60-kDa heat shock protein produce IL-4/IL-10 and IFN-gamma and are protective in adjuvant arthritis.* J Immunol 2000; 165:7270–7277.

[93] Pinchuk, I., Starcher, B.C., Livingston, B., Tvninnereim, A., Wu, S., Appella, E., Sidney, J., Sette, A., Wizel, B. *A CD8+ T cell heptaepitope minigene vaccine induces protective immunity against Chlamydia pneumoniae.* J Immunol 2005; 174:5729–5739.

[94] Probst, H.C., Tschannen, K., Gallimore, A., Martinic, M., Basler, M., Dumrese, T., Jones, E., van den Broek, M.F. *Immunodominance of an antiviral cytotoxic T cell response is shaped by the kinetics of viral protein expression.* J Immunol 2003; 171:5415–5422.

[95] Raz, E., Carson, D.A., Parker, S.E., Parr, T.B., Abai, A.M., Aichinger, G., Gromkowski, S.H., Singh, M., Lew, D., Yankauckas, M.A. *Intradermal gene immunization: the possible role of DNA uptake in the induction of cellular immunity to viruses.* Proc Natl Acad Sci U S A 1994; 91:9519–9523.

[96] Reimann, J., Schirmbeck, R. *Alternative pathways for processing exogenous and endogenous antigens that can generate peptides for MHC class I-restricted presentation.* Immunol Rev 1999; 172:131–152.

[97] Reimann, J., Schirmbeck, R. *DNA vaccines expressing antigens with a stress protein-capturing domain display enhanced immunogenicity* Immunol.Rev. 2004; 199:54–67.

[98] Riedl, P., El Kholy, S., Reimann, J., Schirmbeck, R. *Priming biologically active antibody responses against an isolated, conformational viral epitope by DNA vaccination* J.Immunol. 2002; 169:1251–1260.

[99] Riedl, P., Fissolo, N., Reimann, J., Schirmbeck, R. *A stress protein-facilitated antigen expression system for plasmid DNA vaccines* Methods Mol.Med. 2006; 127:41–53.

[100] Riedl, P., Reimann, J., Schirmbeck, R. *Peptides containing antigenic and cationic domains have enhanced, multivalent immunogenicity when bound to DNA vaccines* J.Mol.Med. 2004; 82:144–152.

[101] Rivoltini, L., Castelli, C., Carrabba, M., Mazzaferro, V., Pilla, L., Huber, V., Coppa, J., Gallino, G., Scheibenbogen, C., Squarcina, P., Cova, A., Camerini, R., Lewis, J.J., Srivastava, P.K., Parmiani, G. *Human tumor-derived heat shock protein 96 mediates in vitro activation and in vivo expansion of melanoma- and colon carcinoma-specific T cells.* J Immunol 2003; 171:3467–3474.

[102] Rodriguez, F., Harkins, S., Slifka, M.K., Whitton, J.L. *Immunodominance in virus-induced CD8(+) T-cell responses is dramatically modified by DNA immunization and is regulated by gamma interferon.* J Virol 2002; 76:4251–4259.

[103] Román, E., Moreno, C. *Synthetic peptides non-covalently bound to bacterial hsp 70 elicit peptide-specific T-cell responses in vivo.* Immunology 1996; 88:487–492.

[104] Rutigliano, J., Ruckwardt, T., Martin, J., Graham, B. *Relative dominance of epitope-specific CD8+ T cell responses in an F1 hybrid mouse model of respiratory syncytial virus infection* Virology 2007; 362:314–319.

[105] Sandberg, J.K., Grufman, P., Wolpert, E.Z., Franksson, L., Chambers, B.J., Kärre, K. *Superdominance among immunodominant H-2Kb-restricted epitopes and reversal by dendritic cell-mediated antigen delivery.* J Immunol 1998; 160:3163–3169.

[106] Saveanu, L., Carroll, O., Lindo, V., Del Val, M., Lopez, D., Lepelletier, Y., Greer, F., Schomburg, L., Fruci, D., Niedermann, G., van Endert, P. *Concerted peptide trimming by human ERAP1 and ERAP2 aminopeptidase complexes in the endoplasmic reticulum* Nat.Immunol. 2005; 6:689–697.

[107] Schirmbeck, R., Fissolo, N., Chaplin, P., Reimann, J. *Enhanced priming of multispecific, murine CD8+ T cell responses by DNA vaccines expressing stress protein-binding polytope peptides* J.Immunol. 2003; 171:1240–1246.

[108] Schirmbeck, R., Gerstner, O., Reimann, J. *Truncated or chimeric endogenous protein antigens gain immunogenicity for B cells by stress protein-facilitated expression* Eur.J.Immunol. 1999; 29:1740–1749.

[109] Schirmbeck, R., Kwissa, M., Fissolo, N., Elkholy, S., Riedl, P., Reimann, J. *Priming polyvalent immunity by DNA vaccines expressing chimeric antigens with a stress protein-capturing, viral J-domain* FASEB J. 2002; 16:1108–1110.

[110] Schirmbeck, R., Riedl, P., Fissolo, N., Lemonnier, F., Bertoletti, A., Reimann, J. *Translation from cryptic reading frames of DNA vaccines generates an extended repertoire of immunogenic, MHC class I-restricted epitopes* J.Immunol. 2005; 174:4647–4656.

[111] Schirmbeck, R., Riedl, P., Kupferschmitt, M., Wegenka, U., Hauser, H., Rice, J., Kroger, A., Reimann, J. *Priming protective CD8 T cell immunity by DNA vaccines encoding chimeric, stress protein-capturing tumor-associated antigen* J.Immunol. 2006; 177:1534–1542.

[112] Schirmbeck, R., Riedl, P., Zurbriggen, R., Akira, S., Reimann, J. *Antigenic epitopes fused to cationic peptide bound to oligonucleotides facilitate Toll-like receptor 9-dependent, but CD4+ T cell help-independent, priming of CD8+ T cells* J.Immunol. 2003; 171:5198–5207.

[113] Schirmbeck, R., Stober, D., El Kholy, S., Riedl, P., Reimann, J. *The immunodominant, Ld-restricted T cell response to hepatitis B surface antigen (HBsAg) efficiently suppresses T cell priming to multiple Dd-, Kd-, and Kb-restricted HBsAg epitopes* J.Immunol. 2002; 168:6253–6262.

[114] Sette, A., Oseroff, C., Sidney, J., Alexander, J., Chesnut, R., Kakimi, K., Guidotti, L., Chisari, F. *Overcoming T cell tolerance to the hepatitis B virus surface antigen in hepatitis B virus-transgenic mice* J.Immunol. 2001; 166:1389–1397.

[115] Singh-Jasuja, H., Scherer, H.U., Hilf, N., Arnold-Schild, D., Rammensee, H.G., Toes, R.E., Schild, H. *The heat shock protein gp96 induces maturation of dendritic cells and down-regulation of its receptor.* Eur J Immunol 2000; 30:2211–2215.

[116] Srivastava, P.K. *Immunotherapy of human cancer: lessons from mice.* Nat Immunol 2000; 1:363–366.

[117] Srivastava, P., Jaikaria, N. *Methods of purification of heat shock protein-peptide complexes for use as vaccines against cancers and infectious diseases* Methods Mol.Biol. 2001; 156:175–186.

[118] Srivastava, P. *Interaction of heat shock proteins with peptides and antigen presenting cells: chaperoning of the innate and adaptive immune responses.* Annu Rev Immunol 2002; 20:395–425.

[119] Suzue, K., Young, R. *Adjuvant-free hsp70 fusion protein system elicits humoral and cellular immune responses to HIV-1 p24* J.Immunol. 1996; 156:873–879.

[120] Suzue, K., Zhou, X., Eisen, H., Young, R. *Heat shock fusion proteins as vehicles for antigen delivery into the major histocompatibility complex class I presentation pathway* Proc.Natl.Acad.Sci.U.S.A 1997; 94:13146–13151.

[121] Thomson, S.A., Elliott, S.L., Sherritt, M.A., Sproat, K.W., Coupar, B.E., Scalzo, A.A., Forbes, C.A., Ladhams, A.M., Mo, X.Y., Tripp, R.A., Doherty, P.C., Moss, D.J., Suhrbier, A. *Recombinant polyepitope vaccines for the delivery of multiple CD8 cytotoxic T cell epitopes.* J Immunol 1996; 157:822–826.

[122] Todryk, S., Melcher, A.A., Hardwick, N., Linardakis, E., Bateman, A., Colombo, M.P., Stoppacciaro, A., Vile, R.G. *Heat shock protein 70 induced during tumor cell killing induces Th1 cytokines and targets immature dendritic cell precursors to enhance antigen uptake.* J Immunol 1999; 163:1398–1408.

[123] Tourdot, S., Gould, K.G. *Competition between MHC class I alleles for cell surface expression alters CTL responses to influenza A virus.* J Immunol 2002; 169:5615–5621.

[124] Trautmann, L., Rimbert, M., Echasserieau, K., Saulquin, X., Neveu, B., Dechanet, J., Cerundolo, V., Bonneville, M. *Selection of T cell clones expressing high-affinity public TCRs within Human cytomegalovirus-specific CD8 T cell responses.* J Immunol 2005; 175:6123–6132.

[125] Trombetta, E.S., Ebersold, M., Garrett, W., Pypaert, M., Mellman, I. *Activation of lysosomal function during dendritic cell maturation.* Science 2003; 299:1400–1403.

[126] Tzelepis, F., de Alencar, B., Penido, M., Claser, C., Machado, A., Bruna-Romero, O., Gazzinelli, R., Rodrigues, M. *Infection with Trypanosoma cruzi Restricts the Repertoire of Parasite-Specific CD8+ T Cells Leading to Immunodominance* J.Immunol. 2008; 180:1737–1748.

[127] Vabulas, R.M., Braedel, S., Hilf, N., Singh-Jasuja, H., Herter, S., Ahmad-Nejad, P., Kirschning, C.J., Costa, C.D., Rammensee, H.G., Wagner, H., Schild, H. *The endoplasmic reticulum-resident heat shock protein Gp96 activates dendritic cells via the Toll-like receptor 2/4 pathway.* J Biol Chem 2002; 277:20847–20853.

[128] Valentinis, B., Capobianco, A., Esposito, F., Bianchi, A., Rovere-Querini, P., Manfredi, A.A., Traversari, C. *Human recombinant heat shock protein 70 affects the maturation pathways of dendritic cells in vitro and has an in vivo adjuvant activity.* J Leukoc Biol 2008; 84:199–206.

[129] van der Burg, S.H., Visseren, M.J., Brandt, R.M., Kast, W.M., Melief, C.J. *Immunogenicity of peptides bound to MHC class I molecules depends on the MHC-peptide complex stability.* J Immunol 1996; 156:3308–3314.

[130] Wallin, R., Lundqvist, A., More, S., von Bonin, A., Kiessling, R., Ljunggren, H. *Heat-shock proteins as activators of the innate immune system* Trends Immunol. 2002; 23:130–135.

[131] Wang, R., Doolan, D.L., Charoenvit, Y., Hedstrom, R.C., Gardner, M.J., Hobart, P., Tine, J., Sedegah, M., Fallarme, V., Sacci, J.B., Kaur, M., Klinman, D.M., Hoffman, S.L., Weiss, W.R. *Simultaneous induction of multiple antigen-specific cytotoxic T lymphocytes in nonhuman primates by immunization with a mixture of four Plasmodium falciparum DNA plasmids.* Infect Immun 1998; 66:4193–4202.

[132] Williams, R.S., Johnston, S.A., Riedy, M., DeVit, M.J., McElligott, S.G., Sanford, J.C. *Introduction of foreign genes into tissues of living mice by DNA-coated microprojectiles.* Proc Natl Acad Sci U S A 1991; 88:2726–2730.

[133] Willis, R., Kappler, J., Marrack, P. *CD8 T cell competition for dendritic cells in vivo is an early event in activation* Proc.Natl.Acad.Sci.U.S.A 2006; 103:12063–12068.

[134] Wolff, J.A., Ludtke, J.J., Acsadi, G., Williams, P., Jani, A. *Long-term persistence of plasmid DNA and foreign gene expression in mouse muscle.* Hum Mol Genet 1992; 1:363–369.

[135] Wolpert, E.Z., Grufman, P., Sandberg, J.K., Tegnesjö, A., Kärre, K. *Immunodominance in the CTL response against minor histocompatibility antigens: interference between responding T cells, rather than with presentation of epitopes.* J Immunol 1998; 161:4499–4505.

[136] Wortmann, A., Vohringer, S., Engler, T., Corjon, S., Schirmbeck, R., Reimann, J., Kochanek, S., Kreppel, F. *Fully Detargeted Polyethylene Glycol-coated Adenovirus Vectors Are Potent Genetic Vaccines and Escape from Pre-existing Anti-adenovirus Antibodies* Mol.Ther. 2008; 16:154–162.

[137] Yang, N.S., Sun, W.H. *Gene gun and other non-viral approaches for cancer gene therapy.* Nat Med 1995; 1:481–483.

[138] Ye, Z., Gan, Y.H. *Flagellin contamination of recombinant heat shock protein 70 is responsible for its activity on T cells.* J Biol Chem 2007; 282:4479–4484.

[139] Yewdell, J.W., Norbury, C.C., Bennink, J.R. *Mechanisms of exogenous antigen presentation by MHC class I molecules in vitro and in vivo: implications for generating CD8+ T cell responses to infectious agents, tumors, transplants, and vaccines.* Adv Immunol 1999; 73:1–77.

[140] Zarozinski, C.C., Fynan, E.F., Selin, L.K., Robinson, H.L., Welsh, R.M. *Protective CTL-dependent immunity and enhanced immunopathology in mice immunized by particle bombardment with DNA encoding an internal virion protein.* J Immunol 1995; 154:4010–4017.

A. Appendix

Chemicals and reagents

Table 9.: Chemicals and reagents

product	**provider**	**cat.no.**
dNTP	NEB	N7552
acetic acid	Applichem	A0820
acrylamid	Roth	3029.1
agar	DIFCO	214010
agarose	Invitrogen	15510
ampicillin	Merck	1.00278
APS	Sigma	A3678
ATP	Sigma	A9187
bactotryptone	DIFCO	0123-07-5
β-ME	BioRad	161-0710
bromphenol blue	Sigma	B-8026
BSA	PAA	K41-001
$CaCl_2$ x $2H_2O$	Merck	1.02383
chloramphenicol	Fluka	2375
Coomassie Brilliant Blue R 250	Serva	17525
desthiobiotin	IBA GmbH	2-1000-002
diethanolamin	Fluka	31590
DMSO	Applichem	67-68-5
EDTA	Fluka	3677
ethanol	VWR	20821.330
ethidium bromide	Applichem	A2273
gelatine	Merck	1.04078

Table 9.: Chemicals and reagents

product	**provider**	**cat.no.**
glycerol	J.T.Baker	7044
glycine	Applichem	A1377
H_2SO_4	Merck	1.00731
HCl	VWR	20252.290
Hepes	Serva	25245
IPTG	Fluka	59740
isopropanol	Fluka	59300
K_2HPO_4	Sigma	P2222
kanamycin	Fluka	60615
KH_2PO_4	Sigma	P5655
leupeptin	Fluka	62070
LiCl	Roth	3739.2
methanol	Fluka	65543
$MgCl_2$ x $6H_2O$	Sigma	M2670
Na_2HPO_4 x $2H_2O$	Merck	1.06345
NaN_3	Serva	30175
NaCl	VWR	27810.364
NH_4Cl	Merck	1.01145
NP40	Sigma	I-3021
ovalbumin	Sigma	A7641
PFA	PFA	158127
PPO	Fluka	43410
saponin	Sigma	S7900
SDS	BioRad	161-0301
TEMED	BioRad	161-0800
Trasylol	Bayer Vital	
trizma base	Sigma	T1503
Tween 20	Fluka	93773
xylencyanol	Merck	1.10590
yeast extract	DIFCO	0127-07-1

List of publications

1. Riedl P.*, **Wieland A.***, Lamberth K., Buus S., Lemonnier F., Reifenberg K., Reimann J., Schirmbeck R. *Elimination of immunodominant epitopes from multispecific DNA-based vaccines allows induction of CD8 T cells that have a striking anti-viral potential.* submitted

2. **Wieland A.***, Riedl P.*, Reimann J., Schirmbeck R. *Silencing an immunodominant epitope of hepatitis B surface antigen reveals an alternative repertoire of CD8 T cell epitopes of this viral antigen.* submitted

3. **Wieland A.**, Denzel M., Schmidt E., Kochanek S., Kreppel F., Reimann J., Schirmbeck R. *Recombinant complexes of antigen with stress proteins are potent CD8 T-cell-stimulating immunogens.* J Mol Med 2008; 86:1067-1079.

4. Karges W., Rajasalu T., Spyrantis A., **Wieland A.**, Boehm B., Schirmbeck R. *The diabetogenic, insulin-specific CD8 T cell response primed in the experimental autoimmune diabetes model in RIP-B7.1 mice.* Eur J Immunol 2007; 37:2097-2103.

* contributed equally

Acknowledgments

I want to thank Prof. Dr. Reinhold Schirmbeck –Reini– who gave me the opportunity to work on this interesting project, for his patience and guidance throughout this thesis.
I would like to thank Prof. Dr. Jörg Reimann who gave me the opportunity to work in his group.
I want to especially thank Dr. Petra Riedl for her help throughout this thesis, her advice in the everyday lab work, familiarizing me with all the immunological methods, the much valued discussions and her 'proof-reading activity'.
I also would like thank my PhD co-fighter and office roommate Michael for his friendship, a lot of fun despite and due to the chaos surrounding him.
I also want thank the other PhD colleagues in the lab: Petra, Helen and 'my coffee partner' Mona for the good times and discussions, and especially Mona for encouraging me to use LaTeX.
I also have to thank 'the commander' Markus for providing me with a lot of plasmid constructs and fun during his diploma thesis.
A special thanks goes out to my intern-in-chief Julia for excellent technical assistance in cloning, delicious cakes and infinite but ineffective attempts to make me nuts.
Thanks to Claudi, Kati and Sarah for their practical help and appreciated distraction. I also want to thank all the other members of the group: Christian, Ivan, Ellen, Ina and Julia. Thank you for three wonderful years of research and fun!

Last but not least, I want to thank the ones I owe it all –my family who supported me all the years.